# Synchronization of Pendulum Like Systems

A THESIS

SUBMITTED TO THE DEPARTMENT OF ELECTRICAL AND

ELECTRONICS ENGINEERING

AND THE GRADUUATE SCHOOL OF ENGINEERING AND SCIENCE

OF BILKENT UNIVERSITY

IN PARTIAL FULFILLMENT OF THE REQUIREMENTS

FOR THE DEGREE OF

MASTER OF SCIENCE

By

Deniz Kerimoğlu

August 2011

I certify that I have read this thesis and that in my opinion it is fully adequate, in scope and in quality, as a thesis for the degree of Master of Science.

Prof. Dr. Ömer Morgül(Supervisor)

I certify that I have read this thesis and that in my opinion it is fully adequate, in scope and in quality, as a thesis for the degree of Master of Science.

Prof. Dr. A. Enis Çetin

I certify that I have read this thesis and that in my opinion it is fully adequate, in scope and in quality, as a thesis for the degree of Master of Science.

Assist. Prof. Dr Melih Çakmakçı

Approved for the Graduate School of Engineering and Science:

Prof. Dr. Levent Onural
Director of Graduate School of Engineering and Science

# ABSTRACT

## Synchronization of Pendulum Like Systems

Deniz Kerimoğlu
M.S. in Electrical and Electronics Engineering
Supervisor: Prof. Dr. Ömer Morgül
August 2011

Synchronization is a phenomenon that is widely encountered in nature, life sciences and engineering. There exist various synchronization definitions in various research fields. The general definition for synchronization is the adjustment of rhythms of oscillating systems due to their weak interaction. Synchronization problem depends on the type of applications that require suitable properties and comparison functions. Different applications require different properties and comparison functions. Throughout our study, we choose the comparison function to be the difference of the states variables of the systems in hand.

In this thesis, we will present types and methods of synchronization which has practical applications, i.e. mechanical systems. Then, we will investigate the passive controlled in-phase synchronization of spring-damper coupled single and double pendulum systems by using various stability analysis for both the system in hand and its appropriately defined error dynamics. We mostly achieved in-phase synchronization in these coupled pendulum systems with a few exceptions which are based on several conditions. Finally, we will explain the master-slave synchronization of two ball hoppers using two different gait controllers, namely, fully-actuated and under-actuated controllers. By using fully-actuated controller for the slave hopper, we achieved apex state synchronization and by

using under-actuated controller for the slave hopper, we achieved apex position synchronization between these two hoppers in master slave configuration.

*Keywords:* In-phase Synchronization, Master Slave Synchronization, Coupled Pendulum System, Ball hopper, Gait Controller.

# ÖZET

## SARKAÇ BENZERİ SİSTEMLERİN EŞZAMANLAMASI

Deniz Kerimoğlu
Elektrik ve Elektronik Mühendisliği Bölümü Yüksek Lisans
Tez Yöneticisi: Prof. Dr. Ömer Morgül
Ağustos 2011

Eşzamanlama doğada, fen bilimlerinde ve mühendislik analarında çokça karşılaş ılan bir olgudur. Çeşitli araştırma alanlarında birçok eşzamanlama tanımı mevcuttur. Genel olarak eşzamanlama pasif bağlı salınan mekanik sistemlerin ritimlerinin uyum sağlaması olarak tanımlanabilir. Eşzamanlama problemi, uygun özellikler ve karşılaştırma fonksiyonları gerektiren uygulama çeşitlerine bağlıdır. Çeşitli uygulamalar çeşitli özellikler ve karşılaştırma fonksiyonları gerektirir. Biz bu çalışmamızda, karşılaştırma fonksiyonunu elimizdeki sistemin durum değişkenlerinin farkı olarak tanımlamaktayız. Bu çalışmamızda, uygulama alanı bulan eşzamanlama çeşitlerini ve yöntemlerini vereceğiz, örneğin mekanik sistemler. Sonra, yay-sönümleyici bağlı basit ve çift sarkaç sistemlerinin pasif-denetleyicili eş-faz eşzamanlamasını hem elimizde bulunan sisteme hem de bu sistemin hata dinamiğine çeşitli kararlılık analizleri uygulayarak inceleyeceğiz. Söz konusu bağlı sarkaç sistemlerin çoğunun eş-faz eşzamanlamasını belirli koşullara bağlı birkaç istisna durum dışında elde ettik. Son olarak, tam tahrikli ve eksik tahrikli olacak şekilde iki farklı hareket denetleyicisi kullanarak iki tane top zıplayanının efendi-köle eşzamanlamasını açıklayacağız. Köle zıplayanı için tam tahrikli denetleyici kullandığımız durumda, efendi ve köle zıplayan arasında tepe

noktası durum eşzamanlaması, eksik tahrikli denetleyici kullandığımız durumda ise tepe noktası pozisyon eşzamanlaması elde ettik.

*Anahtar Kelimeler:* Eş-faz Eşzamanlaması, Efendi-Köle Eşzamanlaması, Bağlı Sarkaç Sistemleri, Top Zıplayanı, Hareket Denetleyicisi.

# ACKNOWLEDGMENTS

Firstly, I would like to thank my supervisor Ömer Morgül for his invaluable guidance and advices. I am also thanful to Uluç Saranlı, Melih Çakmakçı and Orhan Arıkan for their great supports. I also appreciate Kerem Altun, İsmail Uyanık, Murat Cihan Yüksek for their valuable helps.

Finally, I would like to thank to my parents for their endless supports and to my friend Türkan Çakmak for her great encouragement and patience.

# Contents

**1 INTRODUCTION** **1**

1.2 Contributions of the Thesis . . . . . 5

**2 TYPES AND METHODS OF SYNCHRONIZATION** **7**

2.1 Types of Synchronization . . . . . 7

2.1.1 Phase Synchronization . . . . . 8

2.1.2 Full Synchronization . . . . . 9

2.1.3 Frequency Synchronization . . . . . 10

2.1.4 Network Synchronization . . . . . 10

2.2 Methods Of Synchronization . . . . . 11

2.2.1 Active Controlled Synchronization . . . . . 12

2.2.2 Passive Controlled Synchronization . . . . . 13

**3 PASSIVE CONTROLLED IN-PHASE SYNCHRONIZATION OF COUPLED SIMPLE PENDULUMS** **14**

3.1 Two Pendulums Coupled with Series Spring-Mass-Damper . . . . 16

3.2 Two Pendulums Coupled with Series Spring-Damper . . . . . 19

3.3 Two Pendulums Coupled with Parallel Spring-Damper . . . . . 27

3.4 Two Pendulums Coupled with Parallel Spring-Damper in Oblique Form . . . . . 30

3.5 Three Pendulums Coupled with Spring-Damper . . . . . 34

3.6 Four Pendulums Coupled with Two Springs and One Damper(Damper-Spring-Spring Configuration) . . . . . 41

3.7 Four Pendulums Coupled with Two Spring and One Damper(Spring-Damper-Spring-Configuration) . . . . . 46

3.8 Multiple Pendulums Coupled with a Single Damper and Springs . 51

3.9 Discussion and Contribution . . . . . 56

**4 PASSIVE CONTROLLED IN-PHASE SYNCHRONIZATION OF COUPLED DOUBLE PENDULUMS 58**

4.1 Two Double Pendulums Coupled from Upper part with Parallel Spring and Damper . . . . . 60

4.2 Two Double Pendulums Coupled from Lower part with Parallel Spring and Damper . . . . . 66

4.3 Discussion and Contribution . . . . . 72

**5 ACTIVE CONTROLLED MASTER SLAVE SYNCHRONIZATION OF TWO BALL HOPPERS 74**

5.1 Overview of SLIP model and Ball Hopper . . . . . 75

5.2 Master-Slave Synchronization of Two Ball Hoppers using Fully-Actuated Controller . . . . . 79

5.3 Master-Slave Synchronization of Two Ball Hoppers using Under-Actuated Controller . . . . . 82

5.4 Discussion and Contribution . . . . . 87

**6 CONCLUSIONS** **88**

**APPENDIX** **91**

**A Presentation of Positive Routh-Hurwitz First Columns** **91**

# List of Figures

2.1 Mutual Synchronization of Subsystems . . . . . 12

2.2 Master-Slave Synchronization of Subsystems . . . . . 13

3.1 Two Double Pendulums Coupled with Series Spring-Mass-Damper 16

3.2 Simulation of two pendulums coupled with spring, mass, damper. We choose $m_1 = m_2 = 1,\ k = 5,\ c = 1,\ l = 1,\ l_0 = 0.5,\ \theta_1(0) = 8^\circ,\ \dot{\theta}_1(0) = 0^\circ,\ \theta_2(0) = 3^\circ,\ \dot{\theta}_2(0) = 0^\circ,\ x(0) = 0,\ \dot{x}(0) = 0$ for simulation purposes. . . . . 18

3.3 Error simulation of two pendulums coupled with spring, mass, damper. We choose the above parameters for simulation purposes. 19

3.4 Two Double Pendulums Coupled with Series Spring-Damper . . . 20

3.5 Simulation of two pendulums coupled with series spring and damper. We choose $m_1 = m_2 = 1,\ k = 2,\ c = 1,\ l = 1,\ l_0 = 0.75,\ \theta_1(0) = 10^\circ,\ \dot{\theta}_1(0) = 0^\circ,\ \theta_2(0) = -1^\circ,\ \dot{\theta}_2(0) = 0^\circ,\ x(0) = 0$ for simulation purposes. . . . . 26

3.6 Error simulation of two pendulums coupled with series spring and damper. We choose the above parameters for simulation purposes. 26

3.7 Two Double Pendulums Coupled with Parallel Spring-Damper . . 27

3.8 Simulation of two pendulums coupled with parallel spring and damper. In these particular simulations we choose $k = 2,\ c = 1,\ l_0 = 0.75,\ l = 1,\ m_1 = m_2 = 1,\ \theta_1(0) = 9^\circ,\ \dot{\theta}_1(0) = 0^\circ,\ \theta_2(0) = -2^\circ,\ \dot{\theta}_2(0) = 0^\circ$. . . . . 29

3.9 Error simulation of two pendulums coupled with parallel spring and damper. We choose the above parameters for simulation purposes. . . . . 30

3.10 Two Double Pendulums Coupled with Parallel Spring-Damper in Oblique Form . . . . . 31

3.11 Simulation of two pendulums coupled with parallel spring and damper in oblique form. In these particular simulations we choose $k = 10,\ c = 1,\ l = 1,\ l_0 = .75,\ l_1 = .15,\ m_1 = m_2 = 1,\ \theta_1(0) = 10^\circ,\ \dot{\theta}_1(0) = 0^\circ,\ \theta_2(0) = 1^\circ,\ \dot{\theta}_2(0) = 0^\circ$. . . . . 33

3.12 Error simulation of two pendulums coupled with parallel spring and damper in oblique form. We choose the above parameters for simulation purposes. . . . . 34

3.13 Three Pendulums Coupled with Parallel Spring-Damper . . . . . 35

3.14 Simulation of three pendulums coupled with parallel spring and damper. In these particular simulations we choose $k_1 = 4,\ k_2 = 3,\ c_1 = 1,\ c_2 = 1,\ l = 1,\ l_0 = .75,\ m_1 = m_2 = 1,\ \theta_1(0) = 8^\circ,\ \dot{\theta}_1(0) = 0^\circ,\ \theta_2(0) = -2^\circ,\ \dot{\theta}_2(0) = 0^\circ,\ \theta_3(0) = 10^\circ,\ \dot{\theta}_3(0) = 0^\circ$ . 38

3.15 Error simulation of three pendulums coupled with parallel spring and damper. We choose the above parameters for simulation purposes. . . . . 39

3.16 Three Pendulums Coupled with Single Parallel Spring-Damper . . 39

3.17 Simulation of three pendulums coupled with single parallel spring and damper. In these particular simulations we choose $k_1 = 10,\ c_2 = 1,\ l = 1,\ l_0 = .75,\ m_1 = m_2 = 1,\ \theta_1(0) = 8°,\ \dot{\theta}_1(0) = 0°,\ \theta_2(0) = -2°,\ \dot{\theta}_2(0) = 0°,\ \theta_3(0) = 10°,\ \dot{\theta}_3(0) = 0°$ . . . . . 40

3.18 Error simulation of three pendulums coupled with single parallel spring and damper. We choose the above parameters for simulation purposes. . . . . 41

3.19 Four Pendulums Coupled with Two Springs and One Damper. . . 42

3.20 Simulation of four pendulums coupled with two springs and one damper. In these particular simulations we choose $k_1 = 20,\ k_2 = 10,\ c = 1,\ l = 1,\ l_0 = .85,\ m = 1,\ \theta_1(0) = 8°,\ \dot{\theta}_1(0) = 0°,\ \theta_2(0) = -5°,\ \dot{\theta}_2(0) = 0°,\ \theta_3(0) = 2°,\ \dot{\theta}_3(0) = 0°\ \theta_4(0) = 7°,\ \dot{\theta}_4(0) = 0°$ . . . . . 45

3.21 Error simulation of four pendulums coupled with two springs and one damper. We choose the above parameters for simulation purposes. . . . . 45

3.22 Four Pendulums Coupled with Two Springs and One Damper. . . 46

3.23 Simulation of four pendulums coupled with two springs and one damper for $K_1 = K_2$ case. In these particular simulations we choose $k_1 = 10,\ k_2 = 10,\ c = 5,\ l = 1,\ l_0 = .75,\ m = 1,\ \theta_1(0) = 8°,\ \dot{\theta}_1(0) = 0°,\ \theta_2(0) = -5°,\ \dot{\theta}_2(0) = 0°,\ \theta_3(0) = 2°,\ \dot{\theta}_3(0) = 0°\ \theta_4(0) = 7°,\ \dot{\theta}_4(0) = 0°$ . . . . . 50

3.24 Error simulation of four pendulums coupled with two springs and one damper. We choose the above parameters for simulation purposes. . . . . 50

3.25 Simulation of four pendulums coupled with two springs and one damper for $K_1 \neq K_2$ case. In these particular simulations we choose $k_1 = 20,\ k_2 = 10,\ c = 5,\ l = 1,\ l_0 = .75,\ m = 1,\ \theta_1(0) = 8°,\ \dot{\theta}_1(0) = 0°,\ \theta_2(0) = -5°,\ \dot{\theta}_2(0) = 0°,\ \theta_3(0) = 2°,\ \dot{\theta}_3(0) = 0°\ \theta_4(0) = 7°,\ \dot{\theta}_4(0) = 0°$ . . . . . 51

3.26 Error simulation of four pendulums coupled with two springs and one damper. We choose the above parameters for simulation purposes. . . . . 51

3.27 Seven Pendulums Coupled with Five Springs and One Damper. . 52

3.28 Simulation of seven pendulums coupled with five springs and one damper. Parameter values are $k_1 = 20,\ k_2 = 10,\ k_3 = 20,\ k_4 = 20,\ k_5 = 20,\ c = 5,\ l = 1,\ l_0 = .75,\ m = 1,\ \theta_1(0) = 8°,\ \dot{\theta}_1(0) = 0°,\ \theta_2(0) = -1°,\ \dot{\theta}_2(0) = 0°,\ \theta_3(0) = 5°,\ \dot{\theta}_3(0) = 0°,\ \theta_4(0) = 7°,\ \dot{\theta}_4(0) = 0°,\ \theta_5(0) = 6°,\ \dot{\theta}_5(0) = 0°,\ \theta_6(0) = -2°,\ \dot{\theta}_6(0) = 0,°\ \theta_7(0) = -3°,\ \dot{\theta}_7(0) = 0°.$ . . . . . 55

3.29 Error simulation of seven pendulums coupled with five springs and one damper. We choose the above parameters for simulation purposes. . . . . 56

4.1 Two Double Pendulums Coupled from Upper part with Parallel Spring and Damper . . . . . 61

4.2 Simulation of two double pendulums coupled from upper pendulums. In these paticular simulations we choose $m = 1,\ l = 1,\ k = 10,\ c = 5,\ l_0 = 0.75,\ \theta_1(0) = -5°,\ \dot{\theta}_1(0) = 0°,\ \theta_2(0) = -9°,\ \dot{\theta}_2(0) = 0°,\ \theta_3(0) = 8°,\ \dot{\theta}_3(0) = 0°,\ \theta_4(0) = 4°,\ \dot{\theta}_4(0) = 0°.$ . . . 65

4.3 Error simulation of two coupled double pendulums. We choose the above parameters for simulation purposes. . . . . 65

4.4 Two Double Pendulums Coupled from Lower part with Parallel Spring and Damper . . . . . 66

4.5 Plot of eigenvalues of matrix $A$. In this particular simulations we choose $m = 1,\ l = 1,\ l_0 = 0.75,\ k = 0$ to 100 and $c = 0$ to 100. . . 68

4.6 Simulation of two double pendulums coupled from lower pendulums. In these paticular simulations we choose $m = 1,\ l = 1,\ k = 10,\ c = 3,\ l_0 = 0.95,\ \theta_1(0) = -1^\circ,\ \dot{\theta}_1(0) = 0^\circ,\ \theta_2(0) = -3^\circ,\ \dot{\theta}_2(0) = 0^\circ,\ \theta_3(0) = 10^\circ,\ \dot{\theta}_3(0) = 0^\circ,\ \theta_4(0) = 8^\circ,\ \dot{\theta}_4(0) = 0^\circ$. . 71

4.7 Error simulation of two coupled double pendulums. We choose the above parameters for simulation purposes. . . . . 71

4.8 Simulation of two double pendulums coupled from lower pendulums. In these paticular simulations we choose $m = 1,\ l = 1,\ k = 10,\ c = 3,\ l_0 = \frac{1}{\sqrt{2}}l,\ \theta_1(0) = -1^\circ,\ \dot{\theta}_1(0) = 0^\circ,\ \theta_2(0) = -3^\circ,\ \dot{\theta}_2(0) = 0^\circ,\ \theta_3(0) = 10^\circ,\ \dot{\theta}_3(0) = 0^\circ,\ \theta_4(0) = 8^\circ,\ \dot{\theta}_4(0) = 0^\circ$. . 72

4.9 Error simulation of two coupled double pendulums. We choose the above parameters for simulation purposes. . . . . 72

5.1 The SLIP Model . . . . . 75

5.2 The Ball Hopper . . . . . 77

5.3 Master-Slave Synchronization of Two Ball Hoppers. For the master hopper we choose $k = 1$, $\theta = 0$, $\Delta y = 0.05$ as the control inputs and $[y\ z\ \dot{y}\ \dot{z}] = [1\ 0.4\ 1\ 0]$ as the initial conditions. In this particular simulation we choose the initial conditions for the slave hopper as $[y\ z\ \dot{y}\ \dot{z}] = [0.5\ 0.5\ 0.6\ 0]$ . . . . . 80

5.4 Apex states error figures. The $y$, $z$, $\dot{y}$ state variables fully synchronize. . . . . 80

5.5 Touchdown and liftoff position error figures. After the first stride touchdown and litoff positions synchronize. . . . . 81

5.6 Differences of time that is spent between present apex to apex at each stride. . . . . 81

5.7 Simultaneous master-slave synchronization of two ball hoppers when there is no criteria applied to the initial conditions of the slave hopper. . . . . 83

5.8 Simultaneous master-slave synchronization of two ball hoppers when the criteria applied to the initial conditions of the slave hopper. 84

5.9 Master-Slave Synchronization of Two Ball Hoppers. For the master hopper we choose $k = 1$, $\theta = 0$, $\Delta y = 0.05$ as the control inputs and $[y\ z\ \dot{y}\ \dot{z}] = [1\ 0.4\ 1\ 0]$ as the initial conditions. In this particular simulation we choose the initial conditions for the slave hopper as $[y\ z\ \dot{y}\ \dot{z}] = [0.5\ 0.47\ 3\ 0]$ . . . . . 85

5.10 Apex states error figures. . . . . 85

5.11 Touchdown and liftoff position error figures. . . . . 86

5.12 Differences of time that is spent between present apex to apex at each stride. . . . . 86

# List of Tables

3.1 The first column of the Routh table which is obtained by applying Routh-Hurwitz criterion to equations of motion of the coupled system. . . . . 17

3.2 The first column of the Routh table which is obtained by applying Routh-Hurwitz criterion to equations of motion of the coupled system. . . . . 21

3.3 The first column of the Routh table which is obtained by applying Routh-Hurwitz criterion to equations of motion of the coupled system. . . . . 24

3.4 The first column of the Routh table which is obtained by applying Routh-Hurwitz criterion to equations of motion of the coupled system. . . . . 36

3.5 The first column of the Routh table which is obtained by applying Routh-Hurwitz criterion to error equation of the coupled system. . 38

3.6 The first column of the Routh table which is obtained by applying Routh-Hurwitz criterion to equations of motion of the coupled system. . . . . 43

3.7 The first column of the Routh table which is obtained by applying Routh-Hurwitz criterion to error equation of the coupled system. . 44

3.8 The first column of the Routh table which is obtained by applying Routh-Hurwitz criterion to equations of motion of the coupled system. . . . . 47

3.9 The first column of the Routh table which is obtained by applying Routh-Hurwitz criterion to error equation of the coupled system. . 49

4.1 The first column of the Routh table which is obtained by applying Routh-Hurwitz criterion to error equation of the coupled system. . 64

4.2 The first column of the Routh table which is obtained by applying Routh-Hurwitz criterion to error equation of the coupled system. . 70

**Dedicated to my family and Türkan Çakmak.**

# Chapter 1

# INTRODUCTION

Synchronization, a phenomenon that is abundant in science, nature, engineering and social life, in its broadest context is the adjustment of rhythms of oscillating systems due to their weak interaction [1]. Systems such as clocks, singing crickets, cardiac pacemakers, firing neurons, and applauding audiences exhibit a tendency to operate in synchrony and in systems such as robot manipulators, secure communication networks, tele-operated machines, chemical reactions, computers with parallel architecture we desire synchronous operation [2]. These phenomena are universal and can be understood within a common framework based on nonlinear dynamics.

Synchronization phenomenon is widely encountered in the natural world, the chorusing of crickets, synchronous flash light in group of fire-flies, the metabolic synchronicity in yeast cell suspension, see [3]. From an engineering perspective the collective behavior of laser and power generator arrays is of special practical importance. Arrays of microwave oscillators and arrays of super-conducting Josephson junctions are another object of intensive research[2]. In mechanics, synchronization has found wide application in the construction of various

vibro-technical devices [4], robot manipulators [5, 6]. In radio-physics, radio-engineering, radiolocation, radio-measurements and radio-communication, synchronization is employed for frequency stabilization of generators, for synthesizing frequencies and demodulation of signals in Doppler systems, in exact time systems, by designing phase antenna arrays [7]. Several secure and efficient communication schemes are based on chaotic phase synchronization [8, 9]. In social life interpersonally coordinated processes that are organized in time, or sometimes even occur simultaneously, can be subsumed under the notion of synchronization [10].

Synchronization phenomena have been the subject of discussion in various research areas since the $17^{th}$ century, when the synchronization of two pendulum clocks attached to a common support beam was first discovered by Christiaan Huygens [11, 12]. In the middle of the nineteenth century Lord Rayleigh observed synchronization when two distinct but similar pipes sound in unison. A new stage in the investigation of synchronization was related to the development of electrical and radio engineering in the $20^{th}$ century when W. H. Eccles and J. H. Vincent discovered the synchronization property of a triode generator. Since then many interesting synchronization phenomena have been observed and reported in the literature [1]. Today Synchronization has become such a pervasive phenomenon that it is studied in a wide range of research fields and in this study the dynamics of in-phase synchronization of various coupled mechanical systems and master-slave synchronization of two ball hoppers are of interest.

The main concern of synchronization problem is the entrainment of all the sub-systems in such a way that they perform the desired task. This could be accomplished or observed in several ways [13]:

- In case of disconnected systems that present synchronous behavior this is referred to as natural synchronization, e.g. all precise clocks are synchronized in the frequency domain.

- When synchronization is achieved by proper interconnections, i.e. without any artificially introduced external action, then the systems in question are referred to as self-synchronized, e.g. the synchronization of celestial bodies, such as rotation of satellites around planets.

- When there exist external actions (input controls) and/or artificial interconnections then this type of synchronization is called as controlled-synchronization. Examples of this case are most of the practical applications of synchronization theory such as transmitter-receiver systems and synchronized oscillators in communications.

Synchronization phenomenon has various definitions in the literature and to generalize these definitions we introduce synchronization as follows:

Consider two continuous time dynamical systems,

$$\frac{dx}{dt} = f_1(t, x, y) \tag{1.1}$$
$$\frac{dy}{dt} = f_2(t, x, y)$$

Here, $x \in \Re^{d1}$ and $y \in \Re^{d2}$ are vectors that may have different dimensions. The sub-systems in eq.(1.1) are synchronized if there is a comparison function h such that:

$$||h[g(x), g(y)]|| = 0, \tag{1.2}$$

where $||.||$ is some norm, $g(x)$ and $g(y)$ are the measured properties of the systems such as the frequency or coordinates of the sub-systems[14]. In general terms, synchronization problem depends on the type of application that requires suitable properties and comparison functions. Different applications require different properties and comparison functions and those that are suitable for one application are often completely unsuitable for another. For example, the following comparison functions appear in the literature:

$$h[g(x), g(y)] = g(x) - g(y), \tag{1.3}$$

$$h[g(x), g(y)] = \lim_{t\to\infty} [g(x) - g(y)], \tag{1.4}$$

$$h[g(x), g(y)] = \lim_{T\to\infty} \frac{1}{T} \int_t^{t+T} [g(x(s)) - g(y(s))]ds, \tag{1.5}$$

and they all have different purposes. In this thesis we focus on passive and active controlled synchronization and consider (1.4) as our comparison function.

For the control point of view synchronization problem is solved by designing controllers and/or interconnections that guarantee synchronization of multi-composed systems with respect to a certain desired comparison function [15].

The controlled synchronization problem can be divided into two groups as active and passive controlled synchronization problem.

- In active controlled synchronization scheme the problem is to achieve synchronization with the use of external control input [16, 17, 18]. There are numerous ways to choose an appropriate controller to achieve synchronization in the literature. In [19], control of cooperative underactuated manipulators with PD+gravity compensation scheme is studied, in [18] a coupling scheme via a feedback loop with the controller composed of quadratic form is proposed to synchronize oscillators, in [20] feedforward and feedback control laws are designed to synchronize the phase of an oscillator, in [15] computed torque methodology is used to synchronize robotic and mechanical systems, in [16] synchronization of master-slave systems is achieved using non-linear control methods.

- In passive controlled synchronization scheme the problem is to achieve synchronization with the use of passive coupling components such as spring and damper.

In this thesis we mainly deal with passive controlled in-phase synchronization of simple pendulums and double pendulums under various coupling schemes and active controlled master-slave synchronization of two ball hoppers.

This thesis is organized as follows. In Chapter 2 we provide types and methods of synchronization in detail. Chapter 3 and Chapter 4 addresses the analytical analysis and simulation results of coupled simple pendulum and double pendulum, respectively. In Chapter 5 we provide simulation results of master-slave synchronization of two ball hoppers. Finally, we conclude the thesis in Chapter 6.

## 1.2 Contributions of the Thesis

We provide an extensive analysis on the in-phase synchronization of simple pendulums which are coupled under various coupling configurations of spring and damper. Such an extensive research, to the benefit our knowledge, is novel and our basic aim is to provide a simple guideline for passive synchronization of simple pendulum systems. To achieve the aforementioned goal starting with the two pendulums coupled with series spring-mass-damper case we analyze the coupled simple pendulums by using analytical methods and we also provide numerical simulation results which support our conclusions. We show analytically in coupled four pendulums case and numerically in coupled seven pendulums case that the pendulums are synchronized except for certain special cases. For example, we analytically show that for four pendulums case, if the damper is in the middle, and two springs on the right and on left of the damper have the same spring constant then the synchronization can not be achieved. This is in fact the only configuration in four pendulums case in which synchronization can not be achieved. We tried to generalize this idea to higher number of pendulums case and presented some numerical results. Then, we obtain bended matrix forms of system and error matrices of coupled $n$ pendulum system, but the analytical stability analysis of such a general coupled systems remains as an open problem.

Moreover, we investigate the role of spring and damper in synchronization process. While the spring element couples the pendulums, i.e. no effect on synchronization, the damper element synchronizes the pendulums by forcing the velocities of its connection points to be same.

We couple two double pendulums in two different configurations, i.e. from upper pendulums and from lower pendulums, and we show that for every positive system parameters, i.e. $k$, $c$, $m$, $l$, $l_0$, the upper pendulums coupled double pendulums are synchronized and for every positive system parameters except $l_0 = \frac{1}{\sqrt{2}} l$ the lower pendulums coupled double pendulums are also synchronized. We note that these results have been proven analytically, and some numerical simulation results have been added to support our claims.

Finally, we present synchronization of two ball hoppers in master-slave configuration under two different deadbeat gait controllers namely, fully-actuated controller and under-actuated controller. We obtain apex state synchronization between the hoppers by using fully-actuated deadbeat controller and we obtain meaningful apex position synchronization between the hoppers by using under-actuated deadbeat controller. We note that these results are rather novel and require further investigation.

# Chapter 2

# TYPES AND METHODS OF SYNCHRONIZATION

Since there are numerous synchronization applications and observations, various synchronization types exist in the literature [14]. In our researh we restricted the scope of the types of synchronization to practical applications. To achieve synchronization goal, defined by the comparison function, there exist several methods and we will mention about the widely used methods of synchronization in the literature.

## 2.1 Types of Synchronization

Many research fields consider the synchronization in different terms and there is not a unified definition or type of synchronization. Below we address the widely used types of synchronization.

### 2.1.1 Phase Synchronization

Phase synchronization is defined as the appearance of a certain relation between the phases of interacting systems while the amplitudes remain uncorrelated[21, 22]. Since there is not a common definition of phase for regular and chaotic systems, we need to define the phase and phase syncronization based on the application. For regular systems there exist several phase definitions. Consider the equation of motion of the simple harmonic motion,

$$m\frac{d^2x}{dt^2} + kx = 0. \tag{2.1}$$

The solution of the differential equation is,

$$x(t) = Acos(wt + \phi(0)). \tag{2.2}$$

Here $A$ and $\phi(0)$ are determined by the initial conditions of the system. For this periodical solution the phase is defined as,

$$\phi(t) = wt + \phi(0). \tag{2.3}$$

In certain mechanical systems, phase is defined to be the state parameter of the system such as position, velocity and rotational angle [23].

In non-linear systems phase is defined by using the phase-space of the system as,

$$\phi(t) = tan^{-1}\frac{\dot{x}(t)}{x(t).} \tag{2.4}$$

where $x(t)$ is the variable which is of interest, and $\dot{x}(t)$ is its time derivative see e.g. [11].

In limit cycle oscillators phase is defined by the use of limit cycle differential equation as [11], [24]:

$$\dot{\phi}(t) = w. \tag{2.5}$$

and the phase of the system is,

$$\phi(t) = wt + \phi(0). \tag{2.6}$$

For the coupled limit cycle oscillators,which are also used in network synchronization, phase equations are as follows:

$$\dot{\phi_1}(t) = w_1 + h_1(\phi_1, \phi_2), \tag{2.7}$$

$$\dot{\phi_2}(t) = w_2 + h_2(\phi_1, \phi_2), \tag{2.8}$$

and phases are determined once the coupling functions $h_1(\phi_1, \phi_2)$ and $h_2(\phi_1, \phi_2)$ are chosen.

For Chaotic system synchronization see [21].

Phase synchronization is widely used in synchronization of chaotic systems and in secure communication system for receiver-transmitter efficiency.

### 2.1.2 Full Synchronization

Full synchronization is defined as the synchronization of both phase and amplitude of the systems. Full synchronized systems behave in unision. Let $\theta_1(t)$ and $\theta_2(t)$ be the state variables of the systems. In this case if,

$$\lim_{t\to\infty} \theta_1(t) - \theta_2(t) = 0, \tag{2.9}$$

then the systems are in-phase synchronized and if,

$$\lim_{t\to\infty} \theta_1(t) + \theta_2(t) = 0, \tag{2.10}$$

then the systems are anti-phase synchronized[23]. Both types are used in mechanical systems and robotic systems [15], [23].

### 2.1.3 Frequency Synchronization

Frequency synchronization is the entrainment of frequencies of the systems while phases are independent. Let $w_x$ and $w_y$ be the frequencies of the systems, $n_x$ and $n_y$ be some integers. If,

$$n_x w_x - n_y w_y = 0, \tag{2.11}$$

then the frequencies of the systems are synchronized[14]. This type of synchronization is widely used in communication systems.

### 2.1.4 Network Synchronization

Network synchronization is the entrainment of large populations of interacting elements and it is the subject of intense research efforts in physical, biological, chemical, and social systems. A successful approach to the problem of network synchronization, called Kuramoto Model Approach, consists of modeling each member of the population as a phase oscillator. In this way the dynamics of the coupled complex system is reduced and synchronized. The Kuramoto model consists of a population of $N$ coupled phase oscillators $\theta_i(t)$ having natural frequencies $w_i$ distributed with a given probability density $g(w)$, and whose dynamics are governed by:

$$\theta_i' = w_i + \sum_{j=1}^{N} K_{ij} \sin(\theta_j - \theta_i), i = 1, ..., N. \tag{2.12}$$

Thus each oscillator tries to run independently at its own frequency, while the coupling tends to synchronize it to all the others [25]. Network synchronization is widely used in laser arrays, neural networks and chemical oscillators [1].

## 2.2 Methods Of Synchronization

Nowadays, the developments in technology and the requirements on efficiency and quality in production processes have resulted in complex and integrated production systems. In actual production processes such as manufacturing, automotive applications, and teleoperation systems there is a high requirement on flexibility and manoeuvrability of the involved systems. In most of these processes the use of integrated and multi-composed systems is widely spread, and their variety in uses is practically endless; assembling, transporting, painting, welding, just to mention few. All these tasks require large manoeuvrability and manipulability of the executing systems, often even some of the tasks can not be carried out by a single system. In those cases the use of multi-composed systems has been considered as an option. A multi-composed system is a group of individual systems, either identical or different, that work together to execute a task. On the other hand for mechanical systems that require flexibility and manoeuvrability, synchronization is of great importance and these cooperative behaviours can not be achieved by an individual system, e.g. multi finger robot-hands, multi robot systems and multi-actuated platforms [26], [6], teleoperated master-slave systems [27], [28]. In medicine, master-slave teleoperated systems are used in surgery giving rise to more precise and less invasive surgery procedures [29], [30]. In aerospace applications coordination schemes are used to minimize the error of the relative attitude in formations of satellites [31], [32]. The case of group formation of multiple robotic vehicles is addressed in [33].

As we have mentioned before there exist many synchronization applications and observations and as a result numerous methods are applied to these types of synchronization. In this study we constrain our research to the methods which are applied widely in mechanical systems. Methods of synchronizations that are applied to mechanical systems are as follows:

### 2.2.1 Active Controlled Synchronization

The synchronization goal is achieved by designing controllers and/or interconnections that guarantee the synchronous behaviour. In other words, by applying external force, torque generated via feedforward and/or feedback controllers, the synchronization is achieved. Depending on the formulation of the controlled synchronization problem distinction should be made between mutual (internal) synchronization and master-slave (external) synchronization.

- In the first and most general case, all synchronized objects occur on equal terms in the unified multi-composed system. Therefore the synchronous motion occurs as the result of interaction of all elements of the system, e.g. coupled synchronized oscillators, cooperative systems [15].

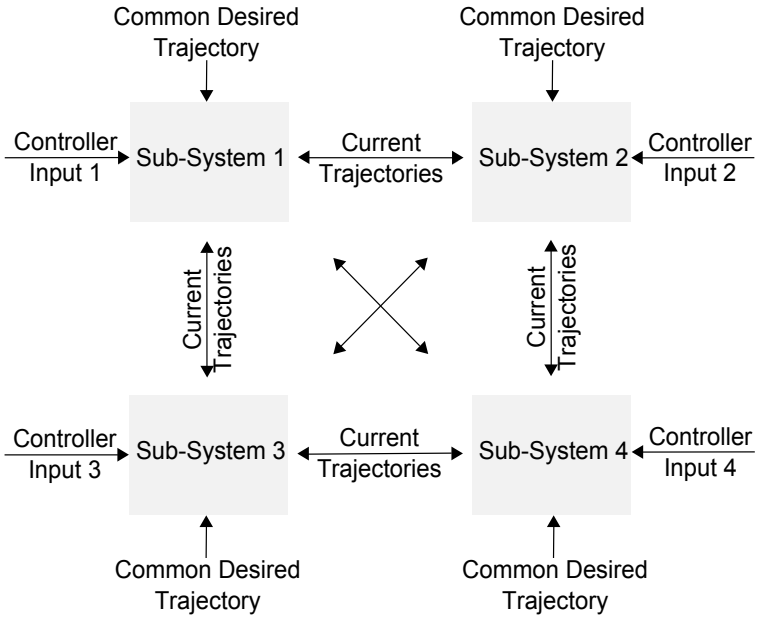


Figure 2.1: Mutual Synchronization of Subsystems

- In the second case, it is supposed that one object in the multi-composed system is more powerful than the others and its motion can be considered

as independent of the motion of the other objects. Therefore the resulting synchronous motion is predetermined by this dominant independent system, e.g. master-slave systems, coordinated system [15].

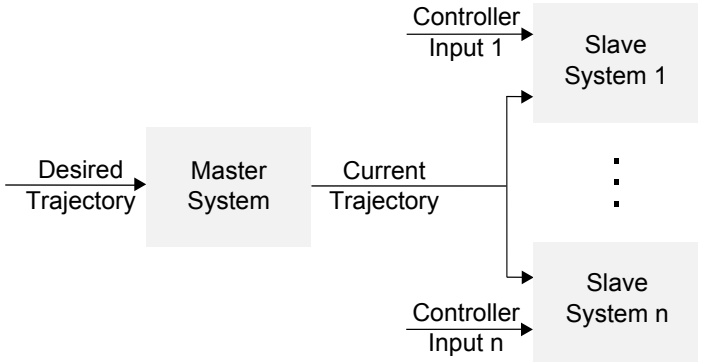


Figure 2.2: Master-Slave Synchronization of Subsystems

### 2.2.2 Passive Controlled Synchronization

Synchronization goal is achieved by using passive coupling elements. No controller is designed and no externel force or torque is applied to synchronize the systems in hand. Such couplings are torsional and translational spring and torsional and translational damper [34].

# Chapter 3

# PASSIVE CONTROLLED IN-PHASE SYNCHRONIZATION OF COUPLED SIMPLE PENDULUMS

In this chapter we will investigate the synchronization dynamics of simple pendulums under various coupling schemes and present equations of motion, linearized system and error equation analysis and stability analysis. The aims of this Chapter are listed as follows:

- The basic aim of this Chapter is to achieve in-phase synchronization between single pendulums by coupling them with various spring-damper combinations and to provide a generalized formula or a guideline that guarantees the synchronization of $n$ pendulums which are coupled with a single damper and $n-2$ springs.

- We want to reveal the role of spring and damper in synchronization process.
- We expect to observe in-phase synchronization between coupled simple pendulums for any positive system parameters and we want to support our findings by using both analytical and numerical analysis.

Starting from the analysis of two pendulums coupled with series spring-mass-damper, we proceed with two pendulums coupled with series spring-damper. Then we analyze two pendulums coupled with parallel spring-damper in normal and oblique forms. Afterwards we analyze three or more pendulums coupled with spring-damper combinations. Throughout the chapter we use several methods and make several assumptions as listed below:

- We use small angle approximation for linearization of equations of motion, i.e. we restrict the pendulum angles not to exceed $10^{\circ}$.
- We assume that the spring and damper compresses and decompresses only in the horizontal direction.
- All of the components in this study are assumed to be frictionless.
- We assume that pendulum rod, spring and damper are weightless.
- Equations of motion are obtained by using both free body diagrams and by Lagrangians.
- For stability analysis Routh-Hurwitz criterion is widely used.
- Simulations are obtained by using the nonlinear equations of motion of the systems under consideration in Matlab environment.

## 3.1 Two Pendulums Coupled with Series Spring-Mass-Damper

Consider the system shown in the Figure 3.1. We couple two pendulums from point $l_0$ with series connected spring, mass and damper and analyze the synchronization dynamics. Suppose that the mass is attached to the beam with a weightless string which does not exert torque but forces the mass to move only in the horizontal direction. Here $k$ is the spring stiffness, $c$ is damping coefficient, $\theta_1$ and $\theta_2$ are pendulum angles and $x$ is the connection point of spring and damper with mass. Let $m_1$, $l_1$, $m_2$, $l_2$ denote the mass and length of the pendulums, respectively. By using either free-body diagrams or performing Lagrangian method, we obtain the following equations of motion:

$$m_1 l_1^2 \ddot{\theta}_1 + m_1 g l_1 \sin\theta_1 + k l_0 \cos\theta_1 (l_0 \sin\theta_1 - x) = 0, \tag{3.1}$$

$$M\ddot{x} - k(l_0 \sin\theta_1 - x) + c(\dot{x} - l_0 \cos\theta_2 \dot{\theta}_2) = 0, \tag{3.2}$$

$$m_2 l_2^2 \ddot{\theta}_2 + m_2 g l_2 \sin\theta_2 - c l_0 \cos\theta_2 (\dot{x} - l_0 \cos\theta_2 \dot{\theta}_2) = 0. \tag{3.3}$$

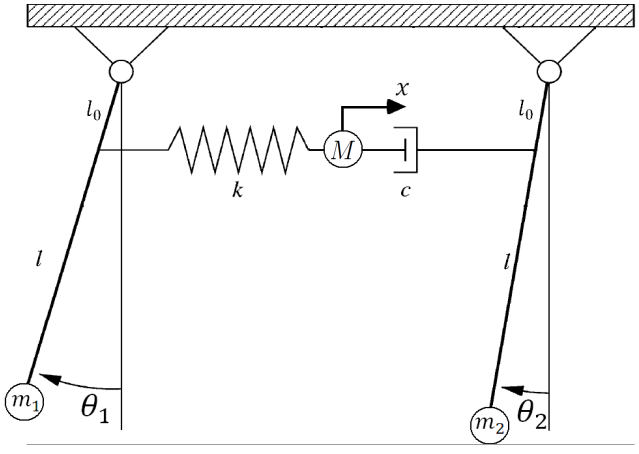


Figure 3.1: Two Double Pendulums Coupled with Series Spring-Mass-Damper

Next, we define the state variables of this system as,

$$z = \begin{bmatrix} \theta_1 & \dot{\theta}_1 & x & \dot{x} & \theta_2 & \dot{\theta}_2 \end{bmatrix}^T. \tag{3.4}$$

Now let assume $m_1 = m_2 = m$, $l_1 = l_2 = l$, which is reasonable for synchronization, i.e. we assume the synchronization of two identical pendulums. When we linearize the equations of motion around the equilibrium point $z = 0$, the linearized equations of motion of the system can be written in matrix form as $\dot{z} = Az$ and $A$ is given as follows:

$$A = \begin{bmatrix} 0 & 1 & 0 & 0 & 0 & 0 \\ -\frac{g}{l} - \frac{kl_0^2}{ml^2} & 0 & \frac{kl_0}{ml^2} & 0 & 0 & 0 \\ 0 & 0 & 0 & 1 & 0 & 0 \\ \frac{kl_0}{m} & 0 & -\frac{k}{m} & -\frac{c}{m} & 0 & -\frac{cl_0}{m} \\ 0 & 0 & 0 & 0 & 0 & 1 \\ 0 & 0 & 0 & \frac{cl_0}{ml^2} & -\frac{g}{l} & -\frac{cl_0^2}{ml^2} \end{bmatrix}. \tag{3.5}$$

Instead of obtaining error equations, applying Routh-Hurwitz criterion to equations of motion for this system is more appropriate. In order to obtain the Routh array, the coefficients of characteric equation of the matrix $A$ is used and the first column of the Routh array is given as:

| | |
|---|---|
| $s^6$ | $1$ |
| $s^5$ | $\frac{c(l^2+l_0^2)}{ml^2}$ |
| $s^4$ | $\frac{kl^3+gl_0^2m}{ml^3+ll_0^2m}$ |
| $s^3$ | $\frac{cl_0^2(2k^2l^2+k^2l_0^2-2gklm+g^2m^2)}{m^2l(kl^3+gl_0^2m)}$ |
| $s^2$ | $\frac{gk(2k^2l^4+2k^2l^2l_0^2+k^2l_0^4-2gkl^3m-gkl_0^2m+(glm)^2)}{ml^3(2k^2l^2+k^2l_0^2-2gklm+g^2m^2)}$ |
| $s^1$ | $\frac{gk^3cl^6}{m^2l^3(2k^2l^4+2k^2l^2l_0^2+k^2l_0^4-2gkl^3m-gkl_0^2m+(glm)^2)}$ |
| $s^0$ | $\frac{kg^2}{ml^2}$ |

Table 3.1: The first column of the Routh table which is obtained by applying Routh-Hurwitz criterion to equations of motion of the coupled system.

After straightforward calculations, it can be shown that all the elements in the first column of Routh array are positive. This analysis is given in the appendix. This shows that the linearized system is exponentially stable, hence the original system given by (3.1)-(3.3) is also locally exponentially stable, i.e. if $z(0)$ is sufficiently small then $z(t) \to 0$, as $t \to \infty$. This is because of the mass we connected between spring and damper. Our simulation results support our findings. In the next section we extract this mass and achieve meaningful synchronization. Typical simulation results for pendulum angles and error between pendulum angles are given in Figures 3.2 and 3.3.

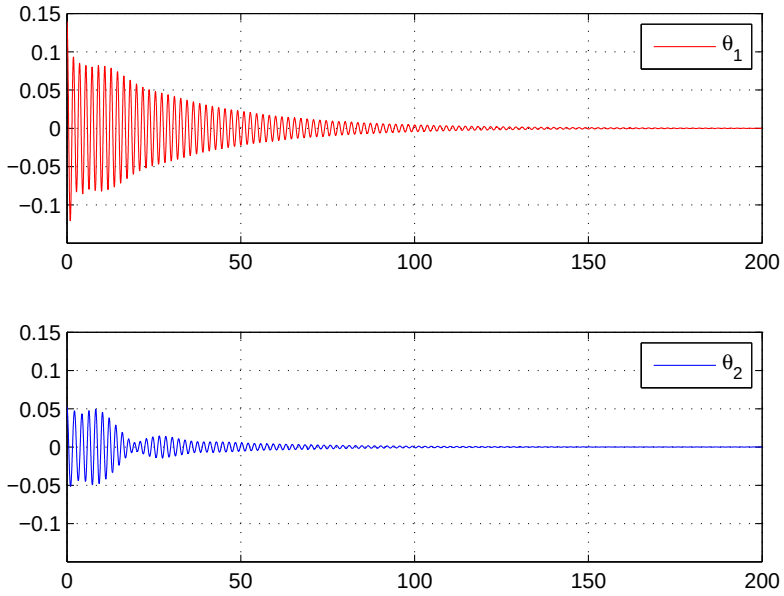


Figure 3.2: Simulation of two pendulums coupled with spring, mass, damper. We choose $m_1 = m_2 = 1,\ k = 5,\ c = 1,\ l = 1,\ l_0 = 0.5,\ \theta_1(0) = 8°,\ \dot{\theta}_1(0) = 0°,\ \theta_2(0) = 3°,\ \dot{\theta}_2(0) = 0°,\ x(0) = 0,\ \dot{x}(0) = 0$ for simulation purposes.

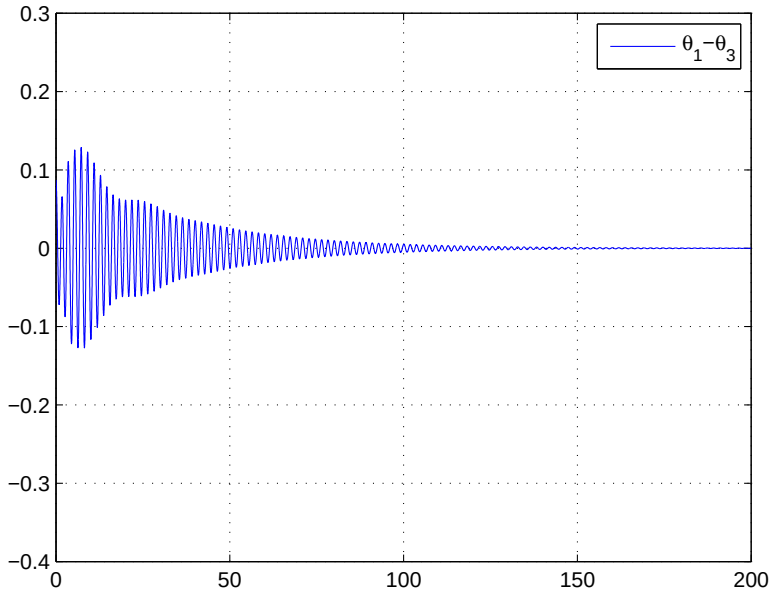


Figure 3.3: Error simulation of two pendulums coupled with spring, mass, damper. We choose the above parameters for simulation purposes.

## 3.2 Two Pendulums Coupled with Series Spring-Damper

Consider the system shown in the Figure 3.4. We couple two pendulums from point $l_0$ with series connected spring and damper and analyze the synchronization dynamics. Here $k$ is the spring stiffness, c is damping coefficient, $\theta_1$ and $\theta_2$ are pendulum angles and $x$ is the connection point of spring and damper. Let $m_1$, $l_1$, $m_2$, $l_2$ denote the mass and length of the pendulums, respectively. By using either free-body diagrams or performing Lagrangian method, we obtain the following equations of motion:

$$m_1 l_1^2 \ddot{\theta}_1 + m_1 g l_1 \sin\theta_1 + k l_0 \cos\theta_1 (l_0 \sin\theta_1 - x) = 0, \tag{3.6}$$

$$k(l_0 \sin\theta_1 - x) - c(\dot{x} - l_0 \cos\theta_2 \dot{\theta}_2) = 0, \tag{3.7}$$

$$m_2 l_2^2 \ddot{\theta}_2 + m_2 g l_2 \sin\theta_2 - c l_0 \cos\theta_2 (\dot{x} - l_0 \cos\theta_2 \dot{\theta}_2) = 0. \tag{3.8}$$

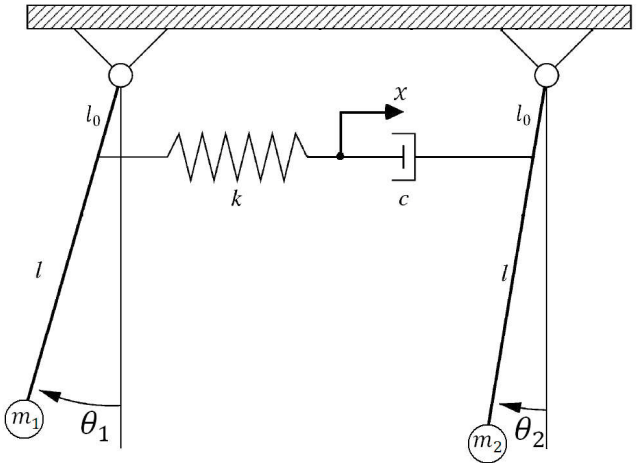


Figure 3.4: Two Double Pendulums Coupled with Series Spring-Damper

Note that we can also obtain (3.6)-(3.8) from (3.1)-(3.3) by simply using $M = 0$. Let us define the following state variables for this system,

$$z = \begin{bmatrix} \theta_1 & \dot{\theta}_1 & x & \theta_2 & \dot{\theta}_2 \end{bmatrix}^T. \tag{3.9}$$

Now let us assume $m_1 = m_2 = m$, $l_1 = l_2 = l$, which is reasonable for synchronization, i.e. we assume the synchronization of two identical pendulums. By linearizing the equations of motion around $z = 0$ we write the equations of motion in $\dot{z} = Az$ form and $A$ is given as:

$$A = \begin{bmatrix} 0 & 1 & 0 & 0 & 0 \\ -\frac{g}{l} - \frac{kl_0^2}{ml^2} & 0 & \frac{kl_0}{ml^2} & 0 & 0 \\ \frac{kl_0}{c} & 0 & -\frac{k}{c} & 0 & l_0 \\ 0 & 0 & 0 & 0 & 1 \\ \frac{kl_0^2}{ml^2} & 0 & -\frac{kl_0}{ml^2} & -\frac{g}{l} & 0 \end{bmatrix}. \tag{3.10}$$

Applying Routh-Hurwitz criterion to the characteristic equation of matrix $A$ we have the first column as in Table 3.2. As it is seen from the Table 3.2, the system is stable as long as $k, c, l_0, l, m$ parameters are positive. Two roots are on the imaginary axis and three roots are on the left half plane. While the roots on the left half plane stabilizes the pendulums, roots on the imaginary axis forces the pendulums oscillate without damping. For further analysis consider the following error dynamics analysis.

| | |
|---|---|
| $s^5$ | $1$ |
| $s^4$ | $\frac{k}{c}$ |
| $s^3$ | $\frac{2kl_0^2}{ml^2}$ |
| $s^2$ | $\frac{gk}{lc}$ |
| $s^1$ | $\epsilon$ |
| $s^0$ | $\frac{g^2k}{l^2c}$ |

Table 3.2: The first column of the Routh table which is obtained by applying Routh-Hurwitz criterion to equations of motion of the coupled system.

Since this system have rotational ($\theta_1$, $\theta_2$) and translational ($x$) generalized coordinates, the error equation, defined as the difference between pendulum angles $z_e = [\theta_1 - \theta_2,\ \dot{\theta}_1 - \dot{\theta}_2]$, can not be written in the $\dot{z}_e = A_e z_e$ form, where $z_e = [\theta_1 - \theta_2,\ \dot{\theta}_1 - \dot{\theta}_2]^T$. In this case we define new state variables for error dynamics and apply similarity transformation to matrix $A$ as follows:

$$\hat{z}_e = \begin{bmatrix} \theta_1 - \theta_2, & \dot{\theta}_1 - \dot{\theta}_2, & x, & \theta_2, & \dot{\theta}_2 \end{bmatrix}^T, \tag{3.11}$$

$$\dot{\hat{z}}_e = TAT^{-1}\hat{z}_e = \hat{A}\hat{z}_e. \tag{3.12}$$

where the transformation matrix is,

$$T = \begin{bmatrix} 1 & 0 & 0 & -1 & 0 \\ 0 & 1 & 0 & 0 & -1 \\ 0 & 0 & 1 & 0 & 0 \\ 0 & 0 & 0 & 1 & 0 \\ 0 & 0 & 0 & 0 & 1 \end{bmatrix}. \tag{3.13}$$

For simplicity we define the following parameter:

$$K = \frac{kl_0}{ml^2}. \tag{3.14}$$

Then $\hat{A}$ given by (3.12) can be computed as:

$$\hat{A} = \begin{bmatrix} 0 & 1 & 0 & 0 & 0 \\ -\frac{g}{l} - 2Kl_0 & 0 & 2K & -2Kl_0 & 0 \\ \frac{kl_0}{c} & 0 & -\frac{k}{c} & \frac{kl_0}{c} & l_0 \\ 0 & 0 & 0 & 0 & 1 \\ Kl_0 & 0 & -K & Kl_0 - \frac{g}{l} & 0 \end{bmatrix}. \tag{3.15}$$

Now let us seperate $\hat{z}_e \in \Re^5$ as $\hat{z}_e = [\hat{z}_{e1}\ \hat{z}_{e2}]^T$ where $\hat{z}_{e1}^T = [e\ \dot{e}]$, $\hat{z}_{e2}^T = [x\ \theta_2\ \dot{\theta}_2]$. Then,

$$\dot{\hat{z}}_{e1} = \hat{A}_{11}\hat{z}_{e1} + \hat{A}_{12}\hat{z}_{e2}, \tag{3.16}$$

$$\dot{\hat{z}}_{e2} = \hat{A}_{21}\hat{z}_{e1} + \hat{A}_{22}\hat{z}_{e2}, \tag{3.17}$$

where

$$\hat{A}_{11} = \begin{bmatrix} 0 & 1 \\ -\frac{g}{l} - 2Kl_0 & 0 \end{bmatrix}, \tag{3.18}$$

$$\hat{A}_{12} = \begin{bmatrix} 0 & 0 & 0 \\ 2K & -2Kl_0 & 0 \end{bmatrix}, \tag{3.19}$$

$$\hat{A}_{21} = \begin{bmatrix} \frac{kl_0}{c} & 0 \\ 0 & 0 \\ Kl_0 & 0 \end{bmatrix}, \tag{3.20}$$

$$\hat{A}_{22} = \begin{bmatrix} -\frac{k}{c} & \frac{kl_0}{c} & l_0 \\ 0 & 0 & 1 \\ -K & Kl_0 - \frac{g}{l} & 0 \end{bmatrix}. \tag{3.21}$$

Differentiating (3.16) and using (3.18)-(3.21) we obtain:

$$\begin{aligned} \ddot{\hat{z}}_{e1} &= \hat{A}_{11}\dot{\hat{z}}_{e1} + \hat{A}_{12}\dot{\hat{z}}_{e2}, \\ &= \hat{A}_{11}\dot{\hat{z}}_{e1} + \hat{A}_{12}(\hat{A}_{21}\hat{z}_{e1} + \hat{A}_{22}\hat{z}_{e2}), \\ &= \hat{A}_{11}\dot{\hat{z}}_{e1} + \hat{A}_{12}\hat{A}_{21}\hat{z}_{e1} + \hat{A}_{12}\hat{A}_{22}\hat{z}_{e2}. \end{aligned} \tag{3.22}$$

On the other hand from (3.19) and (3.21) we obtain:

$$\hat{A}_{12}\hat{A}_{22} = \begin{bmatrix} 0 & 0 & 0 \\ -2K\frac{k}{c} & 2Kl_0\frac{k}{c} & 0 \end{bmatrix} = -\frac{k}{c}A_{12}. \tag{3.23}$$

Using (3.16) and (3.23) in (3.22), we obtain:

$$\ddot{\hat{z}}_{e1} = \hat{A}_{11}\dot{\hat{z}}_{e1} + \hat{A}_{12}\hat{A}_{21}\hat{z}_{e1} - \frac{k}{c}(\dot{\hat{z}}_{e1} - \hat{A}_{11}\hat{z}_{e1}), \tag{3.24}$$

$$= (\hat{A}_{11} - \frac{k}{c}I)\dot{\hat{z}}_{e1} + (\hat{A}_{12}\hat{A}_{21} + \frac{k}{c}\hat{A}_{11})\hat{z}_{e1}.$$

By using (3.18), we obtain:

$$\hat{A}_{11} - \frac{k}{c}I = \begin{bmatrix} -\frac{k}{c} & 1 \\ -2Kl_0 - \frac{g}{l} & -\frac{k}{c} \end{bmatrix}, \tag{3.25}$$

$$\hat{A}_{12}\hat{A}_{21} + \frac{k}{c}\hat{A}_{11} = \begin{bmatrix} 0 & 0 \\ -2Kl_0\frac{k}{c} - \frac{g}{l} & 0 \end{bmatrix} + \frac{g}{l}\hat{A}_{11} = \begin{bmatrix} 0 & \frac{k}{c} \\ -\frac{g}{l}\frac{k}{c} & 0 \end{bmatrix}. \tag{3.26}$$

Using (3.25) and (3.26) in (3.24), we obtain the following error equation for $\hat{z}_{e1}$:

$$\ddot{\hat{z}}_{e1} - (\hat{A}_{11} - \frac{k}{c})\dot{\hat{z}}_{e1} - (\hat{A}_{12}\hat{A}_{21} + \frac{k}{c}\hat{A}_{11})\hat{z}_{e1} = 0, \tag{3.27}$$

$$\ddot{\hat{z}}_{e1} + \begin{bmatrix} \frac{k}{c} & -1 \\ 2Kl_0 + \frac{g}{l} & \frac{k}{c} \end{bmatrix}\dot{\hat{z}}_{e1} + \begin{bmatrix} 0 & \frac{k}{c} \\ \frac{g}{l}\frac{k}{c} & 0 \end{bmatrix}\hat{z}_{e1} = 0.$$

Since $\hat{z}_{e1} = [e\ \dot{e}]^T$, from the first row of (3.27), we obtain $\ddot{e} - \ddot{e} = 0$, which is trivially true. From the second row, we obtain:

$$e^{(3)} + \frac{k}{c}e^{(2)} + (2Kl_0 + \frac{g}{l})e^{(1)} + \frac{g}{l}\frac{k}{c}e = 0. \tag{3.28}$$

The characteristic polinomial of (3.28) can be given as:

$$p(s) = s^3 + \frac{k}{c}s^2 + (2Kl_0 + \frac{g}{l})s + \frac{g}{l}\frac{k}{c}. \tag{3.29}$$

By using Routh-Hurwitz criterion, we have the Routh array as in Table 3.2. Since the first column contains positive elements, it follows that (3.29) is a Hurwitz polinomial, hence the linearized error dynamics given by (3.28) is stable. We can summarize there results in the following theorem.

| | |
|---|---|
| $s^3$ | $1$ |
| $s^2$ | $\frac{k}{c}$ |
| $s^1$ | $\frac{2Kl_0c}{k}$ |
| $s^0$ | $\frac{g}{l}\frac{k}{c}$ |

Table 3.3: The first column of the Routh table which is obtained by applying Routh-Hurwitz criterion to equations of motion of the coupled system.

**Theorem1** : Consider the system given by (3.6)-(3.8). Let us define $e = \theta_1 - \theta_2$. Then the error dynamics are locally exponentially stable, i.e. if $|e(0)|$ and $|\dot{e}(0)|$ are sufficiently small, then both $e(t)$ and $\dot{e}(t)$ converges to zero exponentially fast.

**Proof** : Result follows from the linearization of (3.6)-(3.8) given by (3.9) and (3.10), the error dynamics given by (3.28), and the standard Lyapunov stability arguments, see e.g. [35].

Now let us consider the behaviour of the remaining dynamics given by (3.6)-(3.8) in review of Theorem 1. Let us define $\theta = \theta_1$, then by using $e = \theta_1 - \theta_2$ we obtain $\theta_2 = \theta - e$. Furthermore, let us define a new variable $w$ as follows:

$$w = x - l_0 \sin\theta. \tag{3.30}$$

By using (3.30) in (3.7), we obtain:

$$c\dot{w} + kw = f_0(t), \tag{3.31}$$

where $f_0(t)$ is a function which depends on $e$ and $\dot{e}$ such that $|f_0(t)| < M_1 e^{-\alpha_1 t}$ for some $M_1 > 0$ and $\alpha_1 > 0$. It follows from (3.31) that $w(t) \to 0$ exponentially fast. Moreover, the decay rate of the homogeneous part of (3.31) is given by $-\frac{k}{c}$. By using these in (3.6) and (3.8), we obtain:

$$\ddot{\theta}_i + \frac{g}{l}\sin\theta_i = f_i(t), \quad i = 1, 2. \tag{3.32}$$

where $f_i(t)$ is an appropriate exponentially decaying function which depends on $e$, $\dot{e}$ and $w$. Hence if $e(0)$, $\dot{e}(0)$ and $w(0)$ are sufficiently small, $f_i(t)$ is sufficiently

small as well. This shows that the solution of (3.32) are bounded provided that the initial conditions indicated above are sufficiently small. Moreover, as $t \to \infty$ we have $f_i(t) \to 0$ hence the dynamics of (3.32) converges to the dynamics of,

$$\ddot{\theta}_i + \frac{g}{l} \sin \theta_i = 0, \tag{3.33}$$

i.e. asymptotically each pendulum exhibits standard uncoupled pendulum behaviours. Combining these, we obtain the following result.

**Theorem2** : Consider the system given by (3.6)-(3.8). Let us define the set $\mathcal{S}$ as follows:

$$\mathcal{S} = \{y \in \Re^5 |\ \theta_1 = \theta_2 = \theta,\ \dot{\theta}_1 = \dot{\theta}_2 = \dot{\theta},\ w = x - l_0 \sin \theta = 0\}. \tag{3.34}$$

If $|e(0)|$, $|\dot{e}(0)|$ and $w(0)$ are sufficiently small, then all solutions of (3.6)-(3.8) converges to $\mathcal{S}$ exponentially fast, moreover $\theta_i$ variables satisfy the dynamics given by (3.33).

**Proof** : Since the solutions of (3.6)-(3.8) are bounded the $w$-limit set is well defined and invariant. It also follows that $w$-limit set is a subset of $\mathcal{S}$ given by (3.35). Then the result follows from standard stability arguments, e.g. LaSalle's invarance argument, see e.g. [35].

To further support the results given by Theorem 2 consider the linearized dynamics given by (3.12) and (3.15)-(3.21). Since $e$ and $\dot{e}$ are locally exponentially stable, to study the dynamics of $\hat{z}_{e1}$, we may consider the following equation:

$$\dot{\hat{z}}_{e2} = \hat{A}_{22} \hat{z}_{e2}. \tag{3.35}$$

The behaviour of $\hat{z}_{e2} = [x, \theta_2, \dot{\theta}_2]^T$ is determined by the roots of $\hat{A}_{22}$. After simple calculation we obtain:

$$\hat{p}(s) = det(\lambda I - \hat{A}_{22}) = s^3 + \frac{k}{c} s^2 + \frac{g}{l} s + K \frac{g}{l}, \tag{3.36}$$

$$= (\lambda + \frac{k}{c})(\lambda^2 + \frac{g}{l}). \tag{3.37}$$

Note that the root $-\frac{k}{c}$ corresponds to the decay rate of $w$ given by (3.31), and the complex roots of $\pm j\sqrt{\frac{g}{l}}$ corresponds to the linearized pendulum oscillation frequency. Typical simulation results are given in Figures 3.5 and 3.6.

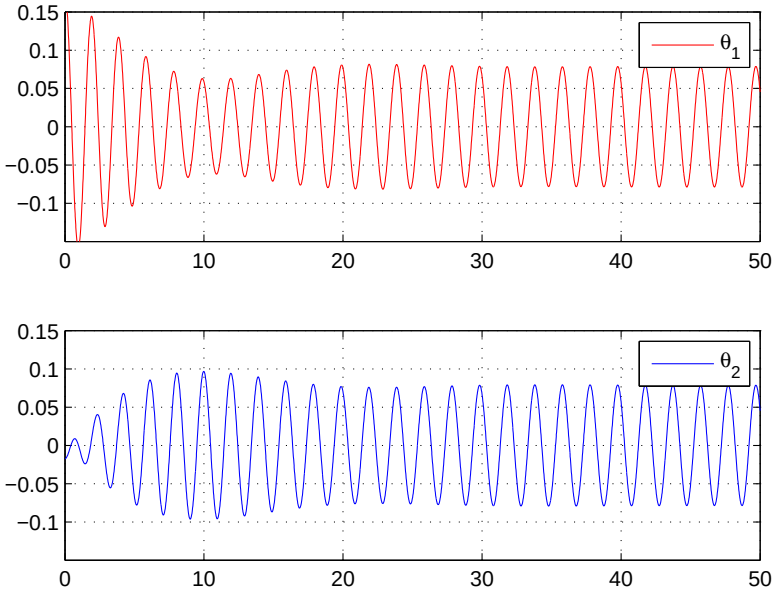


Figure 3.5: Simulation of two pendulums coupled with series spring and damper. We choose $m_1 = m_2 = 1,\ k = 2,\ c = 1,\ l = 1,\ l_0 = 0.75,\ \theta_1(0) = 10°,\ \dot{\theta}_1(0) = 0°,\ \theta_2(0) = -1°,\ \dot{\theta}_2(0) = 0°,\ x(0) = 0$ for simulation purposes.

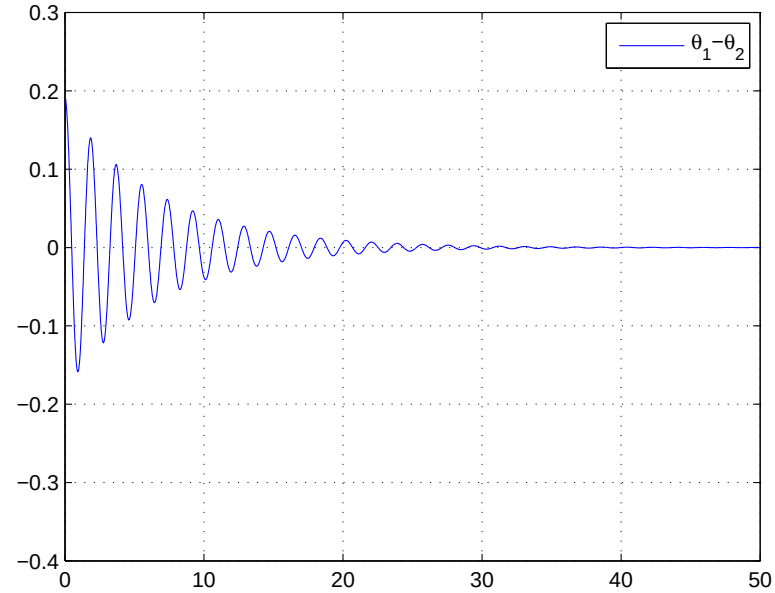


Figure 3.6: Error simulation of two pendulums coupled with series spring and damper. We choose the above parameters for simulation purposes.

Here we simulated the nonlinear system given in equations (3.6)-(3.8) for the below mentioned parameter values. It is clear from Figures 3.5 and 3.6 that,

- Pendulums are synchronized, i.e. $\lim_{t\to\infty} \theta_1(t) - \theta_2(t) = 0$
- $\theta_1(t)$ and $\theta_2(t)$ converges to their natural oscillating frequencies.

## 3.3 Two Pendulums Coupled with Parallel Spring-Damper

Consider the system shown in the Figure 3.7. We couple two pendulums from point $l_o$ with parallel connected spring and damper and analyze the synchronization dynamics. Let $m_1$, $l_1$, $m_2$, $l_2$ denote the mass and length of the pendulums, respectively. By using either free-body diagrams or performing Lagrangian method, we obtain the following equations of motion:

$$m_1 l_1^2 \ddot{\theta}_1 + m_1 g l_1 \sin\theta_1 + k l_o^2 \cos\theta_1(\sin\theta_1 - \sin\theta_2) + c l_0^2 \cos\theta_1(\cos\theta_1\dot{\theta}_1 - \cos\theta_2\dot{\theta}_2) = 0, \tag{3.38}$$

$$m_2 l_2^2 \ddot{\theta}_2 + m_2 g l_2 \sin\theta_2 - k l_o^2 \cos\theta_2(\sin\theta_1 - \sin\theta_2) - c l_0^2 \cos\theta_2(\cos\theta_1\dot{\theta}_1 - \cos\theta_2\dot{\theta}_2) = 0. \tag{3.39}$$

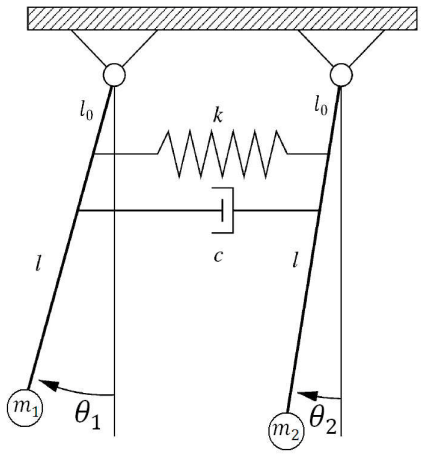


Figure 3.7: Two Double Pendulums Coupled with Parallel Spring-Damper

Now let us assume $m_1 = m_2 = m$, $l_1 = l_2 = l$, which is reasonable for synchronization, i.e. we assume the synchronization of two identical pendulums. Let us define state variables for this system as $z = \begin{bmatrix} \theta_1 & \dot{\theta}_1 & \theta_2 & \dot{\theta}_2 \end{bmatrix}$. Linearizing the equations around $z = 0$ we have $\dot{z} = Az$ and $A$ is given as follows:

$$A = \begin{bmatrix} 0 & 1 & 0 & 0 \\ -\frac{g}{l} - \frac{kl_0^2}{ml^2} & -\frac{cl_0^2}{ml^2} & \frac{kl_0^2}{ml^2} & \frac{cl_0^2}{ml^2} \\ 0 & 0 & 0 & 1 \\ \frac{kl_0^2}{ml^2} & \frac{cl_0^2}{ml^2} & -\frac{g}{l} - \frac{kl_0^2}{ml^2} & -\frac{cl_0^2}{ml^2} \end{bmatrix}. \tag{3.40}$$

The stability analysis for this system is performed by using eigenvalue analysis to the characteristic equation of the matrix $A$. The eigenvalues of the matrix $A$ can be given as:

$$s_1 = \sqrt{\frac{g}{l}}j, \tag{3.41}$$

$$s_2 = -\sqrt{\frac{g}{l}}j, \tag{3.42}$$

$$s_3 = -\frac{cl_0^2}{ml^2} - \sqrt{(\frac{cl_0^2}{ml^2})^2 - \frac{2kl_0^2}{ml^2} - \frac{g}{l}}, \tag{3.43}$$

$$s_4 = -\frac{cl_0^2}{ml^2} + \sqrt{(\frac{cl_0^2}{ml^2})^2 - \frac{2kl_0^2}{ml^2} - \frac{g}{l}}. \tag{3.44}$$

The eigenvalues $s_1$ and $s_2$, which are on the imaginary axis, force the pendulums to oscillate without damping and the eigenvalues $s_3$ and $s_4$, which are on the left half plane since the parameters $k$, $c$, $l$, $l_0$, $m$ are positive, stabilize the pendulum error dynamics. To further justify these claims, let us define the synchronization error $e$ as $e = \theta_1 - \theta_2$. Then by subtracting (3.38) from (3.39) we obtain the nonlinear error equation given as follows:

$$\begin{aligned} &ml^2\ddot{e} + cl_0^2(\cos\theta_1\dot{\theta}_1 - \cos\theta_2\dot{\theta}_2)(\cos\theta_1 + \cos\theta_2) \\ &+mgl(\sin\theta_1 - \sin\theta_2) + kl_0^2(\sin\theta_1 - \sin\theta_2)(\cos\theta_1 + \cos\theta_2) = 0. \end{aligned} \tag{3.45}$$

Then by linearizing (3.45) around $z = 0$ or equivalently using the linearized equations given above, linearized error dynamics can be given as follows:

$$ml^2\ddot{e} + 2cl_0^2\dot{e} + (mgl + 2kl_0^2)e = 0. \tag{3.46}$$

Let $z_e = [e\ \dot{e}]$ be the state variables defined for error equations. Then the error equation is written in the form $\dot{z}_e = A_e z_e$. The error matrix $A_e$ is,

$$A_e = \begin{bmatrix} 0 & 1 \\ -\frac{g}{l} - \frac{2kl_0^2}{ml^2} & -\frac{2cl_0^2}{ml^2} \end{bmatrix}, \tag{3.47}$$

and the eigenvalues of $A_e$ is,

$$\lambda_1 = -\frac{cl_0^2}{ml^2} - \sqrt{(\frac{cl_0^2}{ml^2})^2 - \frac{2kl_0^2}{ml^2} - \frac{g}{l}}, \tag{3.48}$$

$$\lambda_2 = -\frac{cl_0^2}{ml^2} + \sqrt{(\frac{cl_0^2}{ml^2})^2 - \frac{2kl_0^2}{ml^2} - \frac{g}{l}}. \tag{3.49}$$

Note that $\lambda_1$ and $\lambda_2$ given above are exactly the same as $s_3$ and $s_4$ given by (3.43) and (3.44). The eigenvalues of the error equation are on the left half plane and consequently pendulums are synchronized. Since the linearized error dynamics are stable, the error dynamics for the system given by the nonlinear equation (3.45) is also locally asymptotically stable, i.e. synchronization is achieved. Typical simulation results are given in Figue 3.8.

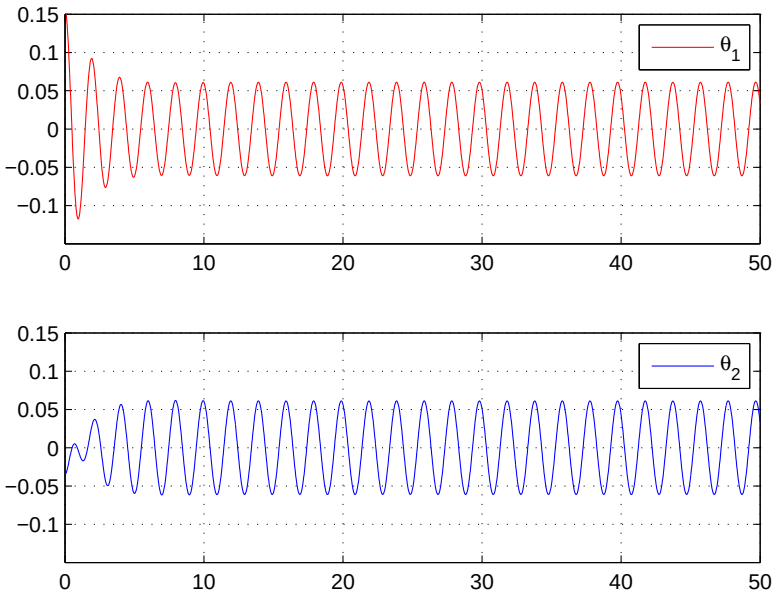


Figure 3.8: Simulation of two pendulums coupled with parallel spring and damper. In these particular simulations we choose $k = 2,\ c = 1,\ l_0 = 0.75,\ l = 1,\ m_1 = m_2 = 1,\ \theta_1(0) = 9°,\ \dot{\theta}_1(0) = 0°,\ \theta_2(0) = -2°,\ \dot{\theta}_2(0) = 0°$.

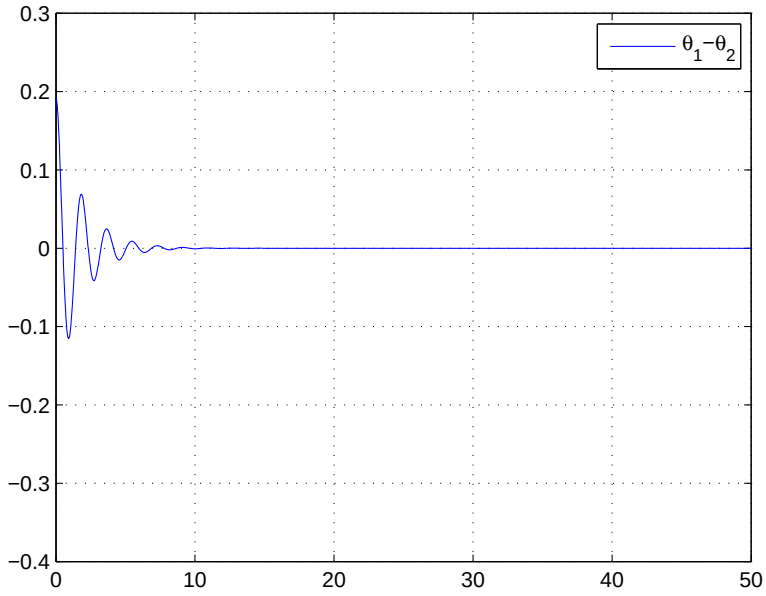


Figure 3.9: Error simulation of two pendulums coupled with parallel spring and damper. We choose the above parameters for simulation purposes.

As can be seen from Figures 3.8 and 3.9:

- $\lim_{t\to\infty} \theta_1(t) - \theta_2(t) = 0$ is achieved,
- $\theta_1(t)$ and $\theta_2(t)$ converges to their natural oscillating frequencies,
- Parallel coupled system synchronizes faster than the series coupled one.

## 3.4 Two Pendulums Coupled with Parallel Spring-Damper in Oblique Form

Consider the system shown in the Figure 3.10. We couple two pendulums from points $l_0$ and $l_1$ with parallel spring-damper in oblique form and analyze the synchronization dynamics. Let $m_1$, $l_1$, $m_2$, $l_2$ denote the mass and length of the pendulums, respectively. By using either free-body diagrams or performing Lagrangian method, we obtain the following equations of motion:

$$m_1 l_1^2 \ddot{\theta}_1 + m_1 g l_1 \sin\theta_1 + k l_0 \sin\alpha_1 (l_0 \sin\theta_1 - \hat{l}_1 \sin\theta_2) \tag{3.50}$$

$$+ cl_0 \sin\alpha_1(l_0 \cos\theta_1\dot{\theta}_1 - \hat{l}_1 \cos\theta_2\dot{\theta}_2) = 0,$$

$$m_2 l_2^2\ddot{\theta}_2 + m_2 g l_2 \sin\theta_2 + k\hat{l}_1 \sin\alpha_2(l_0 \sin\theta_1 - \hat{l}_1 \sin\theta_2) \tag{3.51}$$

$$- cl_1 \sin\alpha_2(l_0 \cos\theta_1\dot{\theta}_1 - \hat{l}_1 \cos\theta_2\dot{\theta}_2) = 0.$$

where $\alpha_1 = \theta_1 + \arctan(\frac{d - l_0 \sin\theta_1 + \hat{l}_1 \sin\theta_2}{|l_0 - \hat{l}_1|})$, $\alpha_2 = \alpha_1 + \theta_2 - \theta_1$ and $d$ is the distance between pendulums.

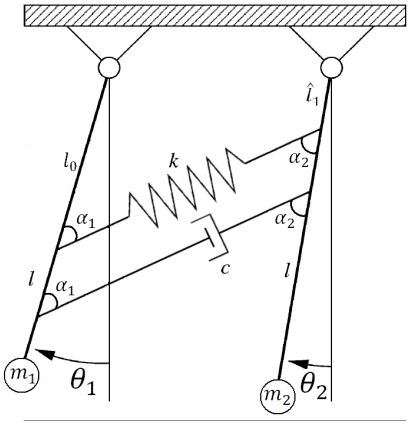


Figure 3.10: Two Double Pendulums Coupled with Parallel Spring-Damper in Oblique Form

As in the previous section let us assume $m_1 = m_2 = m$, $l_1 = l_2 = l$, which is reasonable for synchronization, i.e. we assume the synchronization of two identical pendulums. Let us define the state variables as before, i.e. $z = [\theta_1\ \dot{\theta}_1\ \theta_2\ \dot{\theta}_2]$. By linearizing the equations of motion around $z = 0$, we obtain the linearized equations as $\dot{z} = Az$, where the matrix $A$ is given below:

$$A = \begin{bmatrix} 0 & 1 & 0 & 0 \\ -\frac{g}{l} - \alpha_l K l_0^2 & \alpha_l C l_0^2 & \alpha_l K l_0 l_1 & \alpha_l C l_0 l_1 \\ 0 & 0 & 0 & 1 \\ \alpha_l K l_0 l_1 & \alpha_l C l_0 l_1 & -\frac{g}{l} - \alpha_l K l_1^2 & \alpha_l C l_1^2 \end{bmatrix}, \tag{3.52}$$

where $\alpha_l = \frac{d}{\sqrt{|l_0 - l_1|^2 + d^2}}$. The stability analysis of this system is performed by using eigenvalue analysis since the dynamics resembles the normal spring-damper coupled system explained in the previous section. The eigenvalues of the system

matrix $A$ can be given as follows:

$$s_1 = \sqrt{\frac{g}{l}}j, \tag{3.53}$$

$$s_2 = -\sqrt{\frac{g}{l}}j, \tag{3.54}$$

$$s_3 = \frac{1}{2}(-\alpha_l C(l_0^2 + l_1^2) - \sqrt{(\alpha_l C(l_0^2 + l_1^2))^2 - 4\frac{g}{l} - 4K}), \tag{3.55}$$

$$s_4 = \frac{1}{2}(-\alpha_l C(l_0^2 + l_1^2) + \sqrt{(\alpha_l C(l_0^2 + l_1^2))^2 - 4\frac{g}{l} - 4K}). \tag{3.56}$$

The eigenvalues $s_1$ and $s_2$, which are on the imaginary axis, force the pendulums to oscillate without damping and the eigenvalues $s_3$ and $s_4$, which are on the left half plane since the parameters $m\ l,\ l_0,\ l_1,\ k,\ c,\ \alpha_l$ are positive, stabilize the pendulum error dynamics.

To analyze the error dynamics we needed to define an appropriate error function for this system, i.e. we should be able to write the error dynamics in the form $\dot{z}_e = A_e z_e$ and $z_e = [e,\ \dot{e}]$. In order to do that we define the following error function:

$$e = l_0\theta_1 - l_1\theta_2. \tag{3.57}$$

Then multiplying (3.50) and (3.51) with $l_0$ and $l_1$, respectively and assuming $m_1 = m_2 = m$, $l_1 = l_2 = l$ we subtract the resultant equations with each other to obtain the following nonlinear error equation:

$$ml^2(l_0\ddot{\theta}_1 - l_1\ddot{\theta}_2) + c(l_0\cos\theta_1\dot{\theta}_1 - l_1\cos\theta_2\dot{\theta}_2)(l_0^2\sin\alpha_1 + l_1^2\sin\alpha_2)$$
$$+mgl(l_0\sin\theta_1 - l_1\sin\theta_2) + k(l_0\sin\theta_1 - l_1\sin\theta_2)(l_0^2\sin\alpha_1 - l_1^2\sin\alpha_2) = 0. \tag{3.58}$$

By linearizing (3.58) around $z_e = 0$ the linearized error dynamics can be given as follows:

$$ml^2(l_0\ddot{\theta}_1 - l_1\ddot{\theta}_2) + mgl(l_0\theta_1 - l_1\theta_2) + \alpha_l k(l_0^2 + l_1^2)(l_0\theta_1 - l1\theta_2) \tag{3.59}$$

$$+ \alpha_l C(l_0^2 + l_1^2)(l_0\dot{\theta}_1 - l_1\dot{\theta}_2) = 0.$$

The error dynamics given by (3.59) can be written as $\dot{z}_e = A_e z_e$, where $A_e$ is as given below:

$$A_e = \begin{bmatrix} 0 & 1 \\ -\frac{g}{l} - \alpha_l k(l_0^2 + l_1^2) & \alpha_l c(l_0^2 + l_1^2) \end{bmatrix}, \tag{3.60}$$

and the eigenvalues of the error matrix is,

$$\lambda_1 = \frac{1}{2}(-\alpha_l C(l_0^2 + l_1^2) - \sqrt{(\alpha_l C(l_0^2 + l_1^2))^2 - 4\frac{g}{l} - 4K}), \tag{3.61}$$

$$\lambda_2 = \frac{1}{2}(-\alpha_l C(l_0^2 + l_1^2) + \sqrt{(\alpha_l C(l_0^2 + l_1^2))^2 - 4\frac{g}{l} - 4K}). \tag{3.62}$$

Note that, as before, the eigenvalues $\lambda_1$ and $\lambda_2$ are exactly the same as the eigenvalues $s_3$ and $s_4$ given by (3.55) and (3.56). The eigenvalues of the error equation are on the left half plane and consequently pendulums are synchronized. Since the linearized error dynamics are stable, the error dynamics for the system given by the nonlinear equation (3.58) is also locally asymptotically stable, i.e. synchronization is achieved. Typical simulation results are given in Figures 3.11 and 3.12.

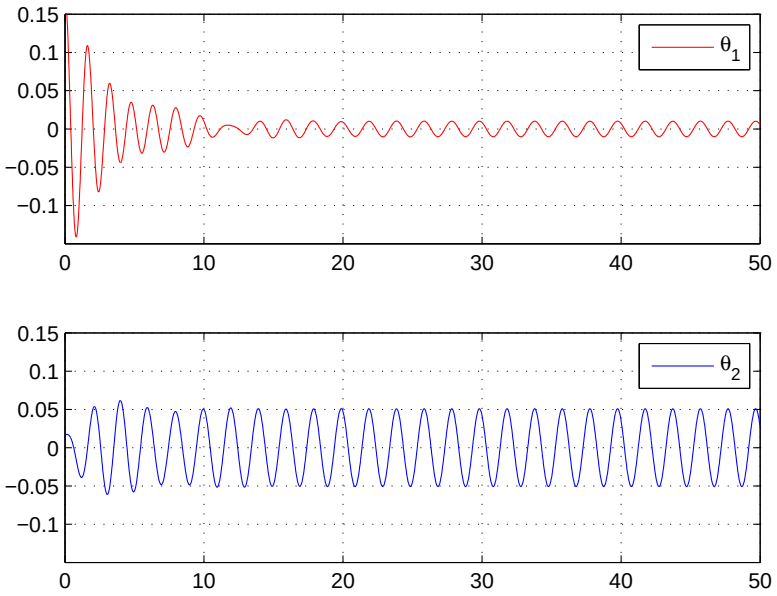


Figure 3.11: Simulation of two pendulums coupled with parallel spring and damper in oblique form. In these particular simulations we choose $k = 10$, $c = 1$, $l = 1$, $l_0 = .75$, $l_1 = .15$, $m_1 = m_2 = 1$, $\theta_1(0) = 10°$, $\dot{\theta}_1(0) = 0°$, $\theta_2(0) = 1°$, $\dot{\theta}_2(0) = 0°$.

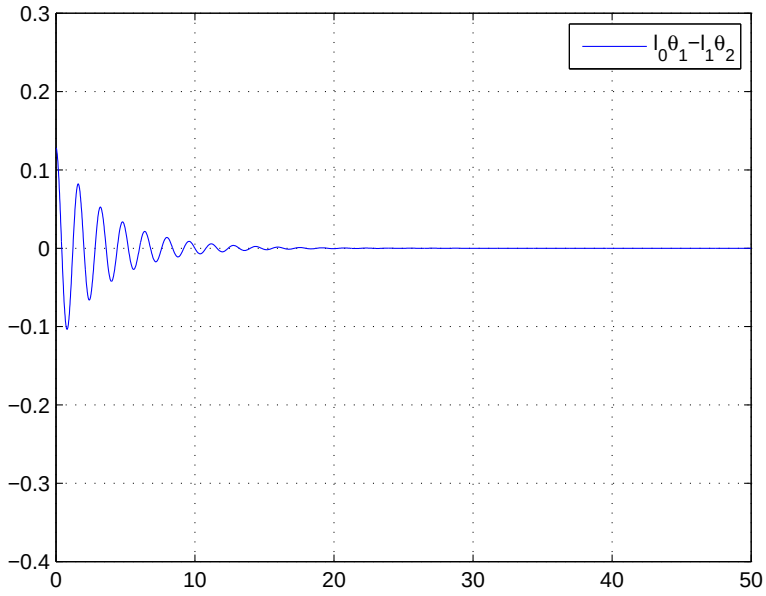


Figure 3.12: Error simulation of two pendulums coupled with parallel spring and damper in oblique form. We choose the above parameters for simulation purposes.

As can be seen from Figures 3.11 and 3.12:

- $\lim_{t\to\infty} l_0\theta_1(t) - l_1\theta_2(t) = 0$ is achieved, i.e. systems are synchronized with different amplitudes,
- $\theta_1(t)$ and $\theta_2(t)$ converges to their natural oscillating frequencies.

## 3.5 Three Pendulums Coupled with Spring-Damper

Consider the system shown in the Figure 3.13. We couple three pendulums from point $l_0$ with double spring-damper and analyze the synchronization dynamics. Let $m_1$, $l_1$, $m_2$, $l_2$, $m_2$, $l_3$ denote the mass and length of the pendulums, respectively. By using either free-body diagrams or performing Lagrangian method,

we obtain the following equations of motion:

$$m_1 l_1^2 \ddot{\theta}_1 + m_1 g l_1 \sin\theta_1 + k_1 l_0^2 \cos\theta_1(\sin\theta_1 - \sin\theta_2) + c_1 l_0^2 \cos\theta_1(\cos\theta_1\dot{\theta}_1 - \cos\theta_2\dot{\theta}_2) = 0, \tag{3.63}$$

$$\begin{aligned} m_2 l_2^2 \ddot{\theta}_2 + m_2 g l_2 \sin\theta_2 - k_1 l_0^2 \cos\theta_2(\sin\theta_1 - \sin\theta_2) - c_1 l_0^2 \cos\theta_2(\cos\theta_1\dot{\theta}_1 - \cos\theta_2\dot{\theta}_2) \\ + k_2 l_0^2 \cos\theta_2(\sin\theta_2 - \sin\theta_3) + c_2 l_0^2 \cos\theta_2(\cos\theta_2\dot{\theta}_2 - \cos\theta_3\dot{\theta}_3) = 0, \end{aligned} \tag{3.64}$$

$$m_3 l_3^2 \ddot{\theta}_3 + m_3 g l_3 \sin\theta_3 - k_2 l_0^2 \cos\theta_3(\sin\theta_3 - \sin\theta_3) - c_2 l_0^2 \cos\theta_3(\cos\theta_2\dot{\theta}_2 - \cos\theta_3\dot{\theta}_3) = 0. \tag{3.65}$$

Now let us assume $m_1 = m_2 = m_3 = m$, $l_1 = l_2 = l_3 = l$, which is reasonable for

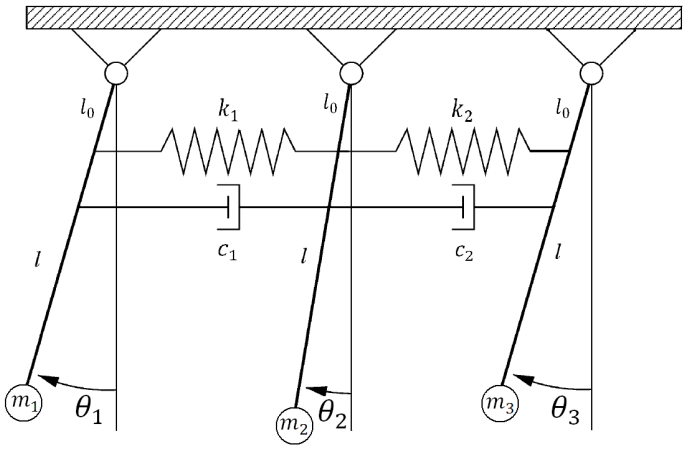


Figure 3.13: Three Pendulums Coupled with Parallel Spring-Damper

synchronization, i.e. we assume the synchronization of three identical pendulums. Let us define the state variables for this system as $z = [\theta_1\ \dot{\theta}_1\ \theta_2\ \dot{\theta}_2\ \theta_3\ \dot{\theta}_3]$. By linearizing (3.63)-(3.65) around $z = 0$ we obtain $\dot{z} = Az$ where $A$ is given below:

$$A = \begin{bmatrix} 0 & 1 & 0 & 0 & 0 & 0 \\ a_{2,1} & -C_1 & K_1 & C_1 & 0 & 0 \\ 0 & 0 & 0 & 1 & 0 & 0 \\ K_1 & C_1 & a_{4,3} & a_{4,4} & K_2 & C_2 \\ 0 & 0 & 0 & 0 & 0 & 1 \\ 0 & 0 & K_2 & C_2 & a_{6,5} & -C_2 \end{bmatrix}, \tag{3.66}$$

and $C_1$, $C_2$, $K_1$, $K_2$ are given as:

$$C_1 = \frac{c_1 l_0^2}{ml^2},\ C_2 = \frac{c_2 l_0^2}{ml^2},\ K_1 = \frac{k_1 l_0^2}{ml^2},\ K_2 = \frac{k_2 l_0^2}{ml^2}. \tag{3.67}$$

For this system the stability and synchronization analysis of both system and error dynamics are performed by using Routh-Hurwitz criterion. Let us define the characteristic polynomial of $A$ as $p(s) = \det(sI - A)$. By applying Routh-Hurwitz criterion to $p(s)$, we obtain the first column of the Routh table as given in Table 3.4.

| | |
|---|---|
| $s^6$ | $1$ |
| $s^5$ | $2(C_1 + C_2)$ |
| $s^4$ | $\frac{g}{l} + \frac{6C_1^2C_2+C_1(6C_2^2+4K_1+K_2)+C_2(K_1+4K_2)}{2(C_1+C_2)}$ |
| $s^3$ | $\frac{3(C_2^2K_1^2l+C_1^3C_2(4g+6K_2l)+2C_1C_2((2K_1^2-3K_1K_2+2K_2^2)l+C_2^2(2g+3K_1l))+C_1^2(K_2^2l+C_2^2(8g+6(K_1+K_2)l)))}{2(C_1+C_2)g+(6C_1^2C_2+C_1(6C_2^2+4K_1+K_2)+C_2(K_1+4K_2))l}$ |
| $s^2$ | $\frac{g^2+2gl(K_1+K_2)+3K_1K_2l^2}{l^2}$ |
| $s^1$ | $\epsilon$ |
| $s^0$ | $\frac{g(g^2+2gl(K_1+K_2)+3K_1K_2l^2)}{l^3}$ |

Table 3.4: The first column of the Routh table which is obtained by applying Routh-Hurwitz criterion to equations of motion of the coupled system.

Unless the parameters $k_1,\ c_1,\ k_2,\ c_2\ , l_0\ , l\ , m$ are not negative we show that the first column of the Routh array is always positive. That means the system has four roots on the left half plane and two roots on the imaginary axis. For further analysis consider the following nonlinear error dynamics, which are obtained by assuming $m_1 = m_2 = m_3 = m$, $l_1 = l_2 = l_3 = l$ and then subtracting (3.63) from (3.64) and subtracting (3.64) from (3.65), respectively:

$$\begin{aligned} ml^2(\ddot{\theta}_1 - \ddot{\theta}_2) + mgl(\sin\theta_1 - \sin\theta_2) + k_1l_0^2(\sin\theta_1 - \sin\theta_2)(\cos\theta_1 + \cos\theta_2) \\ +c_1l_0^2(\cos\theta_1\dot{\theta}_1 - \cos\theta_2\dot{\theta}_2)(\cos\theta_1 + \cos\theta_2) - k_2l_0^2\cos\theta_2(\sin\theta_2 - \sin\theta_3) \\ -c_2l_0^2\cos\theta_2(\cos\theta_2\dot{\theta}_2 - \cos\theta_3\dot{\theta}_3), \end{aligned} \tag{3.68}$$

$$ml^2(\ddot{\theta}_2 - \ddot{\theta}_3) + mgl(\sin\theta_2 - \sin\theta_3) - k_1 l_0^2 \cos\theta_2(\sin\theta_1 - \sin\theta_2$$
$$-c_1 l_0^2 \cos\theta_2(\cos\theta_1\dot{\theta}_1 - \cos\theta_2\dot{\theta}_2) + k_2 l_0^2(\sin\theta_2 - \sin\theta_3)(\cos\theta_2 + \cos\theta_3)$$
$$+c_2 l_0^2(\cos\theta_2\dot{\theta}_2 - \cos\theta_3\dot{\theta}_3)(\cos\theta_2 + \cos\theta_3) = 0. \tag{3.69}$$

Linearizing these equations around $z = 0$, we have the following equations:

$$ml^2(\ddot{\theta}_1 - \ddot{\theta}_2) + 2c_1 l_0^2(\dot{\theta}_1 - \dot{\theta}_2) - c_2 l_0^2(\dot{\theta}_2 - \dot{\theta}_3) + (mgl^2 k_1 l_0^2)(\theta_1 - \theta_2) - k_2 l_0^2(\theta_2 - \theta_3) = 0, \tag{3.70}$$

$$ml^2(\ddot{\theta}_2 - \ddot{\theta}_3) - c_1 l_0^2(\dot{\theta}_1 - \dot{\theta}_2) + 2c_2 l_0^2(\dot{\theta}_2 - \dot{\theta}_3) + (mgl^2 k_2 l_0^2)(\theta_2 - \theta_3) - k_1 l_0^2(\theta_1 - \theta_2) = 0. \tag{3.71}$$

By defining the following state variables for the error equations:

$$z_e = [e_1\ \dot{e}_1\ e_2\ \dot{e}_2]^T, \tag{3.72}$$

where

$$e_1 = \theta_1 - \theta_2,\ \dot{e}_1 = \dot{\theta}_1 - \dot{\theta}_2, \tag{3.73}$$

$$e_2 = \theta_2 - \theta_3,\ \dot{e}_2 = \dot{\theta}_2 - \dot{\theta}_3, \tag{3.74}$$

we are able to write the equations in $\dot{z}_e = A_e z_e$ format and the resultant error matrix $A_e$ is given as:

$$A_e = \begin{bmatrix} 0 & 1 & 0 & 0 \\ -\frac{g}{l} - 2K_1 & -2C_1 & K_2 & C_2 \\ 0 & 0 & 0 & 1 \\ K_1 & C_1 & -\frac{g}{l} - 2K_2 & -2C_2 \end{bmatrix}. \tag{3.75}$$

Let us define the characteristic polynomial $p(s)$ of $A_e$ as $p(s) = \det(sI - A_e)$. Then by applying the Routh-Hurwitz criterion to $p(s)$, we obtain the Routh array as in Table 3.5.

We show that for positive $k_1,\ c_1\ k_2,\ c_2\ , l_0\ , l\ , m$ parameters, all the elements in the first column of the Routh array are always positive in the appendix. The analysis in appendix show that all the eigenvalues of the error equations

| | |
|---|---|
| $s^4$ | $1$ |
| $s^3$ | $2(C_1+C_2)$ |
| $s^2$ | $\frac{g}{l}+\frac{6C_1^2C_2+C_1(6C_2^2+4K_1+K_2)+C_2(K_1+4K_2)}{2(C_1+C_2)}$ |
| $s^1$ | $\frac{3(C_2^2K_1l+C_1^3C_2(4g+6K_2l)+2C_1C_2((2K_1^2-3K_1K_2+2K_2^2)l+C_2^2(2g+3K_1l))+C_1^2(K_2^2l+C_2^2(8g+6(K_1+K_2)l)))}{2(C_1+C_2)g+(6C_1^2C_2+C_1(6C_2^2+4K_1+K_2)+C_2(K_1+4K_2))}$ |
| $s^0$ | $\frac{g^2+2g(K_1+K_2)l+3K_1K_2l^2}{l^2}$ |

Table 3.5: The first column of the Routh table which is obtained by applying Routh-Hurwitz criterion to error equation of the coupled system.

are on the left half plane, hence the linearized error equations are stable so the error dynamics for the system given by the non-linear equations in (3.68)-(3.69) are locally asymptotically stable. In other words, once $|\theta_1(0)-\theta_2(0)|$ and $|\theta_2(0)-\theta_3(0)|$ are sufficiently small the synchronization goal is achieved [35]. On the other hand, the two eigenvalues on the imaginary axis are related to the oscillation of the pendulums without damping, i.e. $[\theta_2,\ \dot{\theta}_2]$. Typical simulation results are given in the Figures 3.14 and 3.15.

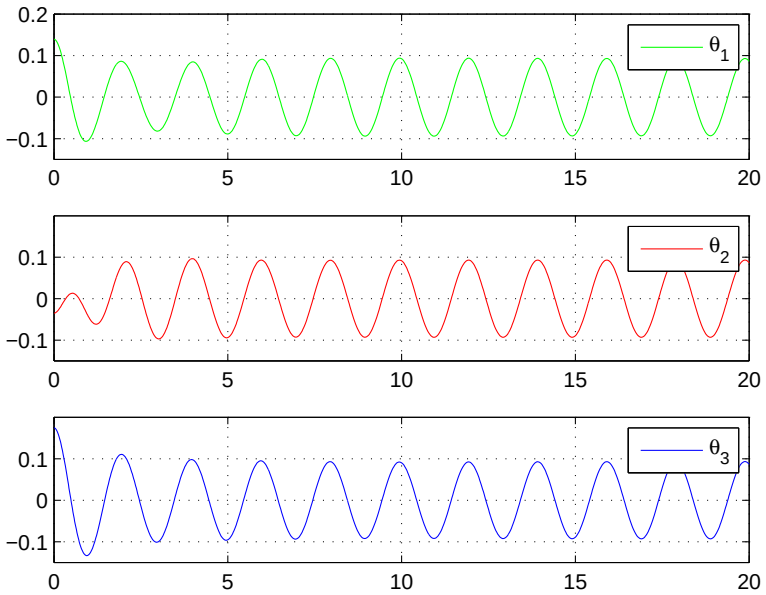


Figure 3.14: Simulation of three pendulums coupled with parallel spring and damper. In these particular simulations we choose $k_1=4,\ k_2=3,\ c_1=1,\ c_2=1,\ l=1,\ l_0=.75,\ m_1=m_2=1,\ \theta_1(0)=8^\circ,\ \dot{\theta}_1(0)=0^\circ,\ \theta_2(0)=-2^\circ,\ \dot{\theta}_2(0)=0^\circ,\ \theta_3(0)=10^\circ,\ \dot{\theta}_3(0)=0^\circ$

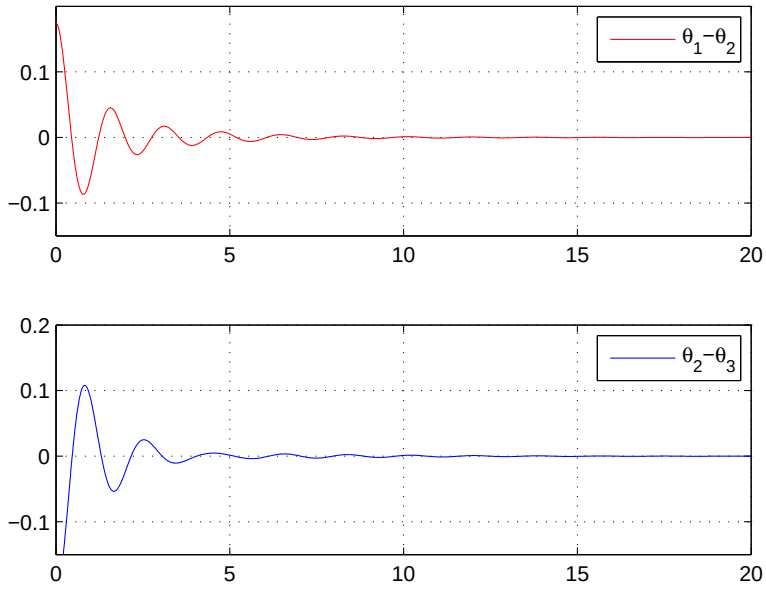


Figure 3.15: Error simulation of three pendulums coupled with parallel spring and damper. We choose the above parameters for simulation purposes.

When $c_1 \geq 0$, $k_1 \geq 0$ and $c_2 \geq 0$, $k_2 \geq 0$ then first column is positive, i.e. $\theta_1 - \theta_2$, $\dot{\theta}_1 - \dot{\theta}_2$, $\theta_2 - \theta_3$, $\dot{\theta}_2 - \dot{\theta}_3$ decays to 0. Further analysis on this system shows that one spring-damper couple is enough for synchronization as explained below:

By choosing $k_2 = 0$ and $c_1 = 0$ we have the coupled system depicted in Figure 3.16.

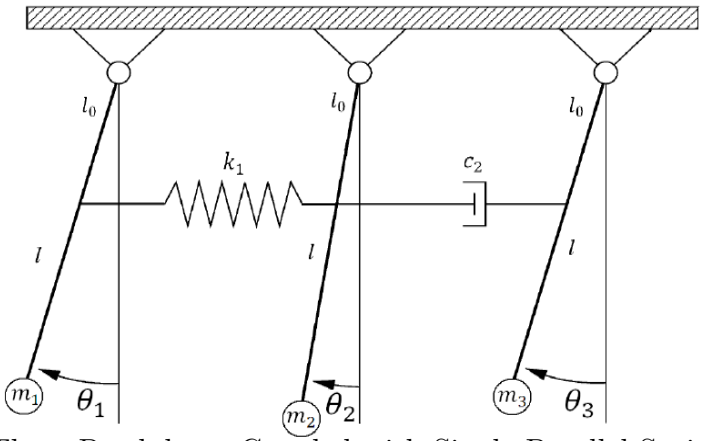


Figure 3.16: Three Pendulums Coupled with Single Parallel Spring-Damper

The equations of motion of the coupled system are given as:

$$m_1 l_1^2 \ddot{\theta}_1 + m_1 g l_1 \sin\theta_1 + k_1 l_0^2 \cos\theta_1(\sin\theta_1 - \sin\theta_2) = 0, \tag{3.76}$$

$$m_2 l_2^2 \ddot{\theta}_2 + m_2 g l_2 \sin\theta_2 + c_2 l_0^2 \cos\theta_2(\cos\theta_2\dot{\theta}_2 - \cos\theta_3\dot{\theta}_3) - k_1 l_0^2 \cos\theta_2(\sin\theta_1 - \sin\theta_2) = 0, \tag{3.77}$$

$$m_3 l_3^2 \ddot{\theta}_3 + m_3 g l_3 \sin\theta_3 - c_2 l_0^2 \cos\theta_3(\cos\theta_2\dot{\theta}_2 - \cos\theta_3\dot{\theta}_3) = 0. \tag{3.78}$$

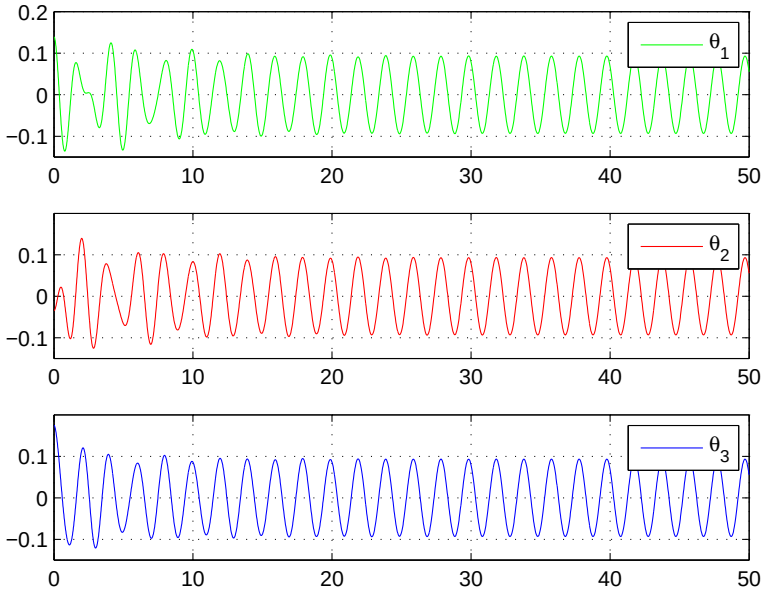


Figure 3.17: Simulation of three pendulums coupled with single parallel spring and damper. In these particular simulations we choose $k_1 = 10$, $c_2 = 1$, $l = 1$, $l_0 = .75$, $m_1 = m_2 = 1$, $\theta_1(0) = 8°$, $\dot{\theta}_1(0) = 0°$, $\theta_2(0) = -2°$, $\dot{\theta}_2(0) = 0°$, $\theta_3(0) = 10°$, $\dot{\theta}_3(0) = 0°$

Figures 3.17 and 3.18 show that this system also synchronizes but due to the lack of one sping-damper couple it synchronizes slowly. Inspired from this configuration, we couple four pendulums with two springs and one damper and analyze it in the next section.

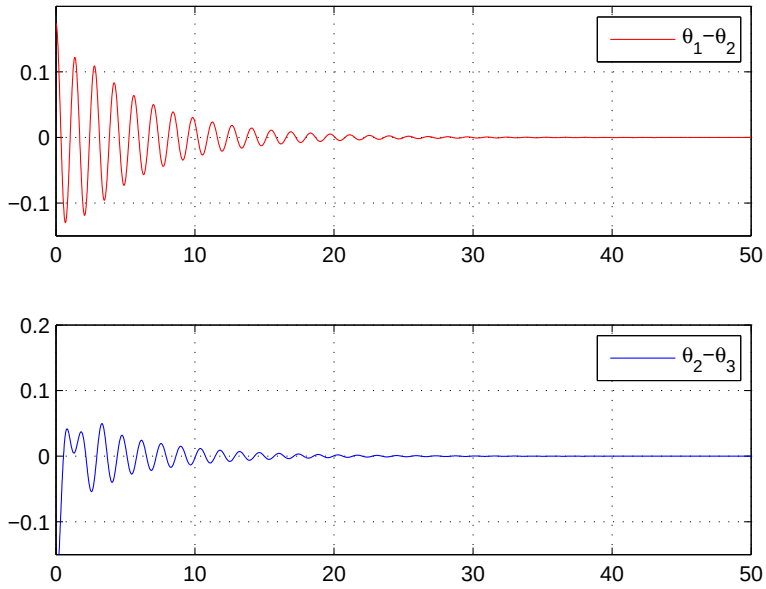


Figure 3.18: Error simulation of three pendulums coupled with single parallel spring and damper. We choose the above parameters for simulation purposes.

## 3.6 Four Pendulums Coupled with Two Springs and One Damper(Damper-Spring-Spring Configuration)

Consider the system shown in the Figure 3.19. We couple four pendulums from point $l_0$ with one damper and two springs, respectively. Then we analyze the synchronization dynamics. Let $m_1$, $l_1$, $m_2$, $l_2$, $m_2$, $l_3$, $m_4$, $l_4$ denote the mass and length of the pendulums, respectively. By using either free-body diagrams or performing Lagrangian method, we obtain the following equations of motion:

$$m_1 l_1^2 \ddot{\theta}_1 + m_1 g l_1 \sin\theta_1 + c l_0^2 \cos\theta_1(\cos\theta_1\dot{\theta}_1 - \cos\theta_2\dot{\theta}_2) = 0, \tag{3.79}$$

$$m_2 l_2^2 \ddot{\theta}_2 + m_2 g l_2 \sin\theta_2 - c l_0^2 \cos\theta_2(\cos\theta_1\dot{\theta}_1 - \cos\theta_2\dot{\theta}_2) + k_1 l_0^2 \cos\theta_2(\sin\theta_2 - \sin\theta_3) = 0, \tag{3.80}$$

$$m_3 l_3^2 \ddot{\theta}_3 + m_3 g l_3 \sin\theta_3 - k_1 l_0^2 \cos\theta_3(\sin\theta_2 - \sin\theta_3) + k_2 l_0^2 \cos\theta_3(\sin\theta_3 - \sin\theta_4) = 0, \tag{3.81}$$

$$m_4 l_4^2 \ddot{\theta}_4 + m_4 g l_4 \sin\theta_4 - k_2 l_0^2 \cos\theta_4(\sin\theta_3 - \sin\theta_4) = 0. \tag{3.82}$$

Now let us assume $m_1 = m_2 = m_3 = m_4 = m$, $l_1 = l_2 = l_3 = l_4 = l$, which is rea-

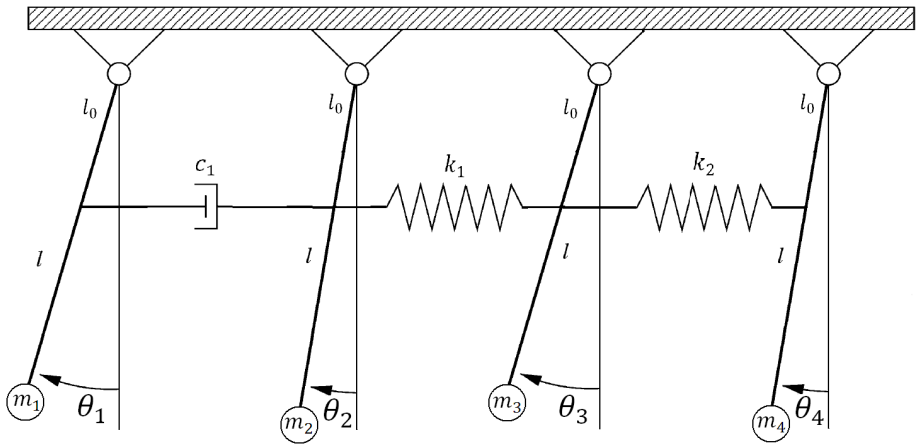


Figure 3.19: Four Pendulums Coupled with Two Springs and One Damper.

sonable for synchronization, i.e. we assume the synchronization of four identical pendulums. As before, we define the state variables as $z = [\theta_1\ \dot{\theta}_1\ \theta_2\ \dot{\theta}_2\ \theta_3\ \dot{\theta}_3\ \theta_4\ \dot{\theta}_4]$. By linearizing (3.79)-(3.82) around $z = 0$ we obtain $\dot{z} = Az$ where $A$ is given below:

$$A = \begin{bmatrix} 0 & 1 & 0 & 0 & 0 & 0 & 0 & 0 \\ -\frac{g}{l} & -c & 0 & c & 0 & 0 & 0 & 0 \\ 0 & 0 & 0 & 1 & 0 & 0 & 0 & 0 \\ 0 & c & -\frac{g}{l} - K_1 & -c & K_1 & 0 & 0 & 0 \\ 0 & 0 & 0 & 0 & 0 & 1 & 0 & 0 \\ 0 & 0 & K_1 & 0 & -\frac{g}{l} - K_1 - K_2 & 0 & K_2 & 0 \\ 0 & 0 & 0 & 0 & 0 & 0 & 0 & 1 \\ 0 & 0 & 0 & 0 & K_2 & 0 & -\frac{g}{l} - K_2 & 0 \end{bmatrix}, \quad (3.83)$$

Let us define the characteristic polynomial $p(s)$ of matrix $A$ given above as $p(s) = \det(sI - A)$. By applying the Routh-Hurwitz criterion to $p(s)$, we obtain the Routh array as in Table 3.6

Once the parameters $k_1$, $k_2$, $c$, $m$, $l$, $l_0$ are positive it is clear that the first column has all positive elements, hence six eigenvalues of the matrix $A$, which are on the left half plane, stabilize the pendulum error dynamics while two eigenvalues of the matrix $A$, which are on the imaginary axis, continuously oscillate the pendulums. For further analysis consider the following nonlinear error dynamics,

| | |
|---|---|
| $s^8$ | $1$ |
| $s^7$ | $2c$ |
| $s^6$ | $\frac{k_1}{2}+\frac{g}{l}$ |
| $s^5$ | $\frac{3ck_1^2l}{2g+k_1l}$ |
| $s^4$ | $\frac{k_1k_2}{3}+\frac{g^2+(2gk_1+\frac{2gk_2}{3})l}{l^2}$ |
| $s^3$ | $\frac{4ck_1^2k_2^2l^2}{3g^2+2gl(3k_1+k_2)+k_1k_2l^2}$ |
| $s^2$ | $\frac{g(g^2+2gl(k_1+k_2)+3k_1k_2l^2)}{l^3}$ |
| $s^1$ | $\epsilon$ |
| $s^0$ | $\frac{g^2(g^2+2gl(k_1+k_2)+3k_1k_2l^2)}{l^4}$ |

Table 3.6: The first column of the Routh table which is obtained by applying Routh-Hurwitz criterion to equations of motion of the coupled system.

which are obtained by assuming $m_1 = m_2 = m_3 = m_4 = m$, $l_1 = l_2 = l_3 = l_4 = l$ and then subtracting (3.79) from (3.80) and subtracting (3.81) from (3.82), respectively,

$$ml^2(\ddot{\theta}_1 - \ddot{\theta}_2) + mgl(\sin\theta_1 - \sin\theta_2) + cl_0^2(\cos\theta_1\dot{\theta}_1 - \cos\theta_2\dot{\theta}_2)$$
$$(\cos\theta_1 + \cos\theta_2) - k_1l_0^2\cos\theta_2(\sin\theta_2 - \sin\theta_3) = 0, \tag{3.84}$$

$$ml^2(\ddot{\theta}_2 - \ddot{\theta}_3) + mgl(\sin\theta_2 - \sin\theta_3) - cl_0^2\cos\theta_2(\cos\theta_1\dot{\theta}_1 - \cos\theta_2\dot{\theta}_2)$$
$$+k_1l_0^2(\sin\theta_2 - \sin\theta_3)(\cos\theta_2 + \cos\theta_3) - k_2l_0^2\cos\theta_3(\sin\theta_3 - \sin\theta_4) = 0, \tag{3.85}$$

$$ml^2(\ddot{\theta}_3 - \ddot{\theta}_4) + mgl(\sin\theta_3 - \sin\theta_4) - k_1l_0^2\cos\theta_3(\sin\theta_2 - \sin\theta_3)$$
$$+k_2l_0^2(\sin\theta_3 - \sin\theta_4)(\cos\theta_3 + \cos\theta_4) = 0. \tag{3.86}$$

By using linearization, we obtain:

$$ml^2(\ddot{\theta}_1 - \ddot{\theta}_2) + mgl(\theta_1 - \theta_2) + 2cl_0^2(\dot{\theta}_1 - \dot{\theta}_2) - k_1l_0^2(\theta_2 - \theta_3) = 0, \tag{3.87}$$

$$ml^2(\ddot{\theta}_2 - \ddot{\theta}_3) + mgl(\theta_2 - \theta_3) - cl_0^2(\dot{\theta}_1 - \dot{\theta}_2) + 2k_1l_0^2(\theta_2 - \theta_3) - k_2l_0^2(\theta_3 - \theta_4) = 0, \tag{3.88}$$

$$ml^2(\ddot{\theta}_3 - \ddot{\theta}_4) + mgl(\theta_3 - \theta_4) - k_1 l_0^2(\theta_2 - \theta_3) + 2k_2 l_0^2(\theta_3 - \theta_4) = 0. \tag{3.89}$$

Let us define the error variables as $e_1 = \theta_1 - \theta_2$, $e_2 = \theta_2 - \theta_3$, $e_3 = \theta_3 - \theta_4$ and the state variable $z_e = [e_1 \ \dot{e}_1 \ e_2 \ \dot{e}_2 \ e_3 \ \dot{e}_3]^T$. By using (3.87)-(3.89), we obtain $\dot{z_e} = A_e z_e$, where $A_e$ is given as:

$$A_e = \begin{bmatrix} 0 & 1 & 0 & 0 & 0 & 0 \\ -\frac{g}{l} & -2C & K_1 & 0 & 0 & 0 \\ 0 & 0 & 0 & 1 & 0 & 0 \\ 0 & C & -\frac{g}{l} - 2K_1 & 0 & K_2 & 0 \\ 0 & 0 & 0 & 0 & 0 & 1 \\ 0 & 0 & K_1 & 0 & -\frac{g}{l} - 2K_2 & 0 \end{bmatrix}, \tag{3.90}$$

where $K_1$, $K_2$ and $C$ are given as:

$$K_1 = \frac{k_1 l_0^2}{ml^2}, \ K_2 = \frac{k_2 l_0^2}{ml^2}, \ C = \frac{c l_0^2}{ml^2}. \tag{3.91}$$

Let us define the characteristic polynomial $p(s)$ of matrix $A$ as $p(s) = \det(sI - A)$. By applying the Routh-Hurwitz criterion to $p(s)$, we obtain the following Routh array:

| | |
|---|---|
| $s^6$ | $1$ |
| $s^5$ | $2C$ |
| $s^4$ | $\frac{K_1}{2} + \frac{g}{l}$ |
| $s^3$ | $\frac{3CK_1^2 l}{2g + K_1 l}$ |
| $s^2$ | $\frac{K_1 K_2}{3} + \frac{g^2 + (2gK_1 + \frac{2gK_2}{3})l}{l^2}$ |
| $s^1$ | $\frac{4CK_1^2 K_2^2 l^2}{3g^2 + 2gl(3K_1 + K_2) + K_1 K_2 l^2}$ |
| $s^0$ | $\frac{g(g^2 + 2gl(K_1 + K_2) + 3K_1 K_2 l^2)}{l^3}$ |

Table 3.7: The first column of the Routh table which is obtained by applying Routh-Hurwitz criterion to error equation of the coupled system.

For positive $K_1$, $K_2$, $C$, $l$, $l_0$ parameters the first column has always positive elements. As a result, the linearized error dynamics are stable. This implies that,

the nonlinear error equations given by (3.84)-(3.86) are locally asymptotically stable. Typical simulation results are given in the Figures 3.20 and 3.21.

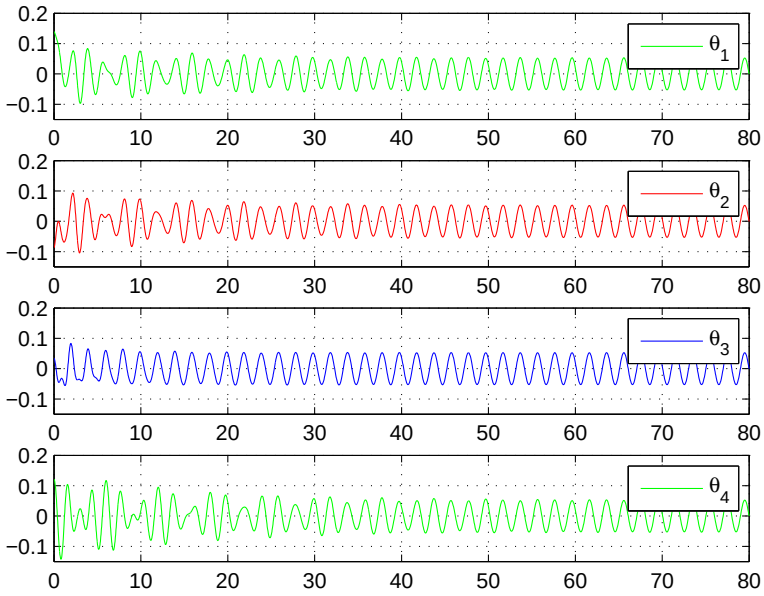


Figure 3.20: Simulation of four pendulums coupled with two springs and one damper. In these particular simulations we choose $k_1 = 20,\ k_2 = 10,\ c = 1,\ l = 1,\ l_0 = .85,\ m = 1,\ \theta_1(0) = 8°,\ \dot{\theta}_1(0) = 0°,\ \theta_2(0) = -5°,\ \dot{\theta}_2(0) = 0°,\ \theta_3(0) = 2°,\ \dot{\theta}_3(0) = 0°\ \theta_4(0) = 7°,\ \dot{\theta}_4(0) = 0°$

.

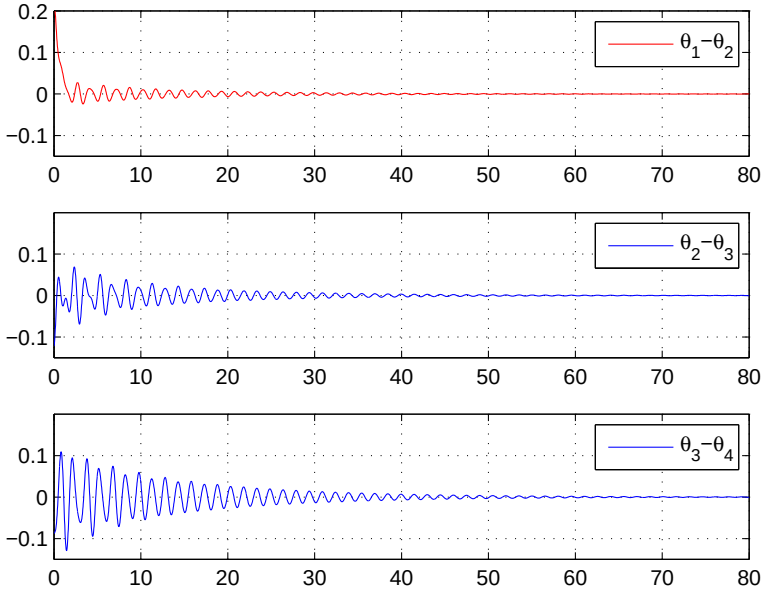


Figure 3.21: Error simulation of four pendulums coupled with two springs and one damper. We choose the above parameters for simulation purposes.

## 3.7 Four Pendulums Coupled with Two Spring and One Damper(Spring-Damper-Spring-Configuration)

Consider the system shown in the Figure 3.22. We couple four pendulums from point $l_0$ with spring, damper and spring respectively. Then we analyze the synchronization dynamics. Let $m_1$, $l_1$, $m_2$, $l_2$, $m_2$, $l_3$, $m_4$, $l_4$ denote the mass and length of the pendulums, respectively as before. By using either free-body diagrams or performing Lagrangian method, we obtain the following equations of motion:

$$m_1 l_1^2 \ddot{\theta}_1 + m_1 g l_1 \sin\theta_1 + k_1 l_0^2 \cos\theta_1(\sin\theta_1 - \sin\theta_2) = 0, \tag{3.92}$$

$$m_2 l_2^2 \ddot{\theta}_2 + m_2 g l_2 \sin\theta_2 + c l_0^2 \cos\theta_2(\cos\theta_2\dot{\theta}_2 - \cos\theta_3\dot{\theta}_3) - k_1 l_0^2 \cos\theta_2(\sin\theta_1 - \sin\theta_2) = 0, \tag{3.93}$$

$$m_3 l_3^2 \ddot{\theta}_3 + m_3 g l_3 \sin\theta_3 - c l_0^2 \cos\theta_3(\cos\theta_2\dot{\theta}_2 - \cos\theta_3\dot{\theta}_3) - k_2 l_0^2 \cos\theta_3(\sin\theta_3 - \sin\theta_4) = 0, \tag{3.94}$$

$$m_4 l_4^2 \ddot{\theta}_4 + m_4 g l_4 \sin\theta_4 - k_2 l_0^2 \cos\theta_4(\sin\theta_3 - \sin\theta_4) = 0. \tag{3.95}$$

Now let us assume $m_1 = m_2 = m_3 = m_4 = m$, $l_1 = l_2 = l_3 = l_4 = l$,

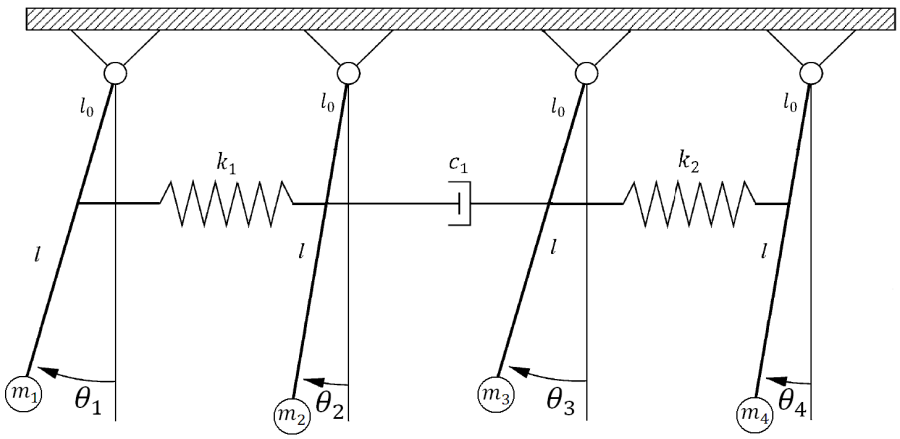


Figure 3.22: Four Pendulums Coupled with Two Springs and One Damper.

which is reasonable for synchronization, i.e. we assume the synchronization of

four identical pendulums. As before, we define the state variable vector as $z = [\theta_1\ \dot{\theta}_1\ \theta_2\ \dot{\theta}_2\ \theta_3\ \dot{\theta}_3\ \theta_4\ \dot{\theta}_4]^T$. By linearizing (3.92)-(3.95) around $z = 0$, we obtain the linearized error dynamics as $\dot{z} = Az$, where the matrix $A$ is as given below:

$$A = \begin{bmatrix} 0 & 1 & 0 & 0 & 0 & 0 & 0 & 0 \\ -\frac{g}{l} - K_1 & 0 & K_1 & 0 & 0 & 0 & 0 & 0 \\ 0 & 0 & 0 & 1 & 0 & 0 & & 0 \\ K_1 & 0 & -\frac{g}{l} - K_1 & -C & 0 & C & 0 & 0 \\ 0 & 0 & 0 & 0 & 0 & 1 & 0 & 0 \\ 0 & 0 & 0 & C & -\frac{g}{l} - K_2 & 0 & K_2 & 0 \\ 0 & 0 & 0 & 0 & 0 & 0 & 0 & 1 \\ 0 & 0 & 0 & 0 & K_2 & 0 & -\frac{g}{l} - K_2 & 0 \end{bmatrix}. \quad (3.96)$$

Let us define the characteristic polynomial $p(s)$ of matrix $A$ given above as $p(s) = \det(sI - A)$. By applying the Routh-Hurwitz criterion to $p(s)$, we obtain the following Routh array:

| | |
|---|---|
| $s^8$ | $1$ |
| $s^7$ | $2C$ |
| $s^6$ | $\frac{K_1+K_2}{2} + \frac{g}{l}$ |
| $s^5$ | $\frac{Cl(2(K_1^2+K_2^2)+(K_1-K_2)^2)}{2g+(K_1+K_2)l}$ |
| $s^4$ | $\frac{g^2(2(K_1^2+K_2^2)+(K_1-K_2)^2)+2g(K_1+K_2)(K_1^2+K_2^2+2(K_1-K_2)^2)l+4K_1(K_1-K_2)^2K_2l^2}{(2(K_1^2+K_2^2)+(K_1-K_2)^2)l^2}$ |
| $s^3$ | $\frac{16CK_1^2(K_1-K_2)^2K_2^2l^2}{g^2(2(K_1^2+K_2^2)+(K_1-K_2)^2)+2g(K_1+K_2)(K_1^2+K_2^2+2(K_1-K_2)^2)l+4K_1(K_1-K_2)^2K_2l^2}$ |
| $s^2$ | $\frac{g(g+2K_1l)(g+2K_2l)}{l^3}$ |
| $s^1$ | $\epsilon$ |
| $s^0$ | $\frac{g^2(g+2K_1l)(g+2K_2l)}{l^4}$ |

Table 3.8: The first column of the Routh table which is obtained by applying Routh-Hurwitz criterion to equations of motion of the coupled system.

Once the parameters $K_1$ $K_2$, $C$, $l$, $l_0$ are positive it is clear that the first column has all positive elements, hence the six roots on the left half plane stabilizes the pendulums and two roots on the imaginary axis continuously oscillates the pendulums. For further analysis consider the following nonlinear error dynamics, which are obtained by assuming $m_1 = m_2 = m_3 = m_4 = m$, $l_1 = l_2 = l_3 = l_4 = l$ and then subtracting (3.92) from (3.93) and subtracting (3.94) from (3.95), respectively,

$$ml^2(\ddot{\theta}_1 - \ddot{\theta}_2) + mgl(\sin\theta_1 - \sin\theta_2) + k_1 l_0^2(\sin\theta_1 - \sin\theta_2)(\cos\theta_1 + \cos\theta_2) \\ -cl_0^2\cos\theta_2(\cos\theta_2\dot{\theta}_2 - \cos\theta_3\dot{\theta}_3) = 0, \tag{3.97}$$

$$ml^2(\ddot{\theta}_2 - \ddot{\theta}_3) + mgl(\sin\theta_2 - \sin\theta_3) + cl_0^2(\cos\theta_2\dot{\theta}_2 - \cos\theta_3\dot{\theta}_3) \\ (\cos\theta_2 + \cos\theta_3) - k_1 l_0^2\cos\theta_2(\sin\theta_1 - \sin\theta_2) \\ -k_2 l_0^2\cos\theta_3(\sin\theta_3 - \sin\theta_4) = 0, \tag{3.98}$$

$$ml^2(\ddot{\theta}_3 - \ddot{\theta}_4) + mgl(\sin\theta_3 - \sin\theta_4) - cl_0^2\cos\theta_3(\cos\theta_2\dot{\theta}_2 - \cos\theta_3\dot{\theta}_3) \\ +k_2 l_0^2(\sin\theta_3 - \sin\theta_4)(\cos\theta_3 + \cos\theta_4) = 0. \tag{3.99}$$

By linearizing (3.97)-(3.99) around $z = 0$, we obtain:

$$ml^2(\ddot{\theta}_1 - \ddot{\theta}_2) + mgl(\theta_1 - \theta_2) + 2k_1 l_0^2(\theta_1 - \theta_2) - cl_0^2(\dot{\theta}_2 - \dot{\theta}_3) = 0, \tag{3.100}$$

$$ml^2(\ddot{\theta}_2 - \ddot{\theta}_3) + mgl(\theta_2 - \theta_3) + 2cl_0^2(\dot{\theta}_2 - \dot{\theta}_3) - k_1 l_0^2(\theta_1 - \theta_2) - k_2 l_0^2(\theta_3 - \theta_4) = 0, \tag{3.101}$$

$$ml^2(\ddot{\theta}_3 - \ddot{\theta}_4) + mgl(\theta_3 - \theta_4) - cl_0^2(\dot{\theta}_2 - \dot{\theta}_3) + 2k_2 l_0^2(\theta_3 - \theta_4) = 0. \tag{3.102}$$

Let us define the error variables as $e_1 = \theta_1 - \theta_2$, $e_2 = \theta_2 - \theta_3$, $e_3 = \theta_3 - \theta_4$ and the error state vector as $z_e = [e_1\ \dot{e}_1\ e_2\ \dot{e}_2\ e_3\ \dot{e}_3]^T$. By using (3.100)-(3.102) we obtain $\dot{z}_e = A_e z_e$, where the matrix $A_e$ is as given below:

$$A_e = \begin{bmatrix} 0 & 1 & 0 & 0 & 0 & 0 \\ -\frac{g}{l} - 2K_1 & 0 & 0 & C & 0 & 0 \\ 0 & 0 & 0 & 1 & 0 & 0 \\ K_1 & 0 & -\frac{g}{l} & -2C & K_2 & 0 \\ 0 & 0 & 0 & 0 & 0 & 1 \\ 0 & 0 & 0 & C & -\frac{g}{l} - 2K_2 & 0 \end{bmatrix}. \tag{3.103}$$

Then let us define the characteristic polynomial $p_e(s)$ of matrix $A_e$ given above as $p_e(s) = \det(sI - A_e)$. By applying the Routh-Hurwitz criterion to $p_e(s)$, we obtain the following Routh array:

| | |
|---|---|
| $s^6$ | $1$ |
| $s^5$ | $2C$ |
| $s^4$ | $\frac{K_1+K_2}{2} + \frac{g}{l}$ |
| $s^3$ | $\frac{Cl(2(K_1^2+K_2^2)+(K_1-K_2)^2)}{2g+(K_1+K_2)l}$ |
| $s^2$ | $\frac{g^2(2(K_1^2+K_2^2)+(K_1-K_2)^2)+2g(K_1+K_2)(K_1^2+K_2^2+2(K_1-K_2)^2)l+4K_1(K_1-K_2)^2K_2l^2}{(2(K_1^2+K_2^2)+(K_1-K_2)^2)l^2}$ |
| $s^1$ | $\frac{16CK_1^2(K_1-K_2)^2K_2^2l^2}{g^2(2(K_1^2+K_2^2)+(K_1-K_2)^2)+2g(K_1+K_2)(K_1^2+K_2^2+2(K_1-K_2)^2)l+4K_1(K_1-K_2)^2K_2l^2}$ |
| $s^0$ | $\frac{g(g+2K_1l)(g+2K_2l)}{l^3}$ |

Table 3.9: The first column of the Routh table which is obtained by applying Routh-Hurwitz criterion to error equation of the coupled system.

Note that for positive parameters $K1$, $K2$, $C$, $l$, $l_0$, when $K_1 \neq K_2$, the first column is always positive. This indicates that the linearized error dynamics are stable as long as all coefficients are positive and $K_1 \neq K_2$. Hence, the original nonlinear error dynamics are also locally exponentially stable. Therefore, the local synchronization can be achieved in this case. When $K_1 = K_2$, the coefficient of the $s^1$ row of Routh array is 0, hence the linearized error dynamics are not stable. Therefore, the stability of nonlinear error dynamics can not be concluded with this approach. We end up with such a result because we have connected the damper right between two springs. The two pendulums which are on the left and on the right of the damper synchronize locally but not globally in case of $K_1 = K_2$. We performed various simulations for the case $K_1 = K_2$ and $K_2 \neq K_2$, which are given in the Figures 3.23-3.26.

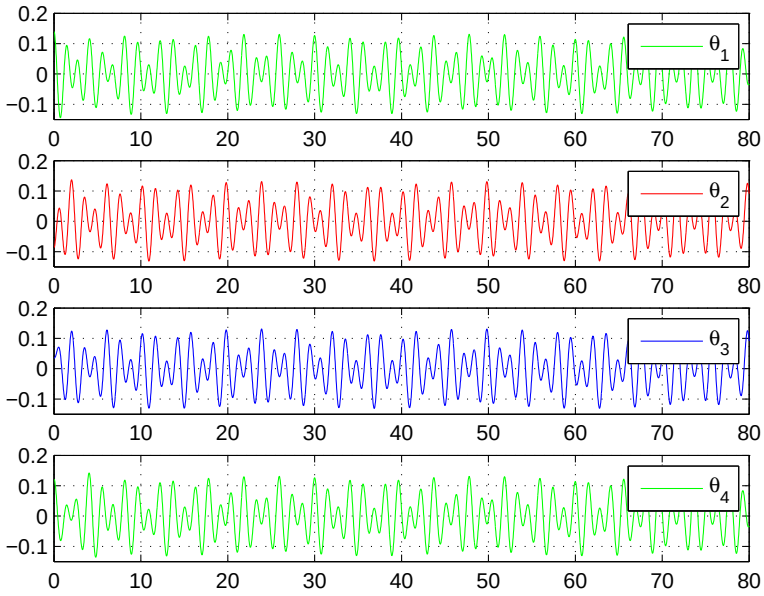


Figure 3.23: Simulation of four pendulums coupled with two springs and one damper for $K_1 = K_2$ case. In these particular simulations we choose $k_1 = 10,\ k_2 = 10,\ c = 5,\ l = 1,\ l_0 = .75,\ m = 1,\ \theta_1(0) = 8°,\ \dot{\theta}_1(0) = 0°,\ \theta_2(0) = -5°,\ \dot{\theta}_2(0) = 0°,\ \theta_3(0) = 2°,\ \dot{\theta}_3(0) = 0°\ \theta_4(0) = 7°,\ \dot{\theta}_4(0) = 0°$

.

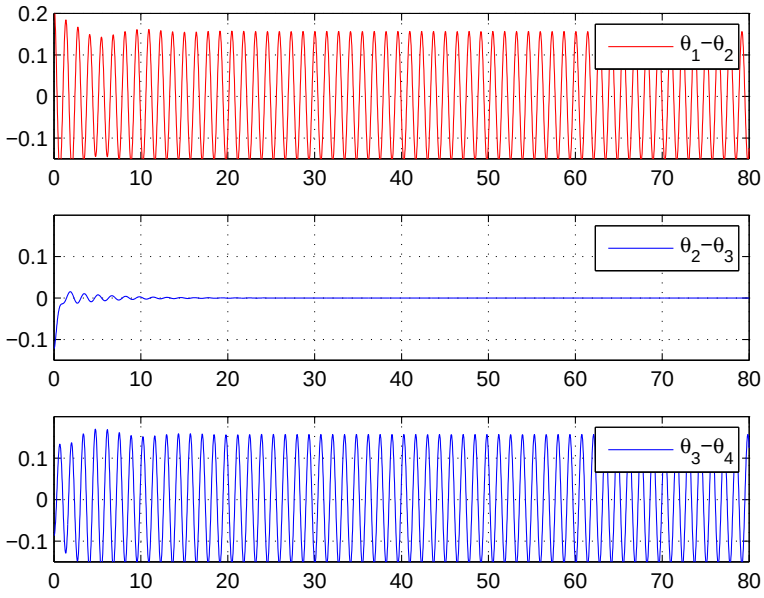


Figure 3.24: Error simulation of four pendulums coupled with two springs and one damper. We choose the above parameters for simulation purposes.

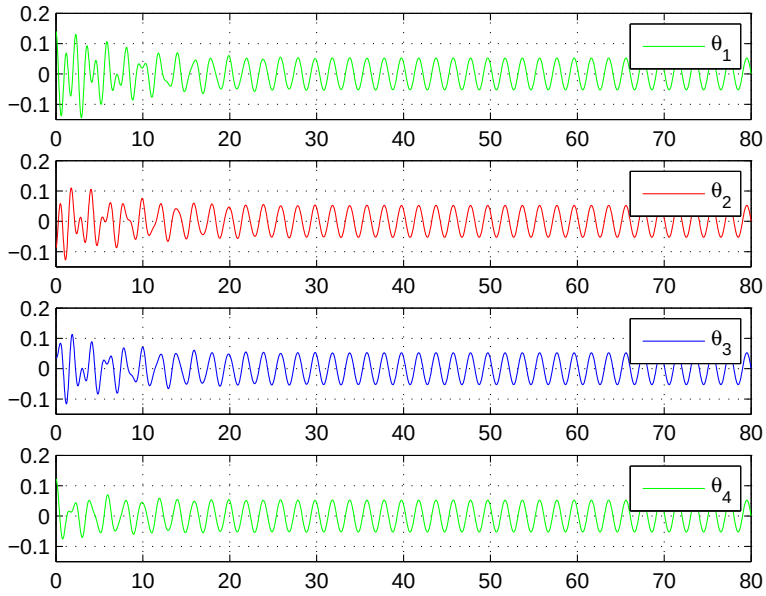


Figure 3.25: Simulation of four pendulums coupled with two springs and one damper for $K_1 \neq K_2$ case. In these particular simulations we choose $k_1 = 20,\ k_2 = 10,\ c = 5,\ l = 1,\ l_0 = .75,\ m = 1,\ \theta_1(0) = 8°,\ \dot{\theta}_1(0) = 0°,\ \theta_2(0) = -5°,\ \dot{\theta}_2(0) = 0°,\ \theta_3(0) = 2°,\ \dot{\theta}_3(0) = 0°\ \theta_4(0) = 7°,\ \dot{\theta}_4(0) = 0°$

.

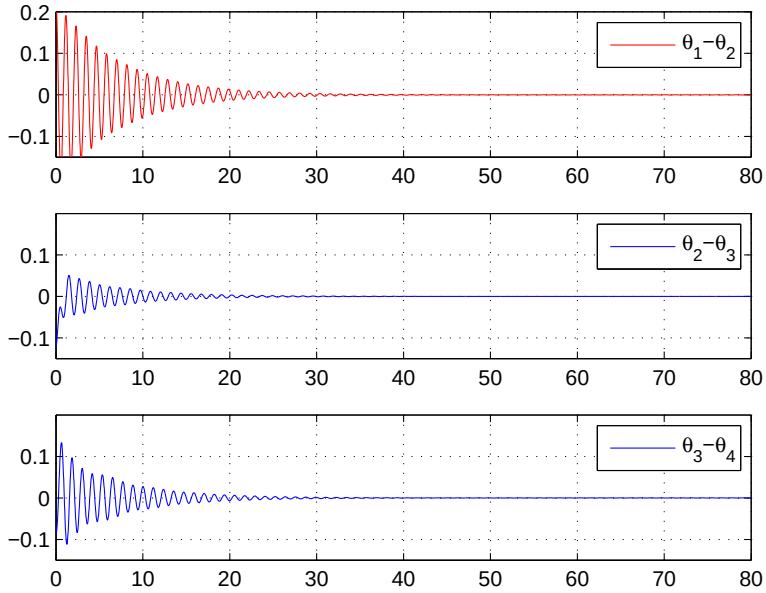


Figure 3.26: Error simulation of four pendulums coupled with two springs and one damper. We choose the above parameters for simulation purposes.

## 3.8 Multiple Pendulums Coupled with a Single Damper and Springs

To generalize the ideas presented in the previous sections, let us consider the case where $n$ pendulums are coupled with a single damper and $n-2$ springs,

respectively. Such a configuration for $n = 7$ is given in Figure 3.27. Let us consider the original nonlinear equations, which will be similar to (3.79)-(3.82) for $n = 4$ case. Such equations can be obtained by either using free-body diagrams or Lagrangian analysis. Assume that all masses are equal and the lengths of the pendulums are equal as well, i.e. we consider the synchronization of identical pendulums as before. Let us denote the state variable $z$ as,

$$z = [\theta_1 \ \dot{\theta}_1 \ ... \ \theta_i \ \dot{\theta}_i \ ... \ \theta_n \ \dot{\theta}_n]^T. \tag{3.104}$$

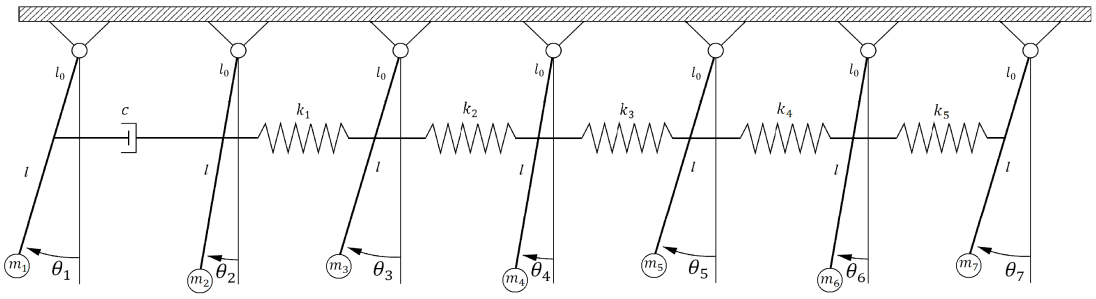


Figure 3.27: Seven Pendulums Coupled with Five Springs and One Damper.

By linearizing the equations of motion around $z = 0$, we obtain the linearized equations as $\dot{z} = Az$, where matrix $A$ will have a bended matrix form similar to (3.83). Let us divide the matrix $A$ in $2x2$ blocks as $A_{i,j} \in \Re^{(2x2)}$, $i = 1, 2, ..., n$, $j = 1, 2, ..., n$. Then, by generalizing (3.83) it is straightforward to show that the matrices $A_{i,j}$ can be given as below:

$$A_{1,1} = \begin{bmatrix} 0 & 1 \\ -\frac{g}{l} & -c \end{bmatrix}, \quad A_{1,2} = A_{2,1} = \begin{bmatrix} 0 & 0 \\ 0 & c \end{bmatrix}, \quad A_{2,2} = \begin{bmatrix} 0 & 1 \\ -\frac{g}{l} - K_1 & -c \end{bmatrix}, \tag{3.105}$$

$$A_{i,i} = \begin{bmatrix} 0 & 1 \\ -\frac{g}{l} - K_{i-2} - K_{i-1} & 0 \end{bmatrix}, \qquad A_{i,i+1} = A_{i+1,i} = \begin{bmatrix} 0 & 0 \\ K_{i-2} & 0 \end{bmatrix}, \tag{3.106}$$

$$A_{n,n} = \begin{bmatrix} 0 & 1 \\ -\frac{g}{l} - K_{n-2} & 0 \end{bmatrix}, \qquad A_{1,j} = A_{2,j} = A_{i,k} = \begin{bmatrix} 0 & 0 \\ 0 & 0 \end{bmatrix}, \tag{3.107}$$

where $i = 3, ..., n-1$, $j = 3, .., n$ $k = 1, ..., n$ and $k \neq i, i-1, i+1$.

For the synchronization error dynamics, let us define the errors as $e_1 = \theta_1 - \theta_2$, $e_i = \theta_i - \theta_{i+1}$, $e_{n-1} = \theta_{n-1} - \theta_n$. Let us define the error state as,

$$z_e = [e_1 \ \dot{e}_1 \ ... \ e_i \ \dot{e}_i \ ... \ e_{n-1} \ \dot{e}_{n-1} \ ]^T. \tag{3.108}$$

The linearized error dynamics can be given as $\dot{z}_e = Ez_e$, here $E \in \Re$. As before, the error matrix $E$ can be divided into $2x2$ blocks as $E_{i,j} \in \Re^{(2x2)}$, $i = 1, 2, ..., n-1$, $j = 1, 2, ..., n-1$. By generalizing (3.90), it is straightforward to show that $E$ has the following form:

$$E_{1,1} = \begin{bmatrix} 0 & 1 \\ -\frac{g}{l} & -2c \end{bmatrix}, \quad E_{2,1} = \begin{bmatrix} 0 & 0 \\ 0 & c \end{bmatrix}, \quad E_{i,i} = \begin{bmatrix} 0 & 1 \\ -\frac{g}{l} - 2k_{i-1} & 0 \end{bmatrix}, \tag{3.109}$$

$$E_{i-1,i} = E_{i+1,i} = \begin{bmatrix} 0 & 0 \\ k_{i-1} & 0 \end{bmatrix}, \quad E_{1,j} = E_{i,k} \begin{bmatrix} 0 & 0 \\ 0 & 0 \end{bmatrix}, \tag{3.110}$$

where $i = 2, ..., n-1$, $j = 3, .., n-1$ $k = 1, ..., n$ and $k \neq i, i-1, i+1$.

Although $E$ has a well-defined structure, we could not be able to find its characteristic polynomial and perform Routh-Hurwitz analysis, as we did for the cases $n = 2, 3, 4$. However, our simulations show that as long as the parameter values are positive and $K_i \neq K_j$, which is an exception only for $n = 4$ spring-damper-spring case, the error dynamics are stable, hence global synchronization is achieved. As an example, we consider $n = 7$ case, as shown in Figure 3.27. The resulting system matrix $A$ and error matrix $E$ can be given as below in abbreviated form:

$$A = \begin{bmatrix} 0 & 1 & 0 & 0 & 0 & 0 & 0 & 0 & 0 & 0 & 0 & 0 & 0 & 0 \\ a_{2,1} & -C & 0 & C & 0 & 0 & 0 & 0 & 0 & 0 & 0 & 0 & 0 & 0 \\ 0 & 0 & 0 & 1 & 0 & 0 & 0 & 0 & 0 & 0 & 0 & 0 & 0 & 0 \\ 0 & C & a_{4,3} & -C & K_1 & 0 & 0 & 0 & 0 & 0 & 0 & 0 & 0 & 0 \\ 0 & 0 & 0 & 0 & 0 & 1 & 0 & 0 & 0 & 0 & 0 & 0 & 0 & 0 \\ 0 & 0 & K_1 & 0 & a_{6,5} & 0 & K_2 & 0 & 0 & 0 & 0 & 0 & 0 & 0 \\ 0 & 0 & 0 & 0 & 0 & 0 & 0 & 1 & 0 & 0 & 0 & 0 & 0 & 0 \\ 0 & 0 & 0 & 0 & K_2 & 0 & a_{8,7} & 0 & K_3 & 0 & 0 & 0 & 0 & 0 \\ 0 & 0 & 0 & 0 & 0 & 0 & 0 & 0 & 0 & 1 & 0 & 0 & 0 & 0 \\ 0 & 0 & 0 & 0 & 0 & 0 & K_3 & 0 & a_{10,9} & 0 & K_4 & 0 & 0 & 0 \\ 0 & 0 & 0 & 0 & 0 & 0 & 0 & 0 & 0 & 0 & 0 & 1 & 0 & 0 \\ 0 & 0 & 0 & 0 & 0 & 0 & 0 & 0 & K_4 & 0 & a_{12,11} & 0 & K_5 & 0 \\ 0 & 0 & 0 & 0 & 0 & 0 & 0 & 0 & 0 & 0 & 0 & 0 & 0 & 1 \\ 0 & 0 & 0 & 0 & 0 & 0 & 0 & 0 & 0 & 0 & K_5 & 0 & a_{14,13} & 0 \end{bmatrix}, \tag{3.111}$$

where $a_{2,1} = -\frac{g}{l}$, $a_{4,3} = -\frac{g}{l} - K_1$, $a_{6,5} = -\frac{g}{l} - K_1 - K_2$, $a_{8,7} = -\frac{g}{l} - K_2 - K_3$, $a_{10,9} = -\frac{g}{l} - K_3 - K_4$, $a_{12,11} = -\frac{g}{l} - K_4 - K_5$, $a_{14,13} = -\frac{g}{l} - K_5$

$$E = \begin{bmatrix} 0 & 1 & 0 & 0 & 0 & 0 & 0 & 0 & 0 & 0 & 0 & 0 \\ e_{2,1} & -2C & K_1 & 0 & 0 & 0 & 0 & 0 & 0 & 0 & 0 & 0 \\ 0 & 0 & 0 & 1 & 0 & 0 & 0 & 0 & 0 & 0 & 0 & 0 \\ 0 & C & e_{4,3} & 0 & K_2 & 0 & 0 & 0 & 0 & 0 & 0 & 0 \\ 0 & 0 & 0 & 0 & 0 & 1 & 0 & 0 & 0 & 0 & 0 & 0 \\ 0 & 0 & K_1 & 0 & e_{6,5} & 0 & K_3 & 0 & 0 & 0 & 0 & 0 \\ 0 & 0 & 0 & 0 & 0 & 0 & 0 & 1 & 0 & 0 & 0 & 0 \\ 0 & 0 & 0 & 0 & K_2 & 0 & e_{8,7} & 0 & K_4 & 0 & 0 & 0 \\ 0 & 0 & 0 & 0 & 0 & 0 & 0 & 0 & 0 & 1 & 0 & 0 \\ 0 & 0 & 0 & 0 & 0 & 0 & K_3 & 0 & e_{10,9} & 0 & K_5 & 0 \\ 0 & 0 & 0 & 0 & 0 & 0 & 0 & 0 & 0 & 0 & 0 & 1 \\ 0 & 0 & 0 & 0 & 0 & 0 & 0 & 0 & K_4 & 0 & e_{12,11} & 0 \end{bmatrix}, \tag{3.112}$$

where $e_{2,1} = -\frac{g}{l}$, $e_{4,3} = -\frac{g}{l} - 2K_1$, $e_{6,5} = -\frac{g}{l} - 2K_2$, $e_{8,7} = -\frac{g}{l} - 2K_3$, $e_{10,9} = -\frac{g}{l} - 2K_4$, $e_{12,11} = -\frac{g}{l} - 2K_5$. We perform various simulations and show that the synchronization occurs. As can be seen from the Figures 3.28 and 3.29 the synchronization of seven pendulums is achieved. The analytical stability analysis of such a generalization remains as an open problem.

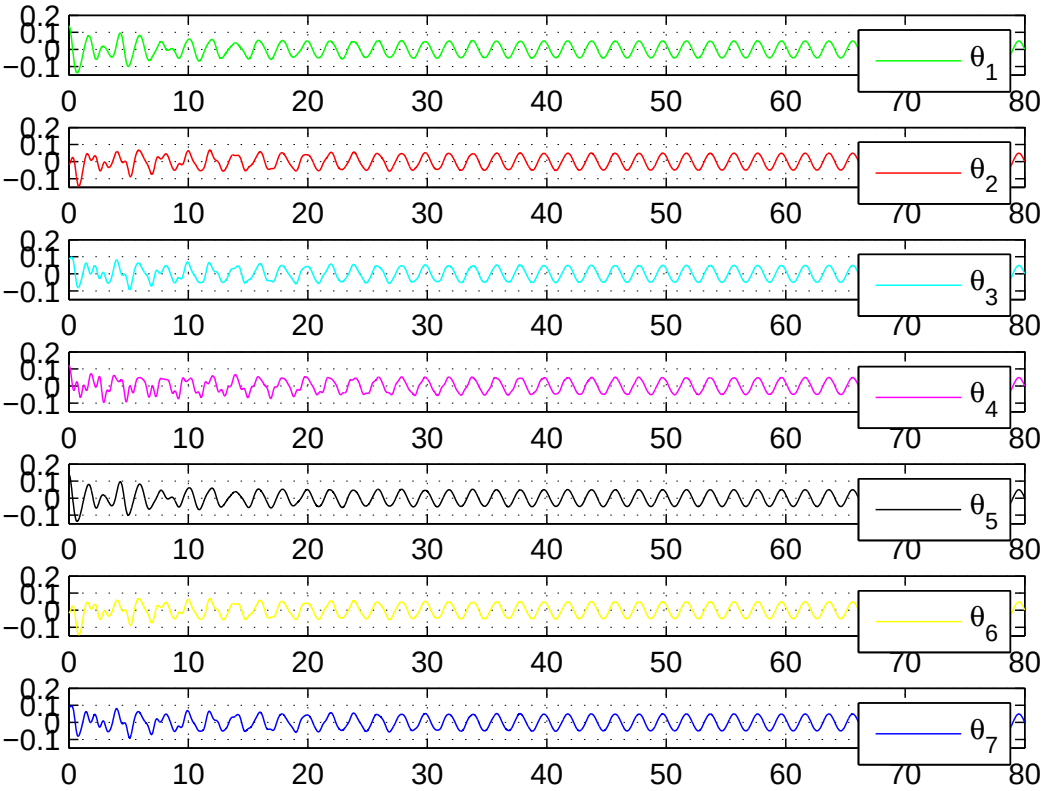


Figure 3.28: Simulation of seven pendulums coupled with five springs and one damper. Parameter values are $k_1 = 20$, $k_2 = 10$, $k_3 = 20$, $k_4 = 20$, $k_5 = 20$, $c = 5$, $l = 1$, $l_0 = .75$, $m = 1$, $\theta_1(0) = 8°$, $\dot{\theta}_1(0) = 0°$, $\theta_2(0) = -1°$, $\dot{\theta}_2(0) = 0°$, $\theta_3(0) = 5°$, $\dot{\theta}_3(0) = 0°$, $\theta_4(0) = 7°$, $\dot{\theta}_4(0) = 0°$, $\theta_5(0) = 6°$, $\dot{\theta}_5(0) = 0°$, $\theta_6(0) = -2°$, $\dot{\theta}_6(0) = 0,°$ $\theta_7(0) = -3°$, $\dot{\theta}_7(0) = 0°$.

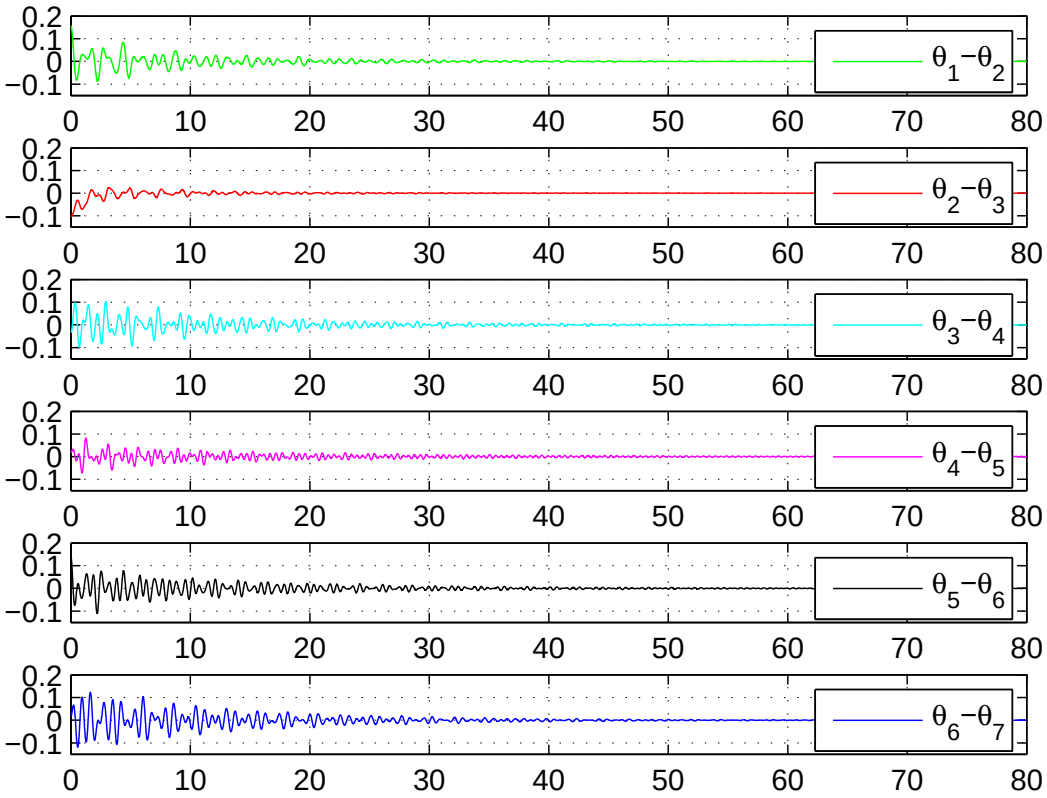


Figure 3.29: Error simulation of seven pendulums coupled with five springs and one damper. We choose the above parameters for simulation purposes.

## 3.9 Discussion and Contribution

In this part of the thesis, we investigated in-phase synchronization between single pendulums which are coupled under various combinations of spring and damper. Initially, we coupled two pendulums with series connected spring and damper and with parallel connected spring and damper to observe and compare the synchronization dynamics under different coupling forms. We observed that the parallel coupled system synchronizes faster than the series coupled system because in parallel coupled case, the damper has a direct connection between pendulums. Then we turned our attention to the analysis of synchronization dynamics of coupled multiple simple pendulums. We observed in-phase synchronization in all of the coupled systems as we have expected by using both analytical and numerical methods except one particular coupling configuration in four pendulums coupled with spring-damper-spring case. This special case consists of a

damper in the middle of pendulums and two springs which have equal spring constants and placed to the right and left of the damper. In fact, this is the only configuration in four pendulums case for which passive synchronization fails. Generalizing this result we conjectured that if there exist equal numbers of springs on the left and right side of the damper and the sum of the coefficients of the springs which are on the left and right sides of the damper are equal, i.e. $k_1 + k_2 + k_3 + ... = ... + k_{n-2} + k_{n-1} + k_n$ then the synchronization can not be achieved. Then we tried to derive a formula that generalizes the stability analysis of $n$ pendulums which are coupled with a single damper and $n-2$ springs and provides a guideline for simple pendulum synchronization. But we could only obtain bended matrix forms of system and error matrices. These points require further investigation.

Finally, we investigated the role of spring and damper in synchronization process. We revealed that the spring element only couples the pendulums, in other words it has no effect on synchronization. On the other hand, the damper element synchronizes the pendulums by equating the velocities of its connecting points.

# Chapter 4

# PASSIVE CONTROLLED IN-PHASE SYNCHRONIZATION OF COUPLED DOUBLE PENDULUMS

In this chapter we will investigate the synchronization dynamics of double pendulums under two different coupling schemes in which we present equations of motion, linearized systems, error equations and stability analysis. Two double pendulums are coupled by using parallel spring-damper in two different configurations namely, upper pendulums coupled and lower pendulums coupled. The aims of this Chapter are listed as follows:

- The basic aim of this Chapter is to achieve in-phase synchronization between double pendulums under two different coupling configurations namely, upper pendulums coupled and lower pendulums coupled, and to

compare the synchronization dynamics between these two coupling configurations.

- As in the previous Chapter we expect to observe in-phase synchronization between coupled double pendulums for any positive system parameters which provides a guideline for double pendulum synchronization. We want to support our findings by using both analytical and numerical methods.

Throughout the chapter we use several methods and make several assumptions as listed below:

- We use small angle approximation for linearization of equations of motion, i.e. we restrict the pendulum angles not to exceed 10°.
- We assume that spring and damper compresses and decompresses only in the horizontal diection.
- All of the components in this study are assumed to be frictionless.
- We assume that the pendulum rod, spring and damper are weightless.
- Equations of motion are obtained by using both free body diagrams and by Lagrangians.
- For stability analysis Routh-Hurwitz criterion is widely used.
- Simulations are obtained by using the nonlinear equations of motion of the systems under consideration in Matlab environment.

For simplicity we define the following parameter to be used thoughout the Chapter:

$$c_1 = \cos\theta_1,\ c_2 = \cos\theta_2,\ c_3 = \cos\theta_3,\ c_4 = \cos\theta_4,\ s_1 = \sin\theta_1,\ s_2 = \sin\theta_2,$$
$$s_3 = \sin\theta_3,\ s_4 = \sin\theta_4,\ c_{12} = \cos(\theta_1 - \theta_2),\ c_{34} = \cos(\theta_3 - \theta_4),$$
$$s_{12} = \sin(\theta_1 - \theta_2),\ s_{34} = \sin(\theta_3 - \theta_4),\ m_{12} = (m_1 + m_2), l_a = l - l_0,$$
$$l_b = l - 2l_0, m_{34} = (m_3 + m_4), \tag{4.1}$$

and let the sum of coupling terms be represented as:

$$S_{c1} = kl_0^2(\sin\theta_1 - \sin\theta_3) + cl_0^2(\cos\theta_1\dot{\theta}_1 - \cos\theta_3\dot{\theta}_3),$$

$$S_{c2} = c[l_1\cos\theta_1\dot{\theta}_1 + l_0\cos\theta_2\dot{\theta}_2 - (l_3\cos\theta_3\dot{\theta}_3 + l_0\cos\theta_4\dot{\theta}_4)] + k[l_1\sin\theta_1 + l_0\sin\theta_2$$
$$- (l_3\sin\theta_3 + l_0\sin\theta_4)]. \tag{4.2}$$

## 4.1 Two Double Pendulums Coupled from Upper part with Parallel Spring and Damper

Consider the system shown in the Figure 4.1. We couple two identical double pendulums from the point $l_0$ of the upper pendulums with parallel spring-damper and analyze the synchronization dynamics.

Let $m_1$, $l_1$, $m_2$, $l_2$, $m_3$, $l_3$, $m_4$, $l_4$ denote the mass and length of the pendulums, respectively. By using either free-body diagrams or performing Lagrangian method, we obtain the following equations of motion:

$$\ddot{\theta}_1 = \frac{-m_2 l_1 c_{12}(l_1 s_{12}\dot{\theta}_1^2 - g s_2) - m_2 l_1 l_2 s_{12}\dot{\theta}_2^2 - m_{12} g l_1 s_1 - c_1 S_{c1}}{m_{12} l_1^2 - m_2 l_1 l_2 {c_{12}}^2} \tag{4.3}$$

$$\ddot{\theta}_2 = \frac{m_{12} l_1(l_1 s_{12}\dot{\theta}_1^2 - g s_2) + c_{12}(m_2 l_1 l_2 s_{12}\dot{\theta}_2^2 + m_{12} g l_1 s_1 + c_1 S_{c1})}{m_{12} l_1 l_2 - m_2 l_1 l_2 {c_{12}}^2} \tag{4.4}$$

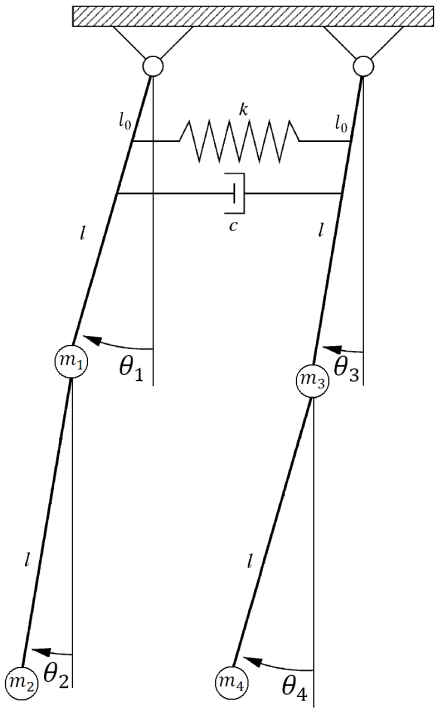


Figure 4.1: Two Double Pendulums Coupled from Upper part with Parallel Spring and Damper

$$\ddot{\theta}_3 = \frac{-m_4 l_3 c_{34}(l_3 s_{34}\dot{\theta}_3^2 - g s_4) - m_4 l_3 l_4 s_{34}\dot{\theta}_4^2 - m_{34} g l_3 s_3 + c_3 S_{c1}}{m_{34} l_3^2 - m_4 l_3 l_4 {c_{34}}^2} \tag{4.5}$$

$$\ddot{\theta}_4 = \frac{m_{34} l_3 (l_3 s_{34}\dot{\theta}_3^2 - g s_4) + c_{34}(m_4 l_3 l_4 s_{34}\dot{\theta}_4^2 + m_{34} g l_3 s_3 - c_3 S_{c1})}{m_{34} l_3 l_4 - m_4 l_3 l_4 {c_{34}}^2} \tag{4.6}$$

Now let us assume $m_1 = m_2 = m_3 = m_4 = m$, $l_1 = l_2 = l_3 = l_4 = l$, which is reasonable for synchronization, i.e. we assume the synchronization of two identical double pendulums. Let us define the state variables for this system as $z = \begin{bmatrix} \theta_1 & \dot{\theta}_1 & \theta_2 & \dot{\theta}_2 & \theta_3 & \dot{\theta}_3 & \theta_4 & \dot{\theta}_4 \end{bmatrix}$. By linearizing (4.3)-(4.6) around $z = 0$ we obtain $\dot{z} = Az$ where $A$ is given below:

$$A = \begin{bmatrix} 0 & 1 & 0 & 0 & 0 & 0 & 0 & 0 \\ -2\frac{g}{l} - K & -C & \frac{g}{l} & 0 & K & C & 0 & 0 \\ 0 & 0 & 0 & 1 & 0 & 0 & 0 & 0 \\ 2\frac{g}{l} + K & C & -2\frac{g}{l} & 0 & -K & -C & 0 & 0 \\ 0 & 0 & 0 & 0 & 0 & 1 & 0 & 0 \\ K & C & 0 & 0 & -2\frac{g}{l} - K & -C & \frac{g}{l} & 0 \\ 0 & 0 & 0 & 0 & 0 & 0 & 0 & 1 \\ -K & -C & 0 & 0 & 2\frac{g}{l} + K & C & -2\frac{g}{l} & 0 \end{bmatrix}. \tag{4.7}$$

and $C$, $K$ are given as:

$$K = \frac{kl_0^2}{ml^2}, C = \frac{cl_0^2}{ml^2}. \tag{4.8}$$

Applying Routh-Hurwitz criterion to the characteristic polynomial of this system matrix, we obtain the first column of the Routh table but it is too large to analyze. So instead we try to obtain the eigenvalues of this matrix, but because of the system matrix is too large we are only able to obtain the eigenvalues which are on the imaginary axis. The eigenvalues of the matrix $A$ which are on the imaginay axis can be given as:

$$s_1 = -\sqrt{\frac{(2+\sqrt{2})g}{l}}j, \tag{4.9}$$

$$s_2 = -\sqrt{\frac{(2-\sqrt{2})g}{l}}j, \tag{4.10}$$

$$s_3 = \sqrt{\frac{(2+\sqrt{2})g}{l}}j, \tag{4.11}$$

$$s_4 = \sqrt{\frac{(2-\sqrt{2})g}{l}}j. \tag{4.12}$$

These eigenvalues are related to the undamped oscillatory motion of the double pendulums. We expect the remaining four eigenvalues to be on the left half

plane to show that the double pendulum error dynamics are stable, hence that they synchronize. To find these eigenvalues we define the state variables vector $\hat{z}_e$ for error dynamics and apply similarity transformation to matrix $A$ as follows:

$$\hat{z}_e = [\theta_1 - \theta_3,\ \dot{\theta}_1 - \dot{\theta}_3,\ \theta_2 - \theta_4,\ \dot{\theta}_2 - \dot{\theta}_4,\ \theta_3,\ \dot{\theta}_3,\ \theta_4,\ \dot{\theta}_4], \tag{4.13}$$

$$\dot{\hat{z}}_e = TAT^{-1}\hat{z}_e = \hat{A}\hat{z}_e, \tag{4.14}$$

where the transformation matrix is given as:

$$T = \begin{bmatrix} 1 & 0 & 0 & 0 & -1 & 0 & 0 & 0 \\ 0 & 1 & 0 & 0 & 0 & -1 & 0 & 0 \\ 0 & 0 & 1 & 0 & 0 & 0 & -1 & 0 \\ 0 & 0 & 0 & 1 & 0 & 0 & 0 & -1 \\ 0 & 0 & 0 & 0 & 1 & 0 & 0 & 0 \\ 0 & 0 & 0 & 0 & 0 & 1 & 0 & 0 \\ 0 & 0 & 0 & 0 & 0 & 0 & 1 & 0 \\ 0 & 0 & 0 & 0 & 0 & 0 & 0 & 1 \end{bmatrix}. \tag{4.15}$$

Then $\hat{A}$ given by (4.14) can be computed as:

$$\hat{A} = \begin{bmatrix} 0 & 1 & 0 & 0 & 0 & 0 & 0 & 0 \\ -2K - 2\frac{g}{l} & -2C & \frac{g}{l} & 0 & 0 & 0 & 0 & 0 \\ 0 & 0 & 0 & 1 & 0 & 0 & 0 & 0 \\ 2K + 2\frac{g}{l} & 2C & -2\frac{g}{l} & 0 & 0 & 0 & 0 & 0 \\ 0 & 0 & 0 & 0 & 0 & 1 & 0 & 0 \\ K & C & 0 & 0 & -2\frac{g}{l} & 0 & \frac{g}{l} & 0 \\ 0 & 0 & 0 & 0 & 0 & 0 & 0 & 1 \\ -K & -C & 0 & 0 & -2\frac{g}{l} & 0 & -2\frac{g}{l} & 0 \end{bmatrix}. \tag{4.16}$$

Since we are interested in the error dynamics, we first define the synchronization errors as $e_1 = \theta_1 - \theta_3$, $e_2 = \theta_2 - \theta_4$ and the state variable $z_e$ as

$e_z = [e_1 \ \dot{e}_1 \ e_2 \ \dot{e}_2]^T$. From (4.16), the linearized error dynamics can be calculated as $\dot{z}_e = \hat{A}_e z_e$, where $\hat{A}_e$ is given below:

$$\hat{A}_e = \begin{bmatrix} 0 & 1 & 0 & 0 \\ -2\frac{g}{l} - 2K & -2C & \frac{g}{l} & 0 \\ 0 & 0 & 0 & 1 \\ 2\frac{g}{l} + 2K & 2C & -2\frac{g}{l} & 0 \end{bmatrix}. \tag{4.17}$$

Let us define the characteristic polynomial of $\hat{A}_e$ as $\hat{p}_e(s) = \det(sI - \hat{A}_e)$. By applying Routh-Hurwitz criterion to $\hat{p}_e(s)$, we obtain the first column of the Routh table as given below:

| | |
|---|---|
| $s^4$ | $1$ |
| $s^3$ | $2C$ |
| $s^2$ | $2K + 3\frac{g}{l}$ |
| $s^1$ | $\frac{2Cg^2}{3gl+2Kl^2}$ |
| $s^0$ | $\frac{2g(g+Kl)}{l^2}$ |

Table 4.1: The first column of the Routh table which is obtained by applying Routh-Hurwitz criterion to error equation of the coupled system.

It can be easily seen from the Table 4.1 that the elements in the first column of the Routh array are always positive which shows that all the eigenvalues of the error equations are on the left half plane, the remaining four eigenvalues as we have mentioned above, hence the linearized error equations are stable. As a result the the nonlinear error dynamics of this system, obtained by subtracting (4.3) from (4.5) and (4.4) from (4.6), are locally asymptotically stable. In other words, once $|e_1(0)|$, $|\dot{e}_1(0)|$, $|e_2(0)|$ and $|\dot{e}_2(0)|$ are sufficiently small the synchronization goal is achieved [35]. On the other hand, since the eigenvalues of $A$ and $\hat{A}$ are the same and the remaining four eigenvalues are on the left half plane, the matrix $A$ has stable and oscillatory eigenvalues as we have observed in the previous sections. Typical simulation results are given in Figures 4.2 and 4.3.

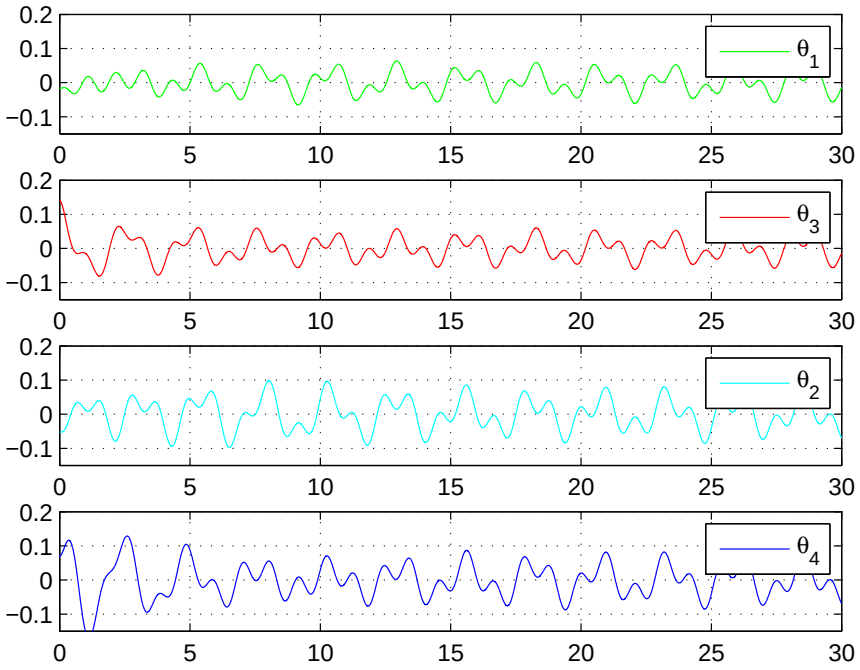


Figure 4.2: Simulation of two double pendulums coupled from upper pendulums. In these paticular simulations we choose $m = 1,\ l = 1,\ k = 10,\ c = 5,\ l_0 = 0.75,\ \theta_1(0) = -5°,\ \dot{\theta}_1(0) = 0°,\ \theta_2(0) = -9°,\ \dot{\theta}_2(0) = 0°,\ \theta_3(0) = 8°,\ \dot{\theta}_3(0) = 0°,\ \theta_4(0) = 4°,\ \dot{\theta}_4(0) = 0°$.

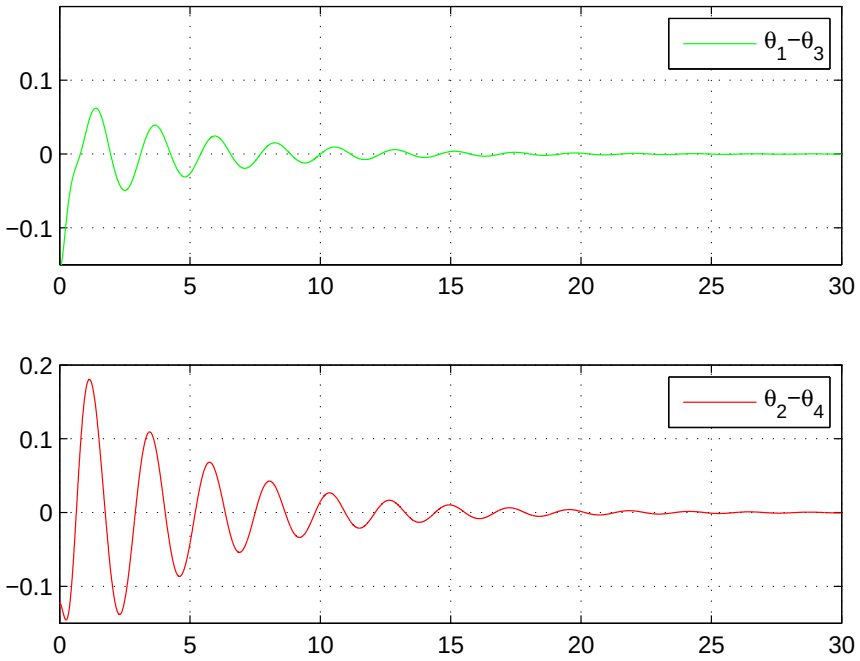


Figure 4.3: Error simulation of two coupled double pendulums. We choose the above parameters for simulation purposes.

## 4.2 Two Double Pendulums Coupled from Lower part with Parallel Spring and Damper

Consider the system shown in the Figure 4.4. We couple two identical double pendulums from the point $l_0$ of the lower pendulums with parallel spring-damper and analyze the synchronization dynamics.

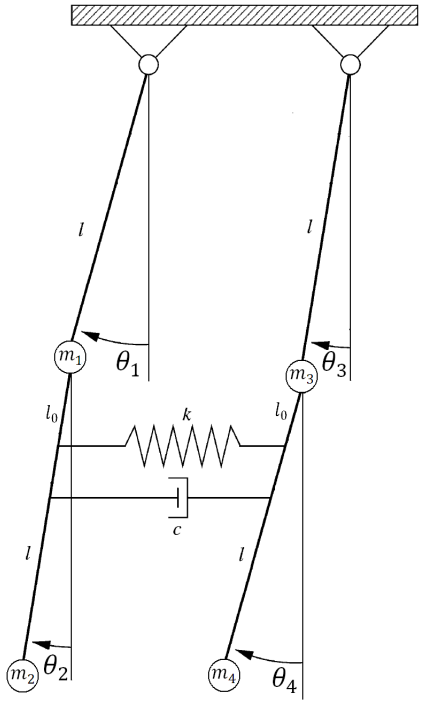


Figure 4.4: Two Double Pendulums Coupled from Lower part with Parallel Spring and Damper

Let $m_1$, $l_1$, $m_2$, $l_2$, $m_3$, $l_3$, $m_4$, $l_4$ denote the mass and length of the pendulums, respectively as before. By using either free-body diagrams or performing Lagrangian method, we obtain the following equations of motion:

$$\ddot{\theta}_1 = \frac{-c_{12}(m_2 l_1 l_2 s_{12}\dot{\theta}_1^2 - m_2 g l_2 s_2 - l_0 c_2 S_{c2}) - m_2 l_2^2 s_{12}\dot{\theta}_2^2 - m_{12} g l_2 s_1 - l_2 c_1 S_{c2}}{m_{12} l_1 l_2 - m_2 l_1 l_2 {c_{12}}^2} \tag{4.18}$$

$$\ddot{\theta}_2 = \frac{m_{12}(m_2 l_2(l_1 s_{12}\dot{\theta}_1^2 - g s_2) - l_0 c_2 S_{c2}) + m_2 l_2 c_{12}(m_2 l_2 s_{12}\dot{\theta}_2^2 + m_{12} g s_1 + c_1 S_{c2})}{m_{12} m_2 l_2^2 - (m_2 l_2 c_{12})^2} \tag{4.19}$$

$$\ddot{\theta}_3 = \frac{-c_{34}(m_4 l_3 l_4 s_{34}\dot{\theta}_3^2 - m_4 g l_4 s_4 + l_0 c_4 S_{c2}) - m_4 l_4^2 s_{34}\dot{\theta}_4^2 - m_{34} g l_4 s_3 + l_4 c_3 S_{c2}}{m_{34} l_3 l_4 - m_4 l_3 l_4 {c_{34}}^2} \tag{4.20}$$

$$\ddot{\theta}_4 = \frac{m_{34}(m_4 l_4(l_3 s_{34}\dot{\theta}_3^2 - g s_4) + l_0 c_4 S_{c2}) + m_4 l_4 c_{34}(m_4 l_4 s_{34}\dot{\theta}_4^2 + m_{34} g s_3 - c_3 S_{c2})}{m_{34} m_4 l_4^2 - (m_4 l_4 c_{34})^2} \tag{4.21}$$

Now let us assume as before $m_1 = m_2 = m_3 = m_4 = m$, $l_1 = l_2 = l_3 = l_4 = l$, which is reasonable for synchronization, i.e. we assume the synchronization of two identical double pendulums. Let us define the state variables for this system as $z = \begin{bmatrix} \theta_1 & \dot{\theta}_1 & \theta_2 & \dot{\theta}_2 & \theta_3 & \dot{\theta}_3 & \theta_4 & \dot{\theta}_4 \end{bmatrix}$ as before. By linearizing (4.18)-(4.21) around $z = 0$ we obtain $\dot{z} = Az$ where $A$ is given below:

$$A = \begin{bmatrix} 0 & 1 & 0 & 0 & 0 & 0 & 0 & 0 \\ a_{2,1} & -Cll_a & a_{2,3} & -Cl_0 l_a & Kll_a & Cll_a & Kl_0 l_a & Cl_0 l_a \\ 0 & 0 & 0 & 1 & 0 & 0 & 0 & 0 \\ a_{4,1} & Cll_b & a_{4,3} & Cl_0 l_b & -Kll_b & -Cll_b & -Kl_0 l_b & -Cl_0 l_b \\ 0 & 0 & 0 & 0 & 0 & 1 & 0 & 0 \\ Kll_a & Cll_a & Kl_0 l_a & Cl_0 l_a & a_{6,5} & -Cll_a & a_{6,7} & -Cl_0 l_a \\ 0 & 0 & 0 & 0 & 0 & 0 & 0 & 1 \\ -Kll_b & -Cll_b & -Kl_0 l_b & -Cl_0 l_b & a_{8,5} & Cll_b & a_{8,7} & Cl_0 l_b \end{bmatrix}. \tag{4.22}$$

where $a_{2,1} = -Kll_a - 2\frac{g}{l}$, $a_{2,3} = \frac{g}{l} - Kl_0 l_a$, $a_{4,1=2\frac{g}{l}+Kll_b}$, $a_{4,3} = -2\frac{g}{l} + Kl_0 l_b$, $a_{6,5} = -Kll_a - 2\frac{g}{l}$, $a_{6,7} = \frac{g}{l} - Kl_0 l_a$, $a_{8,5} = 2\frac{g}{l} + Kll_b$, $a_{8,7} = -2\frac{g}{l} + Kl_0 l_b$

Applying Routh-Hurwitz criterion to the characteristic polynomial of this system matrix or the eigenvalue analysis does not yield meaningful results since the matrix $A$ is too large. Instead of analytical analysis we applied numerical methods to analyze the synchronous behaviour of the coupled system. In this analysis we obtain and plot the eigenvalues of matrix $A$ by spanning $k$ and $c$ parameters between 0 to 100. Figure 4.5 illustrates the results we obtain.

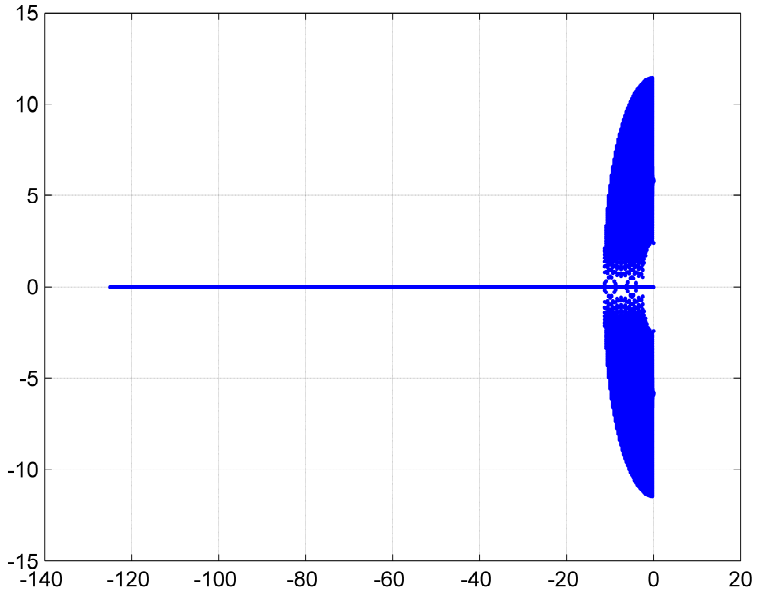


Figure 4.5: Plot of eigenvalues of matrix $A$. In this particular simulations we choose $m = 1,\ l = 1,\ l_0 = 0.75,\ k = 0$ to 100 and $c = 0$ to 100.

It is clear from the Figure 4.5 that the eigenvalues remain either on the left half plane and on the imaginary axis as we have expected. The eigenvalues which are on the imaginary axis, force the double pendulums to oscillate without damping and the eigenvalues which are on the left half plane stabilize the pendulum error dynamics.

For further analysis consider the error dynamics given below. Let us define the state variable vector $\hat{z}_e$ for error dynmamics as follows:

$$\hat{z}_e = [\theta_1 - \theta_3,\ \dot{\theta}_1 - \dot{\theta}_3,\ \theta_2 - \theta_4,\ \dot{\theta}_2 - \dot{\theta}_4,\ \theta_3,\ \dot{\theta}_3,\ \theta_4,\ \dot{\theta}_4], \tag{4.23}$$

and matrix $T$ be the transformation matrix given as:

$$T = \begin{bmatrix} 1 & 0 & 0 & 0 & -1 & 0 & 0 & 0 \\ 0 & 1 & 0 & 0 & 0 & -1 & 0 & 0 \\ 0 & 0 & 1 & 0 & 0 & 0 & -1 & 0 \\ 0 & 0 & 0 & 1 & 0 & 0 & 0 & -1 \\ 0 & 0 & 0 & 0 & 1 & 0 & 0 & 0 \\ 0 & 0 & 0 & 0 & 0 & 1 & 0 & 0 \\ 0 & 0 & 0 & 0 & 0 & 0 & 1 & 0 \\ 0 & 0 & 0 & 0 & 0 & 0 & 0 & 1 \end{bmatrix}. \tag{4.24}$$

Applying similarity transformation to the matrix $A$, i.e. $\hat{A} = TAT^{-1}$, we obtain the matrix $\hat{A}$ as follows:

$$\hat{A} = \begin{bmatrix} 0 & 1 & 0 & 0 & 0 & 0 & 0 & 0 \\ \hat{a}_{2,1} & -2Cll_a & \hat{a}_{2,3} & -2Cl_al_0 & 0 & 0 & 0 & 0 \\ 0 & 0 & 0 & 1 & 0 & 0 & 0 & 0 \\ \hat{a}_{4,1} & 2Cll_b & \hat{a}_{4,3} & 2Cl_bl_0 & 0 & 0 & 0 & 0 \\ 0 & 0 & 0 & 0 & 0 & 1 & 0 & 0 \\ Kll_a & Cll_a & Kl_al_0 & Cl_al_0 & -2\frac{g}{l} & 0 & \frac{g}{l} & 0 \\ 0 & 0 & 0 & 0 & 0 & 0 & 0 & 1 \\ -Kll_b & -Cll_b & -Kl_bl_0 & -Cl_bl_0 & 2\frac{g}{l} & 0 & -2\frac{g}{l} & 0 \end{bmatrix}, \tag{4.25}$$

where $\hat{a}_{2,1} = -2\frac{g}{l} - 2Kll_a$, $\hat{a}_{2,3} = \frac{g}{l} - 2Kl_al_0$, $\hat{a}_{4,1} = 2\frac{g}{l} + 2Kll_b$, $\hat{a}_{4,3} = -2\frac{g}{l} + 2Kl_bl_0$.

Since we are interested in the error dynamics, we first define the synchronization errors as $e_1 = \theta_1 - \theta_3$, $e_2 = \theta_2 - \theta_4$ and the state variable $z_e$ as $z_e = [e_1 \ \dot{e}_1 \ e_2 \ \dot{e}_2]^T$. From (4.25), the linearized error dynamics can be calculated as $\dot{z}_e = \hat{A}_e z_e$, where $\hat{A}_e$ is given below:

$$\hat{A}_e = \begin{bmatrix} 0 & 1 & 0 & 0 \\ -2\frac{g}{l} - 2Kll_a & -2Cll_a & \frac{g}{l} - 2Kl_al_0 & -2Cl_al_0 \\ 0 & 0 & 0 & 1 \\ 2\frac{g}{l} + 2Kll_b & 2Cll_b & -2\frac{g}{l} + 2Kl_bl_0 & 2Cl_bl_0 \end{bmatrix}. \tag{4.26}$$

Let us define the characteristic polynomial of $\hat{A}_e$ as $\hat{p}_e(s) = \det(sI - \hat{A}_e)$. By applying Routh-Hurwitz criterion to $\hat{p}_e(s)$, we obtain the first column of the Routh table as given in Table 4.2. It can be easily seen from the Table 4.2 that all the elements in the first column of Routh array are positive unless $l_0 \neq \frac{1}{\sqrt{2}}l$. This shows that all the eigenvalues of the error equations are on the left half plane as long as $l_0 \neq \frac{1}{\sqrt{2}}l$, hence the linearized error equations are stable. As a result, the the nonlinear error dynamics of this system, obtained by subtracting (4.18) from (4.20) and (4.19) from (4.21), are locally asymptotically stable. In other words, once $|e_1(0)|$, $|\dot{e}_1(0)|$, $|e_2(0)|$ and $|\dot{e}_2(0)|$ are sufficiently small the synchronization goal is achieved [35]. In case of $l_0 = \frac{1}{\sqrt{2}}l$, the term which corresponds to $s^1$ becomes 0 in the first column of the Routh table and the error dynamics become oscillatory, hence synchronization can not be achieved. Typical simulation results are given in Figures 4.6-4.9.

| | |
|---|---|
| $s^4$ | $1$ |
| $s^3$ | $2C(l_0^2 + l_a^2)$ |
| $s^2$ | $2K(l_0^2 + l_a^2) + g\frac{(l-2l_0)^2+2(l-l_0)^2}{l_0^2+l_a^2}$ |
| $s^1$ | $\frac{2Cg^2(l^2-2l_0^2)^2}{l(2Kl(l_0^2+l_a^2)^2+g((l-2l_0)^2+2(l-l_0)^2))}$ |
| $s^0$ | $\frac{2g(g+Kl(l_b^2+2l_0^2))}{l^2}$ |

Table 4.2: The first column of the Routh table which is obtained by applying Routh-Hurwitz criterion to error equation of the coupled system.

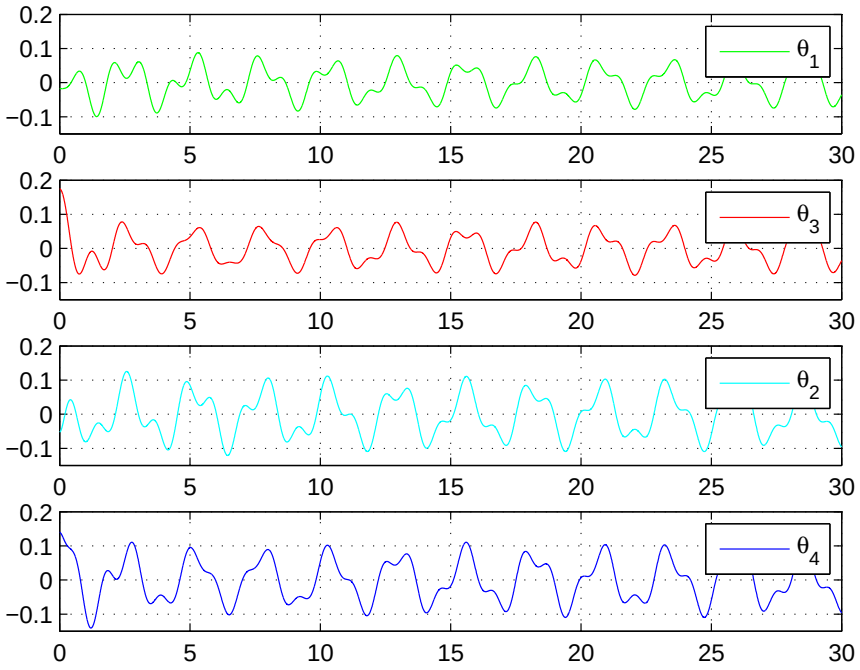


Figure 4.6: Simulation of two double pendulums coupled from lower pendulums. In these paticular simulations we choose $m = 1,\ l = 1,\ k = 10,\ c = 3,\ l_0 = 0.95,\ \theta_1(0) = -1^\circ,\ \dot{\theta}_1(0) = 0^\circ,\ \theta_2(0) = -3^\circ,\ \dot{\theta}_2(0) = 0^\circ,\ \theta_3(0) = 10^\circ,\ \dot{\theta}_3(0) = 0^\circ,\ \theta_4(0) = 8^\circ,\ \dot{\theta}_4(0) = 0^\circ$.

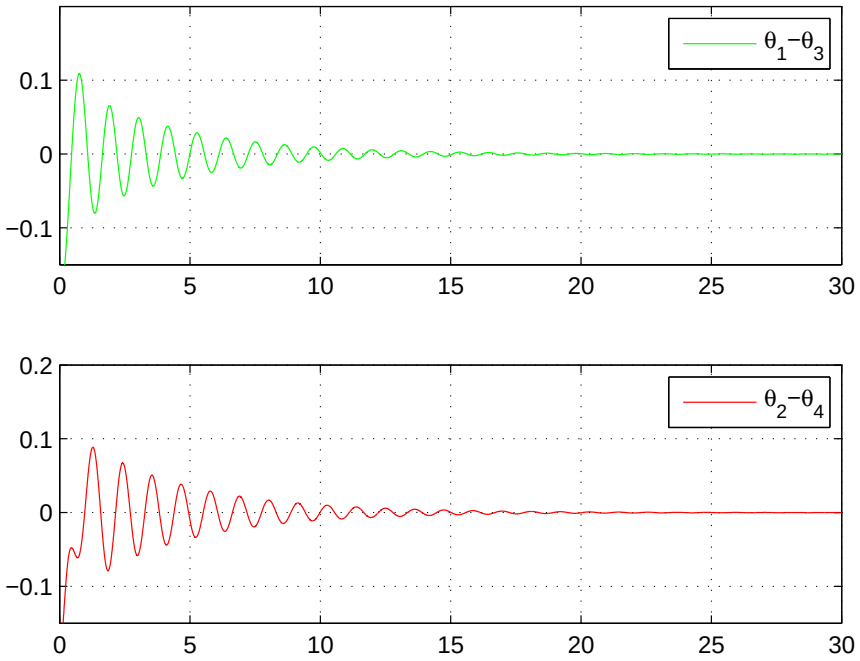


Figure 4.7: Error simulation of two coupled double pendulums. We choose the above parameters for simulation purposes.

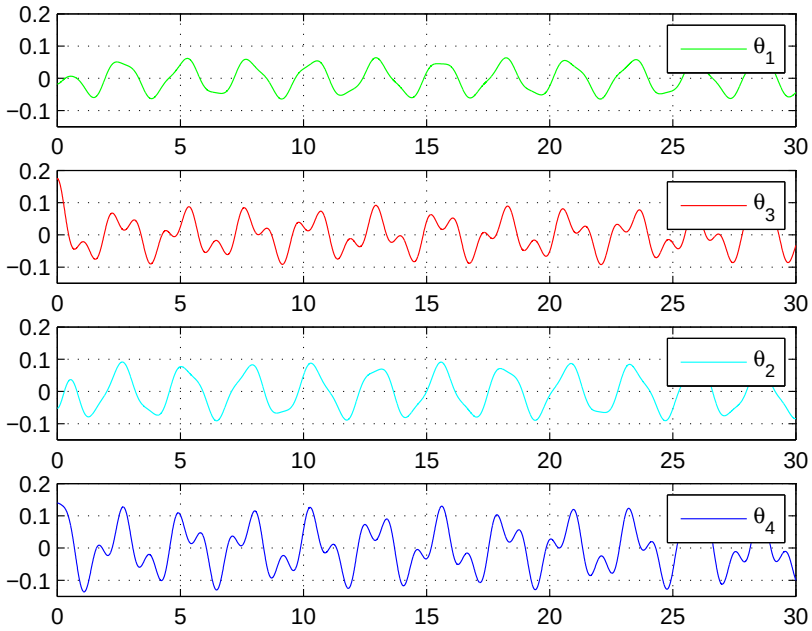


Figure 4.8: Simulation of two double pendulums coupled from lower pendulums. In these paticular simulations we choose $m = 1,\ l = 1,\ k = 10,\ c = 3,\ l_0 = \frac{1}{\sqrt{2}}l,\ \theta_1(0) = -1°,\ \dot{\theta}_1(0) = 0°,\ \theta_2(0) = -3°,\ \dot{\theta}_2(0) = 0°,\ \theta_3(0) = 10°,\ \dot{\theta}_3(0) = 0°,\ \theta_4(0) = 8°,\ \dot{\theta}_4(0) = 0°$.

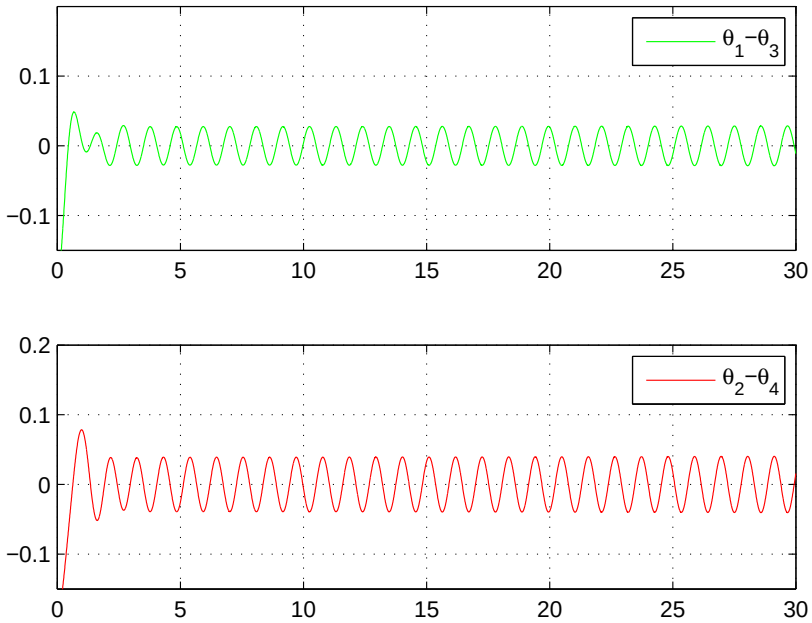


Figure 4.9: Error simulation of two coupled double pendulums. We choose the above parameters for simulation purposes.

## 4.3 Discussion and Contribution

In this part of the thesis, we investigated in-phase synchronization between double pendulums which are coupled under two different coupling configurations.

Initially, we coupled two double pendulums from upper pendulums with parallel connnected spring and damper. We obtained analytically that the double pendulums are synchronized for any positive system paramaters. Then we proceed with coupling two double pendulums from lower pendulums with parallel connected spring and damper. Interestingly, opposed to what we have expected we obtained numerically and analytically that the double pendulums are synchronized for any positive system parameter except for a particular coupling $l_0 = \frac{1}{\sqrt{2}}l$.

Finally, we tried to compare the synchronization dynamics between these two coupling configurations but either by using analytical or numerical methods we could not find meaningful comparison results. This point requires further investigation.

# Chapter 5

# ACTIVE CONTROLLED MASTER SLAVE SYNCHRONIZATION OF TWO BALL HOPPERS

In this Chapter we will present dynamics and synchronization of two ball hoppers in master-slave configuration. We try to achieve master-slave synchronization by using different gait controllers and provide simulation results. The aims of this Chapter are listed as follows:

- The basic aim of this Chapter is to achieve master-slave synchronization between two ball hoppers under two different gait controllers namely, fully-actuated and under-actuated controllers, which is the first step of understanding the synchronious behaviour behind the legged systems.
- In this Chapter we expect to achieve full synchronization, i.e. time and apex state synchronization, between the hoppers in fully-actuated controller case

and we expect to achieve partial apex state synchronization between the hoppers in under-actuated controller case.

## 5.1 Overview of SLIP model and Ball Hopper

In this section, we will briefly present the SLIP (Spring Loaded Inverted Pendulum) model and the simplified hopper model, which is also refered as controllable ball or ball hopper. This simplified model summerizes the dynamics of the SLIP model [36]. Now, let us give definitions of dynamics of the SLIP model first.

The SLIP model consists of a point mass, which represents the total mass for the system of interest, attached to a massless spring leg and it is depicted in the Figure 5.1. SLIP has two seperate dynamics, namely flight and stance dynamics and each of these dynamics is divided into two subdynamics and they are explained as follows [36], [37]:

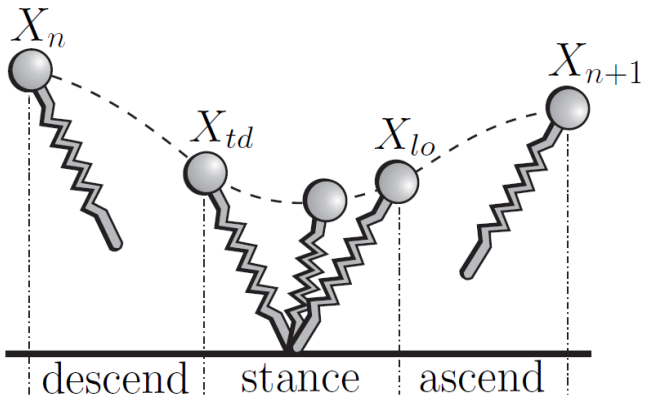


Figure 5.1: The SLIP Model

- In flight, the model follows an uncontrollable ballistic trajectory and depending on the sign of the vertical velocity of the model, SLIP ascents or descent. In ascent phase the vertical velocity is positive and continuously decreases in magnitude until the SLIP reaches it's maximum height. In descent phase the vertical velocity is negative and continuously increases

in magnitude until the spring leg touches the ground. Now let us present the flight dynamics. Let the state variables of the SLIP be given as:

$$b = [b_x \; b_{\dot{x}} \; b_y \; b_{\dot{y}} \; b_{tx}]^T, \tag{5.1}$$

where $b_x$, $b_y$ are horizontal and vertical body (mass) positions, $b_{\dot{x}}$, $b_{\dot{y}}$ are horizontal and vertical body velocities and $b_{tx}$ is the horizontal toe position. Then the flight dynamics of the SLIP is given as follows:

$$\dot{b} = [b_{\dot{x}} \; 0 \; b_{\dot{y}} \; -g \; b_{\dot{x}} \; ]. \tag{5.2}$$

- In stance, the toe, i.e. the spring, touches the ground and remains stationary on the ground and depending on the sign of the rate of change of the leg length, SLIP compresses or decompresses. In compression phase the rate of change of leg length is negative and the stored energy on the spring increases until the mass of the SLIP reaches it's minimum height. In decompression phase the rate of change of leg length is positive and the stored energy on the spring decreases until the SLIP lifts off the ground. The stance dynamics can be given as follows:

$$m\ddot{q}_r = mq_r\dot{q}_\theta^2 + k(l_0 - q_r) - mg\cos(q_\theta), \tag{5.3}$$

$$0 = \frac{d}{dt}(mq_r^2\dot{q}_\theta) + mgq_r\sin q_\theta, \tag{5.4}$$

where $m$, $g$ are body mass and gravitational acceleration; $l_0$, $k$ are leg rest length and leg stiffnessand and $q_r$, $q_\theta$ are leg length and leg angle.

The process of changing from one phase to another is called transition and the transition events of the SLIP play a key role throughout the chapter. Let us give the general properties of these events.

- Apex : This event occurs during the flight phase when the SLIP body reaches its maximum height, i.e. maximum gravitational potential energy, between ascend and descend phases.

- Touchdown : This is the flight to stance transition event, i.e. the transition from descent phase to compression phase. It occurs when the leg touches to the ground.

- Bottom : This event occurs during the stance phase when the SLIP body reaches its mininum height(minimum leg length), i.e. the spring potential energy reaches its maximum value, between compression and decompression phases.

- Liftoff : This is the stance to flight transition event, i.e. the transition from decompression phase to ascent phase. It occurs when the leg lifts off the ground.

The simplified SLIP model or ball hopper, which is depicted in the Figure 5.2, summarizes and mimics the dynamics of the SLIP model.

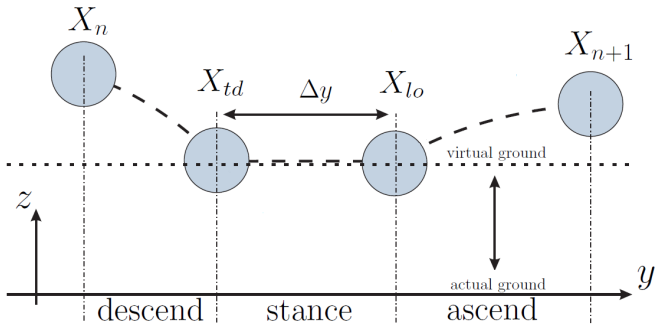


Figure 5.2: The Ball Hopper

Now let us define the dynamics of ball hopper. During flight, the simplified hopper follows an uncontrollable ballistic trajectory. Let the state variables of the ball hopper be given as:

$$X = [y\ z\ \dot{y}\ \dot{z}], \tag{5.5}$$

where $y,\ z,\ \dot{y},\ \dot{z}$ variables denotes the horizontal and vertical system positions and velocities, respectively.

The flight dynamics of the ball hopper can be given as:

$$\dot{X} = [\dot{y}\ \dot{z}\ \ddot{y}\ \ddot{z}] = [\dot{y}\ \dot{z}\ 0\ -g]. \tag{5.6}$$

In the stance dynamics, the compression and decompression of the spring until the liftoff event is realized using a direct, instantaneous touchdown to liftoff map, controlled by the horizontal shift $\Delta y$, the liftoff velocity angle $\theta$, and the liftoff velocity magnitude gain $k$. Let us explain these control parameters which have very close correspondence to control parameters used for the SLIP model [36].

- The liftoff velocity magnitude gain, denoted by k, approximately corresponds to the spring energy control for the SLIP model.
- The liftoff velocity angle adjustment, denoted by $\theta$, closely corresponds to the touchdown leg angle of the SLIP model with respect to ground normal.
- The position shifting control,denoted by $\Delta y$, which corresponds to the average stiffness of the SLIP leg, is used to increase or decrease the horizontal span of the stance phase.

Then the touchdown to liftoff map for the simplified hopper model is given by:

$$X_{lo} = AX_{td} + B, \tag{5.7}$$

where $A$ and $B$ are given as:

$$A = \begin{bmatrix} 1 & 0 & 0 & 0 \\ 0 & 1 & 0 & 0 \\ 0 & 0 & 1-(1+k)\sin^2\theta & 0.5(1+k)\sin 2\theta \\ 0 & 0 & 0.5(1+k)\sin 2\theta & 1-(1+k)\cos^2\theta \end{bmatrix}, \tag{5.8}$$

$$B = \begin{bmatrix} \Delta y \\ 0 \\ 0 \\ 0 \end{bmatrix} \text{[36]}. \tag{5.9}$$

## 5.2 Master-Slave Synchronization of Two Ball Hoppers using Fully-Actuated Controller

In this section, we will present master-slave synchronization of two ball hoppers using fully-actuated controller. By fully-actuated control we mean that all three control parameters, namely $k$, $\theta$ and $\Delta y$ can be utilized by the controller. Synchronization is achieved by finding appropriate control inputs which are necessary to bring the mass hopper from any state $X_n$ to the selected goal point $X_g$. We use a simple deadbeat controller for the simplified hopper. The controller measures the ball hopper's state at every apex and applies a single-step deadbeat controller, i.e. selects control inputs, which brings the hopper to the goal state.

Now assume that a ball hopper, which is called the master hopper, is driven by a controller already designed and is not relevant for the synchronization goal. In other words, this controller ensures convergence of the states of the master hopper to a desired trajectory. Initially, we train the master hopper for a stride to measure the corresponding apex state. Then the slave hopper tries to imitate the motion of the master hopper from one stride behind. We assume that we have the full knowledge about the master hopper, i.e. we precisely measure the apex states of the master hopper. After the first stride of the master hopper by using the deadbeat controller, we try to estimate the control parameters of the master hopper. Then we apply these estimated control parameters to the slave hopper. So applying these control parameters to the slave hopper we obtain master-slave synchronization between these two hopper. Figure 5.3 shows that the controller estimates of the slave hopper perfectly match with the control inputs of the master hopper.

Figure 5.3 states the perfect apex state sychronization of the ball hoppers. Even if we could achieve apex state synchronization and perfect trajectory tracking, the time synchronization of ball hoppers fails due to the use of deadbeat

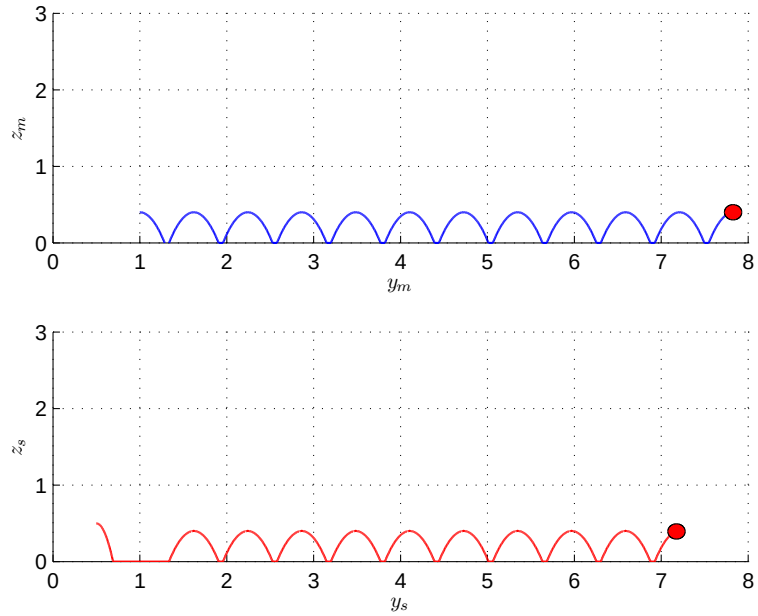


Figure 5.3: Master-Slave Synchronization of Two Ball Hoppers. For the master hopper we choose $k = 1$, $\theta = 0$, $\Delta y = 0.05$ as the control inputs and $[y\ z\ \dot{y}\ \dot{z}] = [1\ 0.4\ 1\ 0]$ as the initial conditions. In this particular simulation we choose the initial conditions for the slave hopper as $[y\ z\ \dot{y}\ \dot{z}] = [0.5\ 0.5\ 0.6\ 0]$

controller. Let us denote the apex state variables of master and slave hoppers as $X_m = [y_m\ z_m\ \dot{y}_m\ \dot{z}_m]$ and $X_s = [y_s\ z_s\ \dot{y}_s\ \dot{z}_s]$, respectively and for further analysis consider the following error figures:

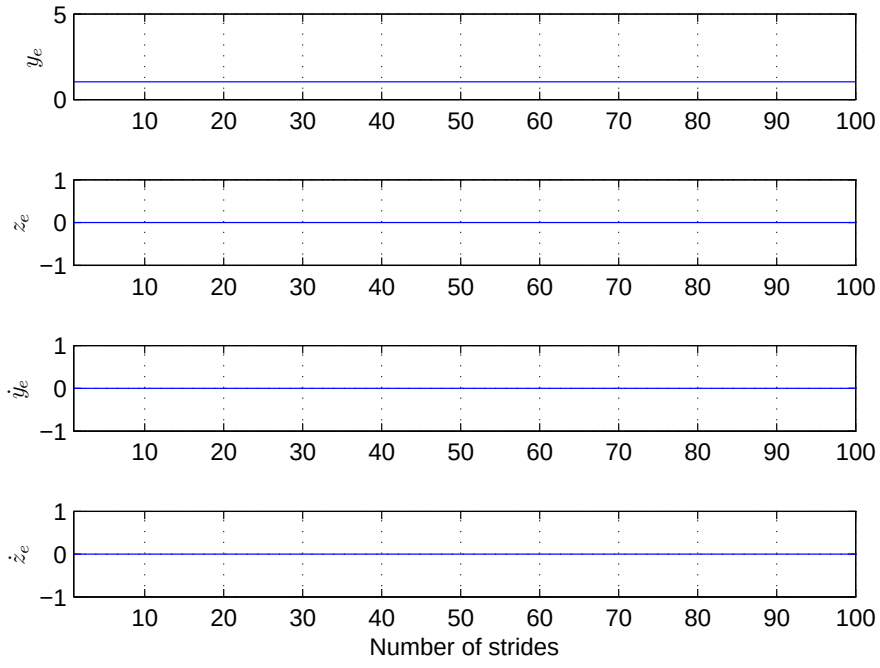


Figure 5.4: Apex states error figures. The $y$, $z$, $\dot{y}$ state variables fully synchronize.

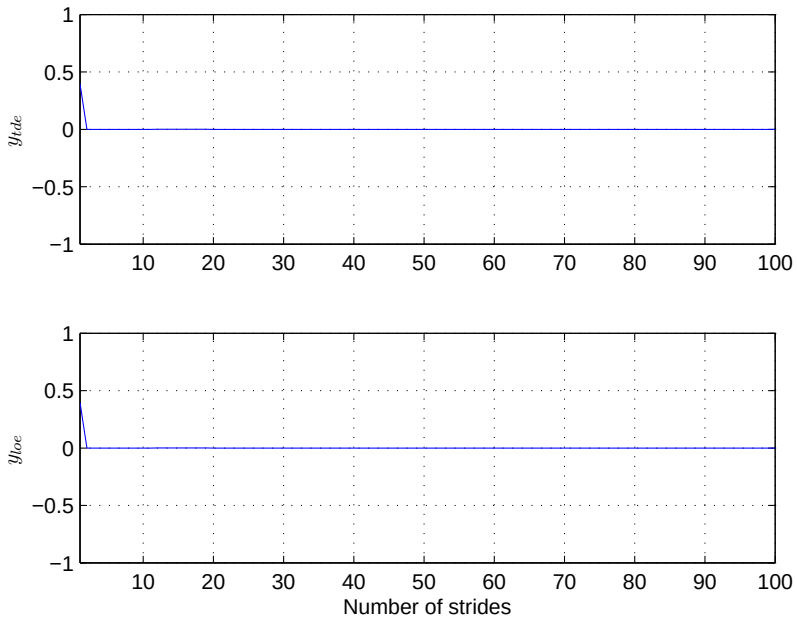


Figure 5.5: Touchdown and liftoff position error figures. After the first stride touchdown and litoff positions synchronize.

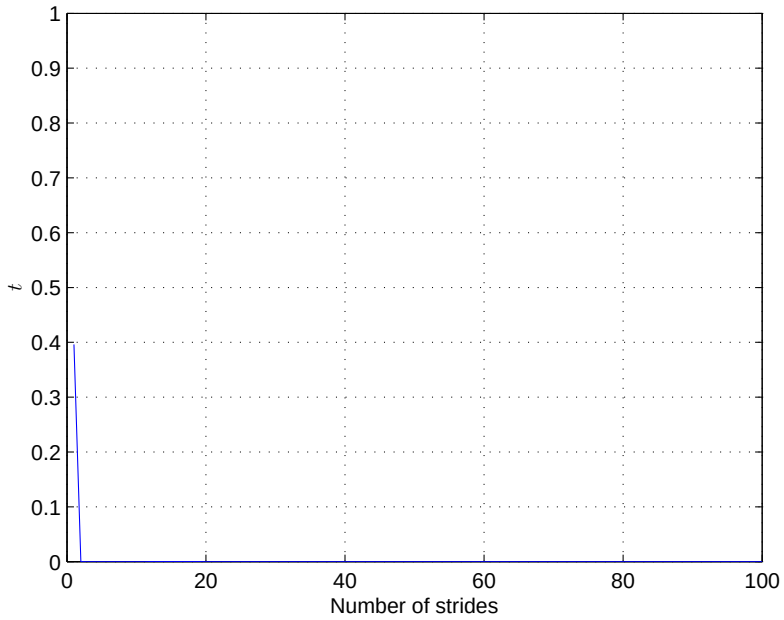


Figure 5.6: Differences of time that is spent between present apex to apex at each stride.

Here $y_e = y_m - y_s$, $z_e = z_m - z_s$, $\dot{y}_e = \dot{y}_m - \dot{y}_s$, $\dot{z}_e = \dot{z}_m - \dot{z}_s$ are the position errors between master and slave hopper, $y_{loe} = y_{lom} - y_{los}$ and $y_{tde} = y_{tdm} - y_{tds}$ are touchdown and liftoff position errors between master and slave hopper. In Figure 5.4 the apex state synchronization can be easily seen between two ball hoppers. Since the slave hopper traces the master hopper from one stride behind,

there is a constant horizontal ($y$) distance between two hoppers which can be seen in the first plot of Figure 5.4. Figure 5.6 states that the master and slave hopper has different initial conditions and in the first stride the present apex to next apex times of master and slave hoppers differ. But after the deatbeat controller is applied, slave hopper traces the master hopper with a constant phase difference due to the different initial conditions. These error figures are obtained by averaging 930 different intial conditions, i.e. $[y_s \; z_s \; \dot{y}_s]$ for 100 strides.

## 5.3 Master-Slave Synchronization of Two Ball Hoppers using Under-Actuated Controller

In this section, we will present master-slave synchronization of two ball hoppers using under-actuated controller. Synchronization is achieved by finding appropriate control inputs $[k, \; \theta]$ in case of fixed control parameter $\Delta y$, which is a reasonable restriction. With the use of under-actuated controller, we achieve the apex position synchronization but due to the fixed control parameter $\Delta y$ the apex velocity synchronization can not be achieved.

Now consider the scenario that we have constructed for the master-slave synchronization of two ball hoppers in the previous section. But this time let the hoppers start moving almost simultaneously, i.e. we assume master hopper hits the ground before the slave hopper and $\Delta y = 0.08$ for the slave hopper. We assume that we have the full knowledge about the master hopper, i.e. we precisely measure the apex states of the master hopper. By using the under-actuated deadbeat controller, i.e. keeping $\Delta y$ fixed, we try to choose such control parameters $k$ and $\theta$ that the slave hopper imitates the master hoppers trajectory. We choose $k$ and $\theta$ by using the nonlinear equations obtained from (5.7)-(5.9). In Figure 5.7, which shows the syncronization of two hoppers with respect to time, the slave hopper jumps forth and back continuosly, which is meaningless. We

come up with such a result because, the under-actuated controller achieves only apex position synchronization but the apex velocity synchronization fails. To achieve meaningful master-slave synchronization between the hoppers we define two criteria as follows which depend on the initial conditions:

- The liftoff horizontal position of the slave hopper is desired to be smaller than the next apex horizontal position of the master hopper:

$$y_s(0)+\dot{y}_s(0)\sqrt{\frac{2z_s(0)}{g}}+\Delta y_s < y_m(0)+\dot{y}_m(0)(\sqrt{\frac{2z_m(0)}{g}}+\frac{\dot{z}_{mlo}(0)}{g})+\Delta y_m(0). \tag{5.10}$$

- The touchdown horizontal position of the slave is desired to be larger than the apex horizontal position of the master hopper:

$$y_s(0)+\dot{y}_s(0)\sqrt{\frac{2z_s(0)}{g}} > y_m(0). \tag{5.11}$$

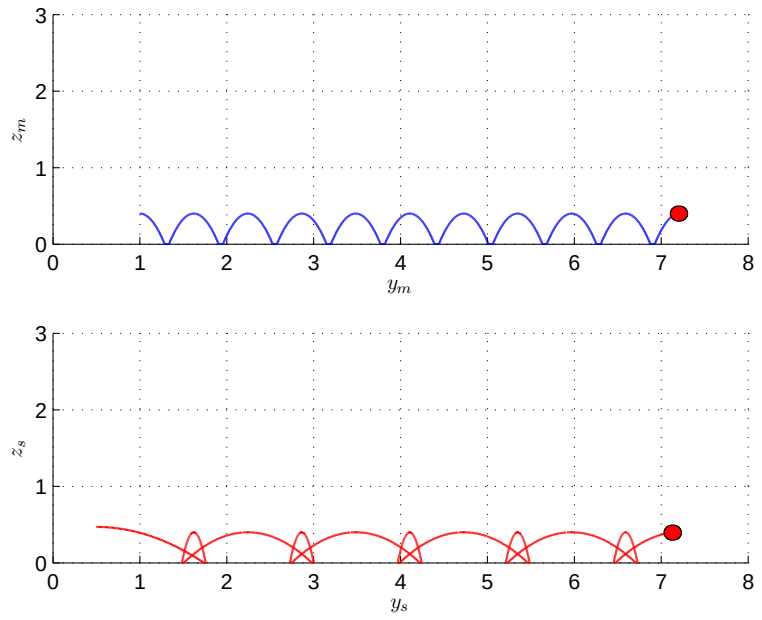


Figure 5.7: Simultaneous master-slave synchronization of two ball hoppers when there is no criteria applied to the initial conditions of the slave hopper.

Now, let the hoppers start moving almost simultaneously and satisfy the conditions given below. To visualize the gaits consider the following figure:

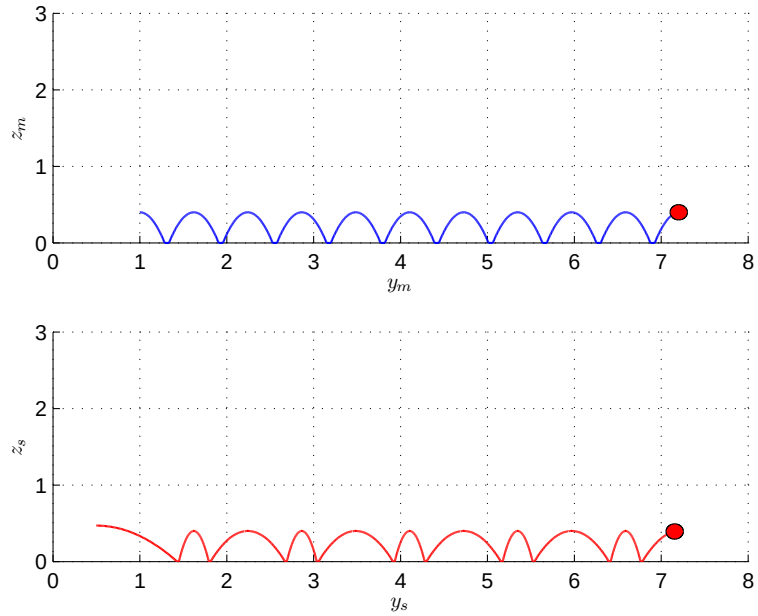


Figure 5.8: Simultaneous master-slave synchronization of two ball hoppers when the criteria applied to the initial conditions of the slave hopper.

So, in Figure 5.8 we solved the moving back and forth problem. But this time the collision of the masses problem occurs. Due to the simulataneous gaits of the hoppers, they collide. To overcome this problem let the master hopper move one stride ahead from the slave hopper. The aforementioned case is illustrated in Figure 5.9. Now, we achieve meaningful synchronization between master and slave hoppers. For further analysis consider the error figures. Figure 5.10 shows that the slave hopper traces the apex position of the master hopper from one stride behind, i.e. $y_e$ is constant, but the oscillating $\dot{y}_e$ means that the slave hopper fails to synchronize the horizontal velocity with the master hopper at the apex. In Figure 5.11, we can reach the same result, i.e. horizontal velocity of the master and slave hoppers are not synchronized. Figure 5.12 states that the slave hopper traces the master hopper with two different time phases, namely lead and lag time phases. These error figures are obtained by averaging 460 different intial conditions, i.e. $[y_s \; z_s \; \dot{y}_s]$ for 100 strides.

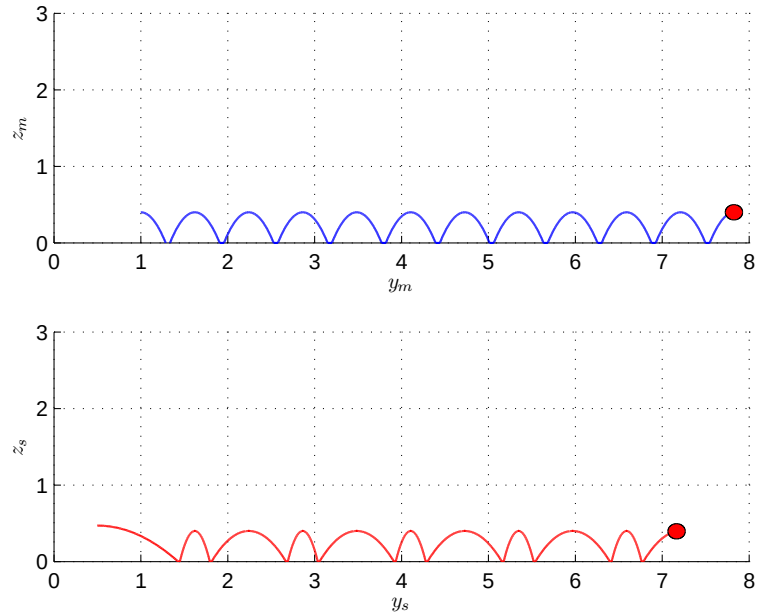


Figure 5.9: Master-Slave Synchronization of Two Ball Hoppers. For the master hopper we choose $k = 1$, $\theta = 0$, $\Delta y = 0.05$ as the control inputs and $[y\ z\ \dot{y}\ \dot{z}] = [1\ 0.4\ 1\ 0]$ as the initial conditions. In this particular simulation we choose the initial conditions for the slave hopper as $[y\ z\ \dot{y}\ \dot{z}] = [0.5\ 0.47\ 3\ 0]$

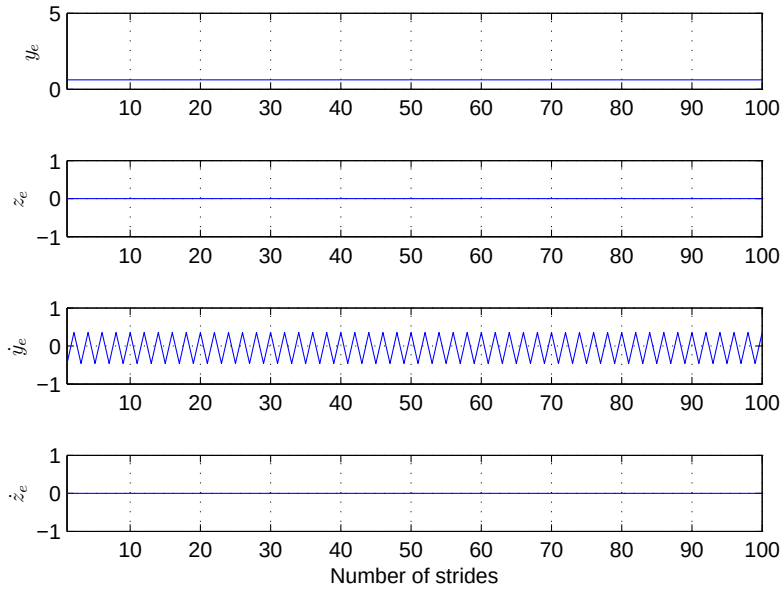


Figure 5.10: Apex states error figures.

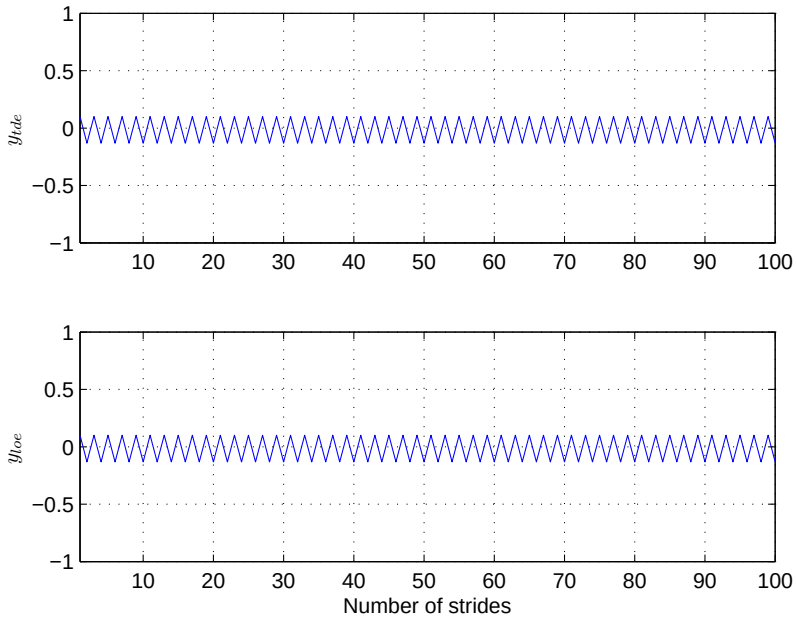


Figure 5.11: Touchdown and liftoff position error figures.

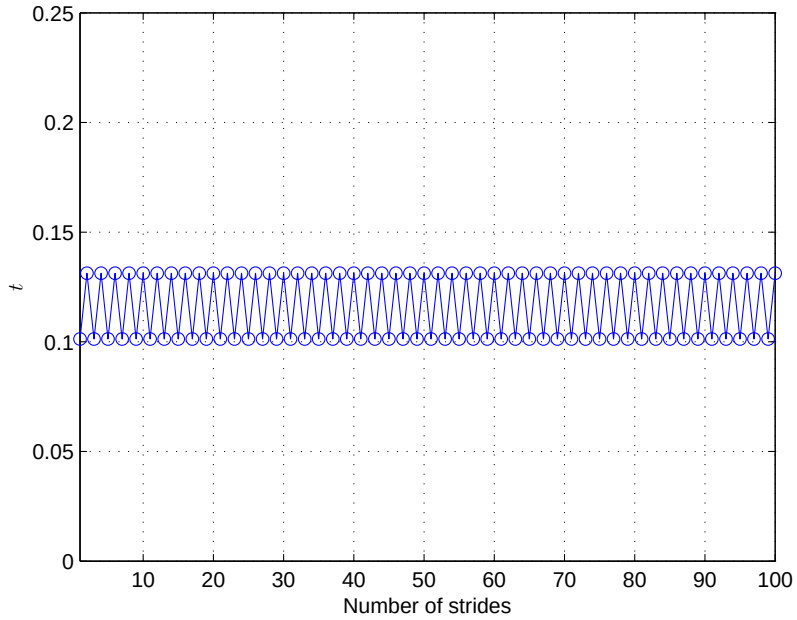


Figure 5.12: Differences of time that is spent between present apex to apex at each stride.

## 5.4 Discussion and Contribution

In this part of the thesis, we presented synchronization of two ball hoppers in master-slave configuration under two different deadbeat gait controllers namely, fully-actuated controller and under-actuated controller. The apex state synchronization between hoppers is easily achieved by using fully-actuated controller, in other words we successfully estimated the control parameters of the master hopper ($k$, $\theta$ $\Delta y$) by using the deadbeat controller. But the deadbeat controller synchronized the slave hopper in one stride which made it impossible to synchronize hoppers in time.

Finally, meaningful apex position synchronization between hoppers is achieved by using under-actuated controller ($k$, $\theta$, and fixed $\Delta y$), i.e. we used nonlinear touchdown to liftoff equations to choose appropriate $k$ and $\theta$ control inputs, if we apply several criteria to the initial conditions of the slave hopper. The fixed $\Delta y$ control parameter prevented us to control the horizontal velocity of the slave hopper, so the apex velocity synchronization is failed. Due to the use of deadbeat controller, as in the fully-actuated case, time synchronization also failed, but both the apex velocity and time differences are shown to be bounded in simulations. We note that the results presented in this chapter are novel and require further investigation for the synchronization of multiple ball hoppers and SLIP systems.

# Chapter 6

# CONCLUSIONS

In this thesis, we firstly introduced the general notion about synchronization phenomenon and then we provided the general types and methods of synchronization which are widely used in practical applications. Afterwards we investigated the passive controlled in-phase synchronization between coupled simple and double pendulum systems. Finally we considered the master-slave synchronization of the two ball hoppers.

In Chapter 1, we introduced various examples of synchronization which are widely encountered in natural events, life sciences and engineering applications. Then we gave the definitions of synchronization and problems of synchronization which are existed in the literature. In this study, we defined the synchronization as the adjustment of rhythms of oscillating systems due to their weak interaction.

In Chapter 2, we provided the types and methods of synchronization which are widely used in practical applications. Throughout the thesis we used full synchronization, i.e. in-phase synchronization and master-slave synchronization.

In Chapter 3, we coupled simple pendulums under various configurations by using spring and damper motivated by the idea of providing a generalized formula

or a guideline for simple pendulum synchronization. To analyze and show the synchronous behaviour between the coupled pendulums we firstly linearized the equations of motion using the small angle approximation, i.e. pendulum angles are restricted to be smaller than $10^{\circ}$. The linearization process enabled us to write the equations of motion of the systems in hand and its appropriately defined error dynamics in matrix forms $A$ and $A_e$, respectively. The analytical analysis applied to matrices $A$ and $A_e$ showed that all of the pendulums we coupled are synchronized except for some special cases. For example, in four pendulums case we showed analytically that if there is a single damper in the middle pendulum and a single spring on the left and a single spring on the right of the damper with equal spring constants, then the synchronization can not be achieved. In fact, this is the only configuration in four pendulums case where passive synchronization fails. By generalizing this conclusion to multiple pendulums case, we conjectured that if there exist equal numbers of springs on the left and right side of the damper and the sum of the coefficients of the springs which are on the left and right sides of the damper are equal, i.e. $k_1 + k_2 + k_3 + ... = ... + k_{n-2} + k_{n-1} + k_n$ then the synchronization can not be achieved. Analytical proof of this conjecture requires further investigation. Then we revealed the role of spring and damper in synchronization process. The spring element had no effect on synchronization other than coupling the pendulums and the damper element had the effect of synchronizing pendulums by equating the velocities of its connection points.

In Chapter 4, we coupled double pendulums under two different coupling configurations, i.e. upper pendulums coupled and lower pendulums coupled, to show that the double pendulums are synchronized for any positive system parameters $k,\ c,\ m,\ l,\ l_0$ and to compare the synchronization dynamics between these two coupling configurations. The analytical and numerical analysis we applied to matrices $A$ and $A_e$ showed that the upper pendulums coupled double pendulum system synchronizes for all positive $k,\ c,\ m,\ l,\ l_0$ parameter values and the lower pendulums coupled double pendulum system synchronizes for all

positive $k,\ c,\ m,\ l,\ l_0$ except $l_0 = \frac{1}{\sqrt{2}}l$. Either by using analyitcal or numerical methods we could not find meaningful comparison results between upper and lower coupled double pendulums.

In Chapter 5, we tried to synchronize two ball hoppers in master-slave configuration by using two different gait controllers namely, fully-actuated controller ($k$, $\theta$, $\Delta y$) and under-actuated controller ($k$, $\theta$, $\Delta y$ is fixed). In the fully-actuated controller case, we achieved apex state synchronization between the hoppers by successfully estimating the control parameters of the master hopper. The time synchronization of the hoppers could not be achieved due to the use of deadbeat controller. In the under-actuated controller case, by making use of the nonlinear touchdown to liftoff nonlinear equations to choose appropriate $k$ and $\theta$ and by finding appropriate criteria for the initial conditions of the slave hopper, we were able to achieve meaningful apex position synchronization between hoppers, but the fixed $\Delta y$ control parameter constrained the control on the horizontal velocity of the slave hopper. As a result, the apex velocity synchronization is failed and the slave hopper traced the master hopper with leading and lagging time phases. The simulation results show that both the apex velocity and time differences between present apex to next apex are bounded. These results are, to the best of our knowledge, novel and require further investigation.

# APPENDIX A

# Presentation of Positive Routh-Hurwitz First Columns

Consider the Table 3.1. We need to show that the terms correspond to the $s^2$ and $s^3$ are positive. The $s^3$ term can be written as $2k^2l^2+kl_0^2+(kl_0-gm)^2$ by making use of the square form and $s^2$ can be written as $k^2l^4+gkl_0^2m+(kl^2+kl_0^2-glm)^2$ by adding and subtracting $gkl_0^2m$ from the term and by making use of the square form.

Consider the Table 3.4. We need to show that the term corresponds to $s^3$ is positive once we show $2K_1^2-3K_1K_2+2K_2^2$ is positive. By adding and subtracting $K_1K_2$ from the term and by making use of the square form the above term can be written as $2(K_1-K_2)^2+K_2$. The same method applies to the Table 3.5 for $s^1$ term.

# Bibliography


[1] A. Pikovsky, M. Rosenblum, and J. Kurtis, *Synchronization - A Universal Concept in Nonlinear Science*. Springer, 2002.

[2] G. V. Osipov, J. Kurths, and Ch. Zhou, *Synchronization in Oscillatory Networks*. Berlin: Springer, 2007.

[3] Winfree, A. T., *The Geometry of Biological Time*. New York: Springer, 1980.

[4] I.I. Blekhman, *Synchronization in Science and Technology*. New York: ASME Press, 1988.

[5] A. Rodriguez-Angeles and H. Nijmeijer, "Coordination of Two Robot Manipulators Based on Position Measurements Only," *Int. J. Control*, vol. 74, pp. 1311–1323, 2001.

[6] Y. H. Liu, Y. S. Xu, and M. Bergerman, "Cooperation control of multiple manipulators with passive joints," *IEEE Trans. Robot. Autom.*, vol. 15, no. 2, pp. 258–267, Apr. 1999.

[7] W.C. Lindsey and M.K. Simon, *Phase-Locked Loops and Their Applications*. New York: IEEE Press, 1978.

[8] L.M. Pecora and T.L. Carroll, "Synchronization in chaotic systems," *Phys. Rev. Lett.*, vol. 64, pp. 821–824, 1990.

[9] A.S. Dmitriev and A.I. Panas, *Dynamical chaos: new information carrier in communication systems*. Moscow: Fizmatlit, 2002.

[10] Kleinspehn, A., *Goal-directed interpersonal action synchronization across the lifespan: A dyadic drumming study. Doctoral dissertation*. PhD thesis, Freie Universitt Berlin, Germany, 2008.

[11] Belykh, V., Pankratova, E., Pogromski, A.Y. and Nijmeijer, H., "Two Van Der Pol–Duffing Oscillators With Huygens Coupling," in *Proceedings of the 6th EUROMECH Nonlinear Dynamics Conference (ENOC'08)*, (Saint Petersburg, RUSSIA), June 30 - July 4, 2008.

[12] Hugenii C., *Horoloquim Oscilatorium*. 1673.

[13] Blekhman, I. I., A. L. Fradkov, H. Nijmeijer and A. Yu Pogromsky, "On self-synchronization and controlled synchronization," *Systems and Control Letters*, vol. 31, p. 299305, 1997.

[14] R. Brown, L. Kocarev, "A unifying definition of synchronization for dynamical systems," *CHAOS*, vol. 10, p. 344349, 2000.

[15] A. Rodriguez-Angeles, *Synchronization of Mechanical Systems*. PhD thesis, Eindhoven Univ. Technol., 2002.

[16] H. Nijmeijer, "A dynamical control view on synchronization," *Physica D*, vol. 154, p. 219228, 2001.

[17] I.I. Blekhman, A.L. Fradkov, H. Nijmeijer, A.Yu. Pogromsky, "On self-synchronization and controlled synchronization," *Syst. Contr. Lett.*, vol. 31, p. 299305, 1997.

[18] Vladimir N. Belykh, Grigory V. Osipov, Nina Kucklander., Bernd Blasius, Jurgen Kurths, "Automatic control of phase synchronization in coupled complex oscillators," *Physica D*, vol. 200, pp. 81–104, 2005.

[19] Yun-Hui Liu, Yangsheng Xu and Marcel Bergerman, "Cooperation Control of Multiple Manipulators with Passive Joints," *IEEE TRANSACTIONS ON ROBOTICS AND AUTOMATION*, vol. 15, no. 2, pp. 258–267, APRIL 1999.

[20] Efimov, D.; Sacre, P.; Sepulchre, R., "Controlling the phase of an oscillator: A phase response curve approach," in *Decision and Control, 2009 held jointly with the 2009 28th Chinese Control Conference*, pp. 7692–7697, 15-18 Dec. 2009.

[21] A.S. Pikovsky, M.G. Rosenblum, and J. Kurths, "Phase Synchronization in Regular and chaotic systems," *International Journal of Bifurcation and Chaos*, vol. 10, no. 10, pp. 2291–2305, 2000.

[22] Rosenblum M, Pikovsky A, Kurths J, Schafer C, Tass PA., *Phase synchronization: from theory to data analysis, Handbook of biological physics.* Amsterdam, Netherland: Elsevier, 2001.

[23] R. Dilo, "On the problem of synchronization of identical dynamical systems: The Huygens clocks," *Variational Analysis and Aerospace Engineering*, vol. 33, pp. 163–181, 2009.

[24] O. Makarenkov, P. Nistri, D. Papini, "Synchronization problems for unidirectional feedback coupled nonlinear systems," *Dyn. Contin. Discrete Impuls. Syst., Ser. A, Math. Anal.*, vol. 15, no. 4, pp. 453–468, 2008.

[25] J.A. Acebron, L.L. Bonilla, C.J. Perez, F. Ritort and R. Spigler, "The Kuramoto model: a simple paradigm for synchronization phenomena," *Rev. Mod. Phys.*, vol. 77, p. 137185, 2005.

[26] Brunt, M., *Coordination of Redundant Systems. PhD thesis.* PhD thesis, Technical University Delft, The Netherlands., 1998.

[27] Dubey, R. V., T. F. Chan and S. E. Everett, "Variable damping impedance control of a bilateral telerobotics system," *IEEE Control and Systems*, vol. 17, p. 3745, 1997.

[28] Lee, H. K. and M. J. Chung, "Adaptive controller of a master-slave system for transparent teleoperation," *Journal of Robotic Systems*, vol. 15, p. 465475, 1998.

[29] Hills, J. W. and J. F. Jensen, "Telepresence technology in medicine: principles and applications," *Proceedings of the IEEE*, vol. 86, p. 569580, 1998.

[30] Guthart, G. S. and J. K. Salisbury Jr., "The $intuitive_TM$ telesurgery system: overview and application," *Proceedings of the IEEE International Conference on Robotics and Automation*, p. 618621, 2000.

[31] Wang, P.K.C., A. Sparks and S. Banda, "Co-ordination and control of multiple microspacecraft moving in formation," *The Journal of the Astronautical Sciences*, vol. 44, p. 315355, 1996.

[32] Kang, W. and H. Yeh, "Co-ordinated attitude control of multi-satellite systems," *International Journal of Robust and Nonlinear Control*, vol. 12, p. 185205, 2002.

[33] Yamaguchi, H., T. Arai and G. Beni, "A distributed control scheme for multiple robotic vehicles to make group formations," *Robotics and Autonomous Systems*, vol. 36, p. 125147, 2001.

[34] R. C. Dorf, R. H. Bishop, *Modern Control Systems.* Upper Saddle River, N.J.: Prentice Hall, 2005.

[35] H. K. Khalil, *Nonlinear Systems.* Elnglewood Cliffs, NJ: Prentice-Hall, 2.

[36] . Arslan., *Model-Based Methods for the Control and Planning of Running Robots. M.Sc. thesis,.* PhD thesis, Bilkent University, Ankara, Turkey,.

[37] W. J. Schwind., *Spring loaded inverted pendulum running: a plant model. PhD thesis,*. PhD thesis, University of Michigan, Ann Arbor, MI, USA,, 1998.